Coastal Protection and Restoration Authority
150 Terrace Avenue, Baton Rouge, LA 70802 | coastal@la.gov | www.coastal.la.gov

2017 Coastal Master Plan

Attachment C3-23: ICM Calibration, Validation, and Performance Assessment

Report: Final

Date: April 2017

Prepared By: Stokka Brown (Moffatt & Nichol), Brady Couvillion (U.S. Geological Survey), Zhifei Dong (CB&I), Ehab Meselhe (The Water Institute of the Gulf), Jenneke Visser (University of Louisiana at Lafayette), Yushi Wang (The Water Institute of the Gulf), and Eric White (The Water Institute of the Gulf)

Coastal Protection and Restoration Authority

This document was prepared in support of the 2017 Coastal Master Plan being prepared by the Coastal Protection and Restoration Authority (CPRA). CPRA was established by the Louisiana Legislature in response to Hurricanes Katrina and Rita through Act 8 of the First Extraordinary Session of 2005. Act 8 of the First Extraordinary Session of 2005 expanded the membership, duties, and responsibilities of CPRA and charged the new authority to develop and implement a comprehensive coastal protection plan, consisting of a master plan (revised every five years) and annual plans. CPRA's mandate is to develop, implement, and enforce a comprehensive coastal protection and restoration master plan.

Suggested Citation:

Brown, S., Couvillion, B., Dong, Z., Meselhe, E., Visser, J., Wang, Y., and White, E. (2017). *2017 Coastal Master Plan: Attachment C3-23: ICM Calibration, Validation, and Performance Assessment*. Version Final. (pp. 1-95). Baton Rouge, Louisiana: Coastal Protection and Restoration Authority.

Acknowledgements

This document was developed as part of a broader Model Improvement Plan in support of the 2017 Coastal Master Plan under the guidance of the Modeling Decision Team (MDT):

- The Water Institute of the Gulf - Ehab Meselhe, Alaina Grace, and Denise Reed
- Coastal Protection and Restoration Authority (CPRA) of Louisiana - Mandy Green, Angelina Freeman, and David Lindquist

This effort was funded by the Coastal Protection and Restoration Authority (CPRA) of Louisiana under Cooperative Endeavor Agreement Number 2503-12-58, Task Order No. 03.

Executive Summary

The Integrated Compartment Model (ICM) is the primary landscape model used in the Louisiana Coastal Master Plan to analyze restoration and protection projects. The ICM comprises the following subroutines: hydrology, morphology, barrier islands, and vegetation. Output from these subroutines is used to drive several habitat suitability indices (HSI) and a food web fish and shellfish biomass model (Ecopath with Ecosim, EwE). Further, the ICM provides output used by a storm surge model (ADCIRC) and risk analysis model (CLARA), which focuses on evaluating protection projects.

This report documents the calibration and validation effort for the coast wide ICM. Once validated, the ICM was used to evaluate and analyze the landscape and ecosystem effects of individual projects and alternatives (groups of projects) under a variety of environmental scenarios.

This report provides a description of the list of model parameters selected to perform the calibration and validation. The modeling team carefully fine-tuned these parameters while ensuring that values assigned to these parameters remained within the acceptable values in the literature. The model performance was quantitatively assessed through comparison with available field observations and measurements. In addition to the model performance assessment described in this report, an uncertainty analysis was performed and is documented separately in Attachment C3-24: ICM Uncertainty Analysis.

Overall, the ICM compared well and captured the temporal and spatial trends and patterns of field observations. Therefore, the model is considered suitable as a planning-level predictive tool to analyze and evaluate restoration projects and strategies under various environmental scenarios. Understandably, the environmental scenarios allow for examining the landscape response to drivers such as sea level rise, subsidence, precipitation, and evapotranspiration. These conditions exceed the environmental conditions used to calibrate and validate the model and cause a challenge regarding the ability of the ICM to capture the landscape response to these drivers. Some of these challenges are addressed in the uncertainty analysis presented in Attachment C3-24: ICM Uncertainty Analysis.

The calibration and validation effort also resulted in feedback regarding additional data needs. Water quality and sediment information, for example, are quite limited not only within the model domain (for calibration purposes) but also at the model boundaries (for boundary condition purposes). It is strongly recommended to improve the data collection effort for these parameters.

Table of Contents

List of Tables

List of Figures

List of Abbreviations

ADCIRC	Advanced Circulation (model)
AVGE	*Avicennia germinans*
BD	Bulk Density
BICM	Barrier Island Comprehensive Monitoring
BIMODE	Barrier Island Model
CERC	Coastal Engineering Research Center
CLARA	Coastal Louisiana Risk Assessment (model)
CPRA	Coastal Protection and Restoration Authority
CRMS	Coastwide Reference Monitoring System
CWPPRA	Coastal Wetlands Planning, Protection and Restoration Act
DISP	*Distichlis spicata*
EwE	Ecopath with Ecosim
HSI	Habitat Suitability Index
ICM	Integrated Compartment Model
KZM	Keyhole Markup Language
LAVegMod	Louisiana Vegetation Model
LDEQ	Louisiana Department of Environmental Quality
LCA S&T	Louisiana Coastal Area Science and Technology
LiDAR	Light Detection And Ranging
NAVD88	North American Vertical Datum of 1988
NH4	Ammonium
NO3	Nitrate
NOAA	National Oceanic and Atmospheric Administration
OM	Organic Matter
ppt	Parts per Thousand

RE	Relative Error
RMSE	Root Mean Square Error
SPAL	*Spartina alterniflora*
SPPA	*Spartina patens*
SSURGO	Soil Survey Geographic Database
TKN	Total Kjeldahl Nitrogen
TMP	Temperature
TPH	Total Phosphorus
TSS	Total Suspended Solids
USGS	United States Geological Survey
WIS	Wave Information Studies

1.0 Introduction

The Integrated Compartment Model (ICM) replaces four previously independent models (eco-hydrology, wetland morphology, barrier shoreline morphology, and vegetation) with a single model coded for all regions of the coast. It also includes the components of the previous ecosystem-related models that are being carried forward for 2017, and it enables integrated execution of the new fish and shellfish community model. Such integration allows for coupling of processes and removes the inefficiency of manual data handoffs and the potential human error that may occur during the transfer of information from one model to another. The ICM serves as the central modeling platform for the 2017 Coastal Master Plan and is used to analyze the landscape and ecosystem performance of individual projects and alternatives (groups of projects) under a variety of future environmental scenarios.

As in the 2012 Coastal Master Plan modeling effort, the hydrodynamic, morphology (including barrier islands), and vegetation subroutines of the ICM underwent calibration and validation. However, due to the integrated nature of the ICM, the automated data handoff and frequent feedback allowed for a much more systematic calibration effort than was possible for many of the 2012 components. For the 2017 effort, calibration of ICM subroutines was conducted to the extent possible considering data availability and time in the overall project schedule.

1.1 Importance of Calibration and Validation

In any long-term coastal planning effort, especially one as critical as the Louisiana Coastal Master Plan, it is important to continuously advance the suite of technical tools used to inform decision making. With continued advancements and incorporation of new capabilities also comes the need to calibrate, validate the model performance, and consider the effects of parametric uncertainties on modeled outcomes. This document provides a detailed description of the calibration, validation, and performance assessment of the 2017 Coastal Master Plan ICM. Results and discussions for parametric uncertainties can be found in the separate uncertainty analysis report (Attachment C3-24: ICM Uncertainty Analysis).

1.2 Overview of ICM Parameters used for Calibration

The first step toward calibrating and validating the ICM was to conduct a sensitivity analysis of a broad list of parameters that were identified by the modeling team. Parameters were chosen for analysis based on the team's expert understanding of: how the natural system works, how the respective model subroutines behave, and the understanding of how these parameters could potentially influence model output. Table 1 shows the parameters that were included in the sensitivity analysis. These parameters were adjusted across a range of permissible values, which were identified by subject matter experts associated with each subroutine based on previous experience with their respective model code. The relative impact on model output from each parameter value informed the modeling team of the relative sensitivity of the ICM to the range in potential parameter values. The results of these sensitivity runs were used as qualitative indicators of relative importance of these parameters on ICM outputs. These qualitative sensitivities were then used to guide the calibration process by alerting the modeling team to which parameters should be manually adjusted during calibration. A description of the general adjustments made and the impact on ICM output is provided in later sections for each subroutine.

Table 1: Summary of Model Parameters Used in the Sensitivity Analysis.

Test Parameter	Model Output Examined
Roughness - channel links	Stage
	Tidal Range
Roughness - marsh links	Stage
	Tidal Range
Link diffusivity	Salinity
Kadlec & Knights Coefficient 1	Stage
Kadlec & Knights Coefficient 2	Stage
Kadlec & Knights Exponent	Stage
Excess shear exponent	Stage
Remove all islands to assess change in hydrology	Tidal Range
	Salinity
Non-sand sediment resuspension coefficient	Accretion
Sand sediment resuspension coefficient	Accretion
Topography/elevation	Stage
	Tidal Range
	Accretion
Sediment denitrification rate, m/day	NO3
	Chl-A (ALG)
Salinity at which algal growth is halved, ppt	Chl-A (ALG)
Phytoplankton mortality rate at 20 deg C, day-1	Chl-A (ALG)
Minimum nitrification rate, per day	NO3
	NH4

Test Parameter	**Model Output Examined**
Detritus dissolution rate at 20 deg C, day-1	Organic N
	Organic P
	TKN
Phytoplankton respiration rate at 20 deg C, day-1	TKN
	Total P
Initial vegetation dispersal probability	Percent cover of key species: *Typha* spp*, Salix Nigra, Sagitaria lancifolia*
Vegetation establishment	Percent cover of key species: *Spartina alterniflora* (SPAL), *S. patens* (SPPA), *Sagitaria lancifolia* (SALA), *Panicum hemitomon* (PAHE2), *Panicum amarum* (PAAM2)
Vegetation mortality	Percent cover of key species: *Taxodium distchum* (TADI2), *Quercus spp.* (QULA3, QULY, QUNI, QUTE), *Panicum amarum* (PAAM2)
Tree establishment	% cover of key species: *Taxodium distchum* (TADI2), *Quercus spp.* (QULA3, QULY, QUNI, QUTE)
Bathymetry/Topography	Land area
Bulk density	Land area
Turn off marsh edge erosion to see RSLR effects	Land area
Barrier island long-shore transport	Long-shore sediment transport rates
Barrier island cross shore transport (Overwash transport parameter in SBEACH)	Cross-shore profiles

Table 2 summarizes key model output compared to observed data in this calibration and validation analysis. In the calibration phase, the key model parameters listed in Table 1 were fine-tuned until the model output compared well to the field/laboratory observations. Parameter values set during calibration were maintained for the rest of the model runs. In the validation phase, additional model simulations, using a completely independent input dataset, were performed using calibrated parameters to assess the model performance and how well it replicates the natural system. Calibration was performed on observed data ranging from 1/1/2010 through 12/31/2013. The independent data used to validate the calibrated model came from the same sources but covered a separate time period, ranging from 1/1/2006 through 12/31/2009.

Since the hydrodynamic subroutine is the primary driving force for other ICM subroutines, it was calibrated and validated before proceeding with calibration of the other subroutines. The vegetation subroutine was calibrated second, followed by the calibration of the wetland morphology subroutine. The barrier island subroutine, due to the relatively limited interaction with the other subroutines, was calibrated independent of the other subroutines. An overview of how the subroutines interact is provided in Appendix C: Chapter 3 (Model Components and Overview). A discussion of the process used to calibrate each respective subroutine, as well as a discussion of the calibration results is provided in the following sections.

Upon calibration of the hydrodynamic, vegetation, wetland morphology, and barrier island subroutines, the (now-calibrated) ICM output was used to develop and calibrate the Ecopath with Ecosim (EwE) fisheries biomass model using observed data. A full discussion of this process is provided in Attachment C3-20: Ecopath with Ecosim. The habitat suitability indices (HSI) were not quantitatively calibrated due to a lack of appropriate observed data and are not discussed here; refer to Attachments C3-6 through C3-19 for a full discussion of the development and application of each HSI.

Table 2: Overview of the ICM Calibration and Validation Data Sources and Performance Targets.

Model Output	Data Used	Available Record	Approach/Metrics	Model Parameters to Adjust During Calibration
Stage	LDEQ[1], CRMS[2], USGS[3], NOAA[4]	2006-2013	RMSE of 10-20%/Bias of 0.15 m	Cell/link dimensions Observed tidal datum corrections Hydraulic equations
Flow	USGS	2006-2013	RMSE of 20-30%	Same as stage
Salinity	LDEQ, CRMS, USGS	2006-2013	RMSE of 20-30%	Diffusivity
Total Suspended Sediment	Long term averages of grab TSS samples from USGS and LDEQ & reflectance imagery	Varied	Best professional judgment based on long term average TSS & TSS grab samples	Resuspension coefficients, see Table 3 for a full list
Sediment Accumulation	CRMS soil properties & measured accretion	Varied	Best professional judgment based on marsh accumulation	Resuspension coefficients Marsh exchange flow

[1] Louisiana Department of Environmental Quality
[2] Coastwide Reference Monitoring System
[3] U.S. Geological Survey
[4] National Oceanographic and Atmospheric Administration

Model Output	Data Used	Available Record	Approach/Metrics	Model Parameters to Adjust During Calibration
	rates		and mean suspended sediment concentration	
Nitrogen	LDEQ	2006-2013	Best professional judgment based on grab sample datasets	Sediment denitrification rate Minimum nitrification rate
Phosphorus	LDEQ	2006-2013	Best professional judgment based on grab sample datasets	Detritus dissolution rate Phytoplankton respiration rate
Long-term (25-yr) accretion	Cesium cores (>100 cores)	2006-2013	Best professional judgment based on comparison to measured mean annual accretion by ICM region by wetland type	Bulk density Organic matter
Multi-year land area change rates	Historic land change rates from satellite imagery (Landsat)	2006-2013	Best professional judgment based on comparison to measured land change rates by CWPPRA[5] basin by wetland type	Marsh collapse threshold Only if needed: • Storm sediment distribution • Background land change rate • 2-zone sediment deposition
Percent cover per modeled vegetation species	CRMS vegetation data	2006-2013	Best professional judgment based on capturing stability or trajectories of change at 392 CRMS stations for all species	Mortality and establishment tables for species for which the distributions are over or under estimated
Barrier island long-shore	BICM[6], LiDAR[7],	2003-2012	Best professional judgment based	Long-shore transport coefficients (to obtain net

[5] Coastal Wetlands Planning, Protection and Restoration Act
[6] Barrier Island Comprehensive Monitoring

Model Output	Data Used	Available Record	Approach/Metrics	Model Parameters to Adjust During Calibration
transport	historic reports		on accepted long-shore transport rates	long-shore transport rates that match sediment budgets presented in historic reports)
Barrier island cross shore transport	BICM	2010	Best professional judgment based on overwash extent as calibrated for previous SBEACH efforts	SBEACH transport rate coefficient, slope dependent coefficient, transport rate decay coefficient, and overwash

2.0 Hydrology

2.1 Data and Methods

Observed stage, flow, salinity, sediment, and water quality data were collected from monitoring stations across the Louisiana coast from the United States Geological Survey (USGS), the National Oceanic and Atmospheric Administration (NOAA), the Louisiana Department of Environmental Quality (LDEQ), and the Coastwide Reference Monitoring System (CRMS) to calibrate and validate the ICM. The following sections identify the stations from which data were collected and used for model comparison.

2.1.1 Stage

Figure 1 shows the spatial extent of the observed stage monitoring stations. The shape of the point indicates the agency which collected the data, and the color of the point indicates the vertical datum reference. Circles indicate data collected by CRMS, triangles indicate data collected by NOAA, and squares indicate data collected by USGS. A fill color of green indicates the data were referenced to the fixed datum North American Vertical Datum of 1988 and Geoid 12A (NAVD88 Geoid12A), yellow indicates the data were referenced to only NAVD88 with no Geoid specified, and orange indicates the data were not referenced to any fixed datum. Table 1 in Attachment C3-23.1 identifies the stations' agency, identification number, name, latitude, longitude, and the vertical reference datum.

[7] Light Detection and Ranging

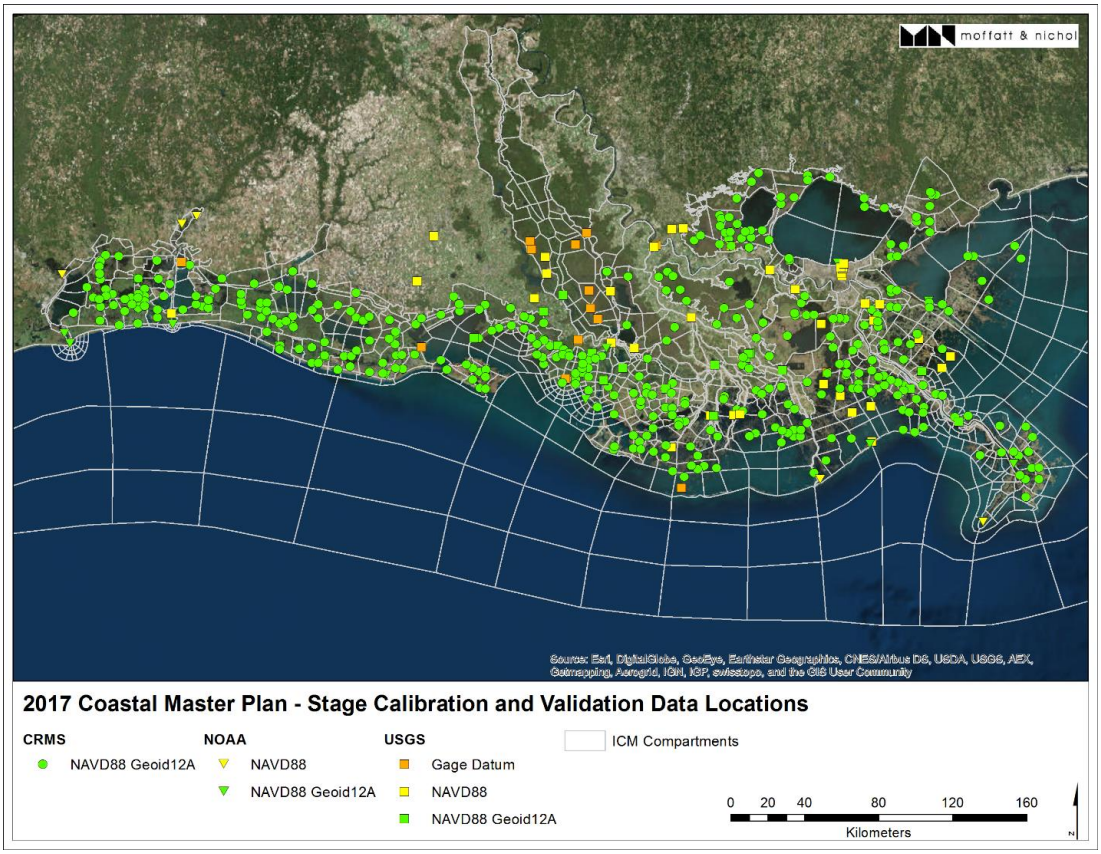

Figure 1: Stage Calibration and Validation Stations.

2.1.2 Flow

Figure 2 shows the spatial extent of the observed flow monitoring stations. All observed flow data were collected from USGS monitoring stations. Table 3 in Attachment C3-23.1 identifies the stations' agency, identification number, name, latitude, and longitude.

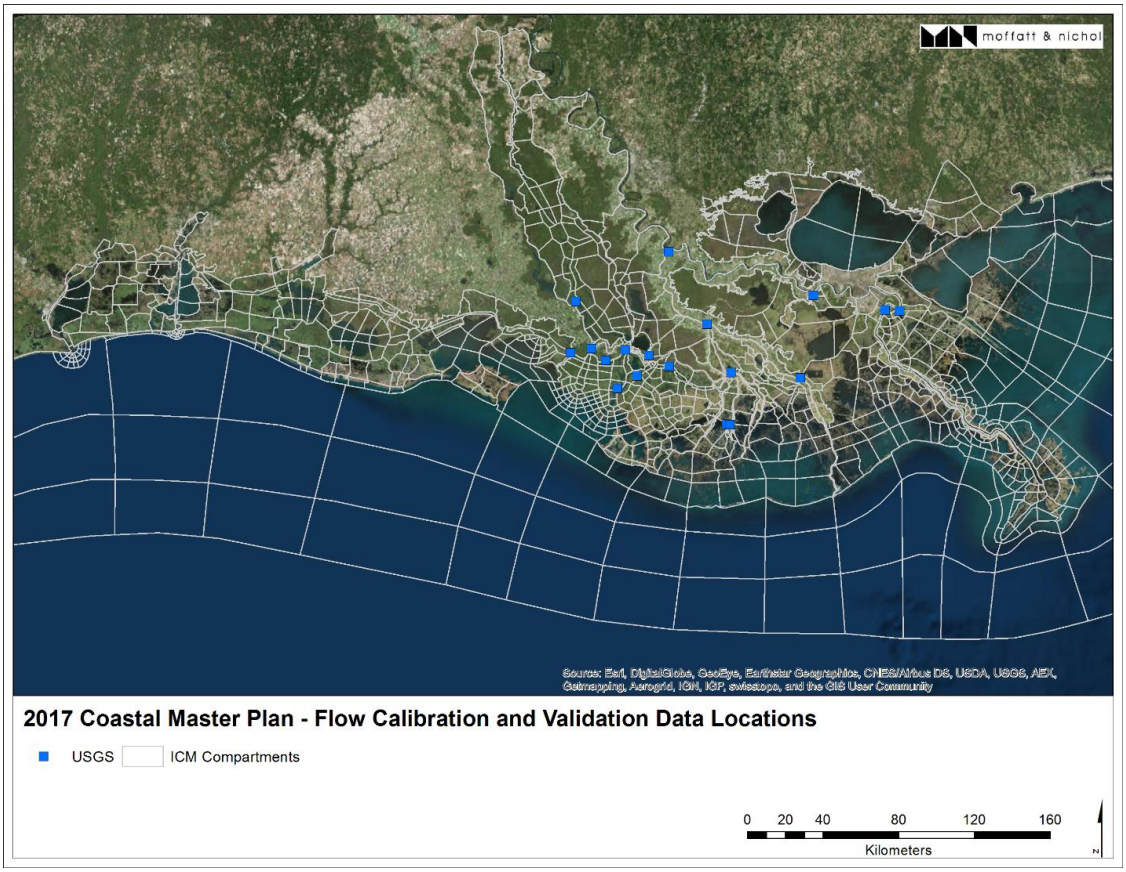

Figure 2: Flow Calibration and Validation Stations.

2.1.3 Salinity

Figure 3 shows the spatial extent of the observed salinity monitoring stations. Circles indicate CRMS stations, triangles indicate LDEQ stations, and squares indicate USGS stations. Table 2 in Attachment C3-23.1 identifies the stations' agency, identification number, name, latitude, and longitude.

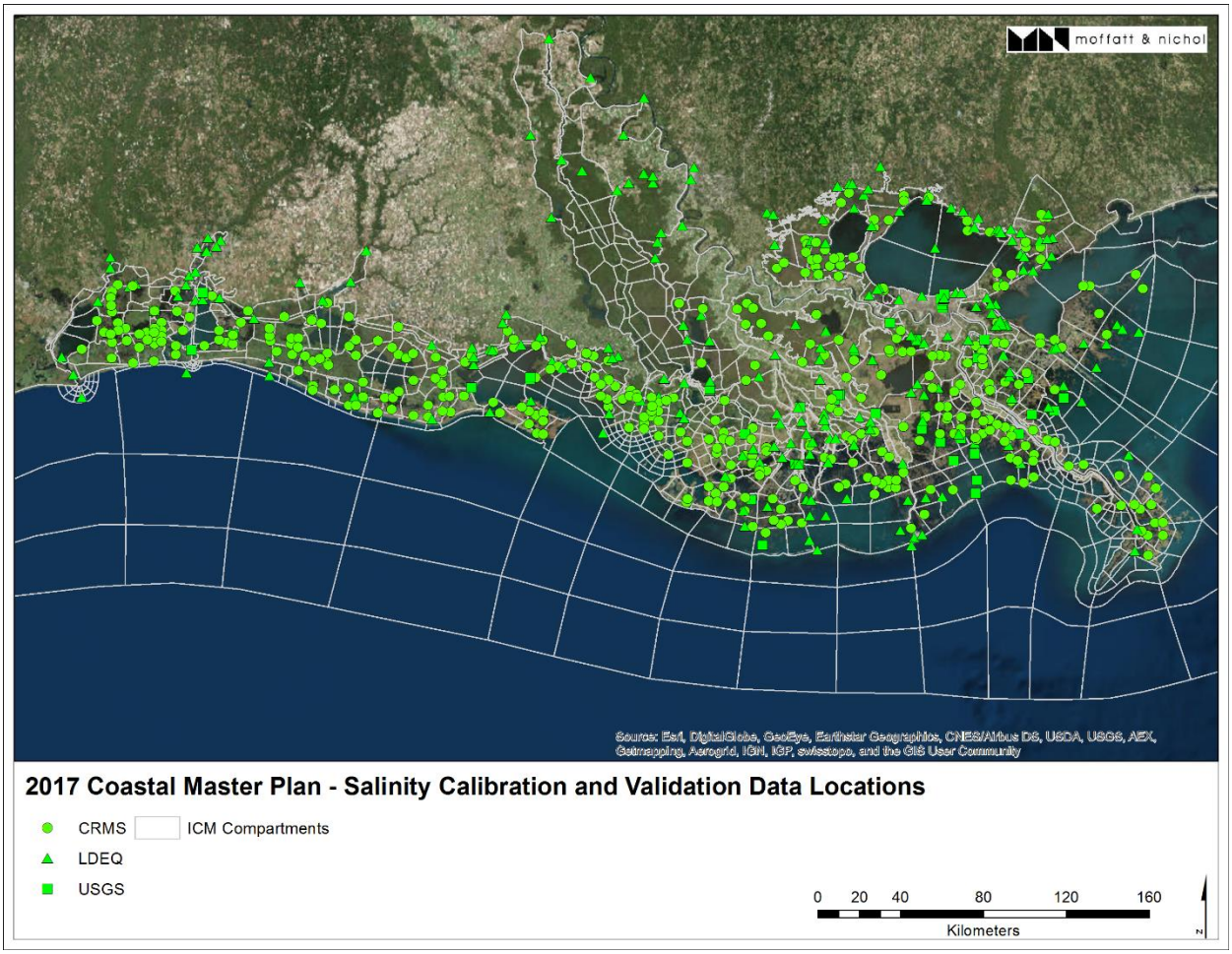

Figure 3: Salinity Calibration and Validation Stations.

2.1.4 Suspended Sediment

The observed total suspended solids (TSS) monitoring stations are shown in Figure 4. The hydrodynamic subroutine only modeled inorganic suspended sediments (sand, silt, clay and flocculated clay); however, due to data availability the observed total suspended sediment concentrations were used for model comparison. Throughout the remainder of this report, TSS will be used to reference both modeled inorganic sediments and observed total sediments.

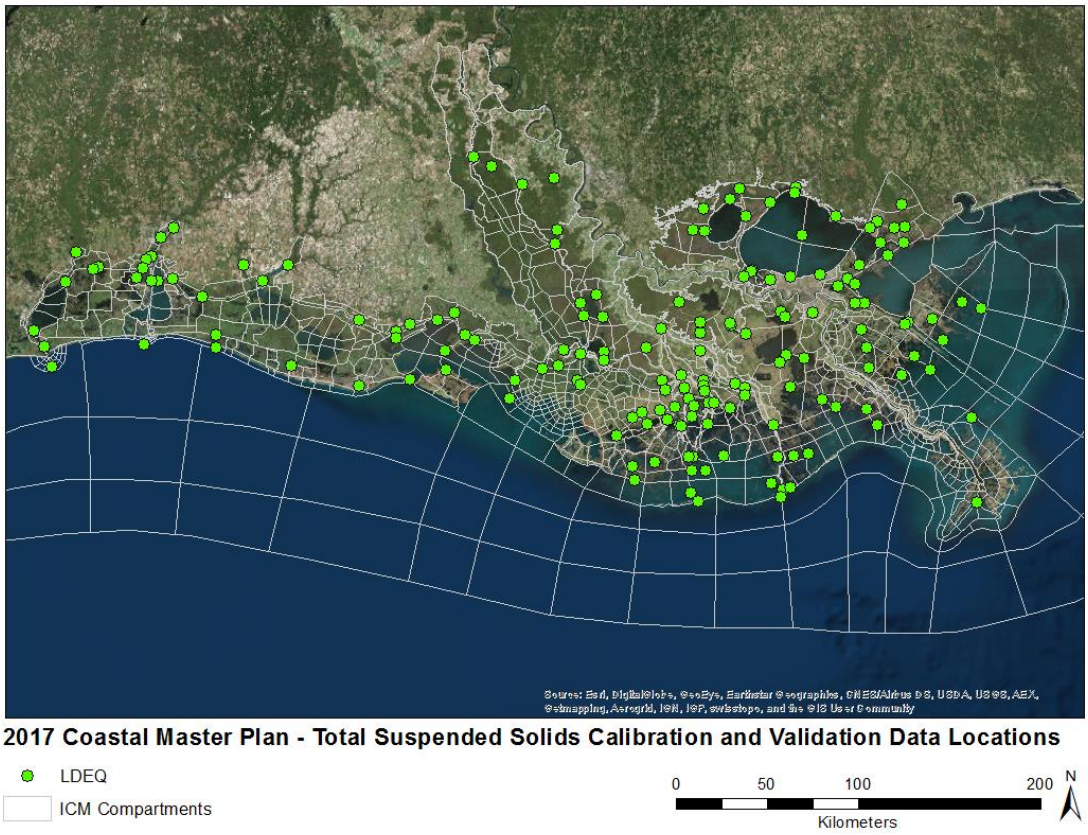

Figure 4: Total Suspended Solids Stations.

2.1.5 Temperature and Water Quality

Water quality monitoring stations for temperature (TMP), nitrate (NO3), ammonium (NH4), total Kjeldahl nitrogen (TKN), and total phosphorus (TPH) are shown in Figure 5. Observed data were all collected from LDEQ stations.

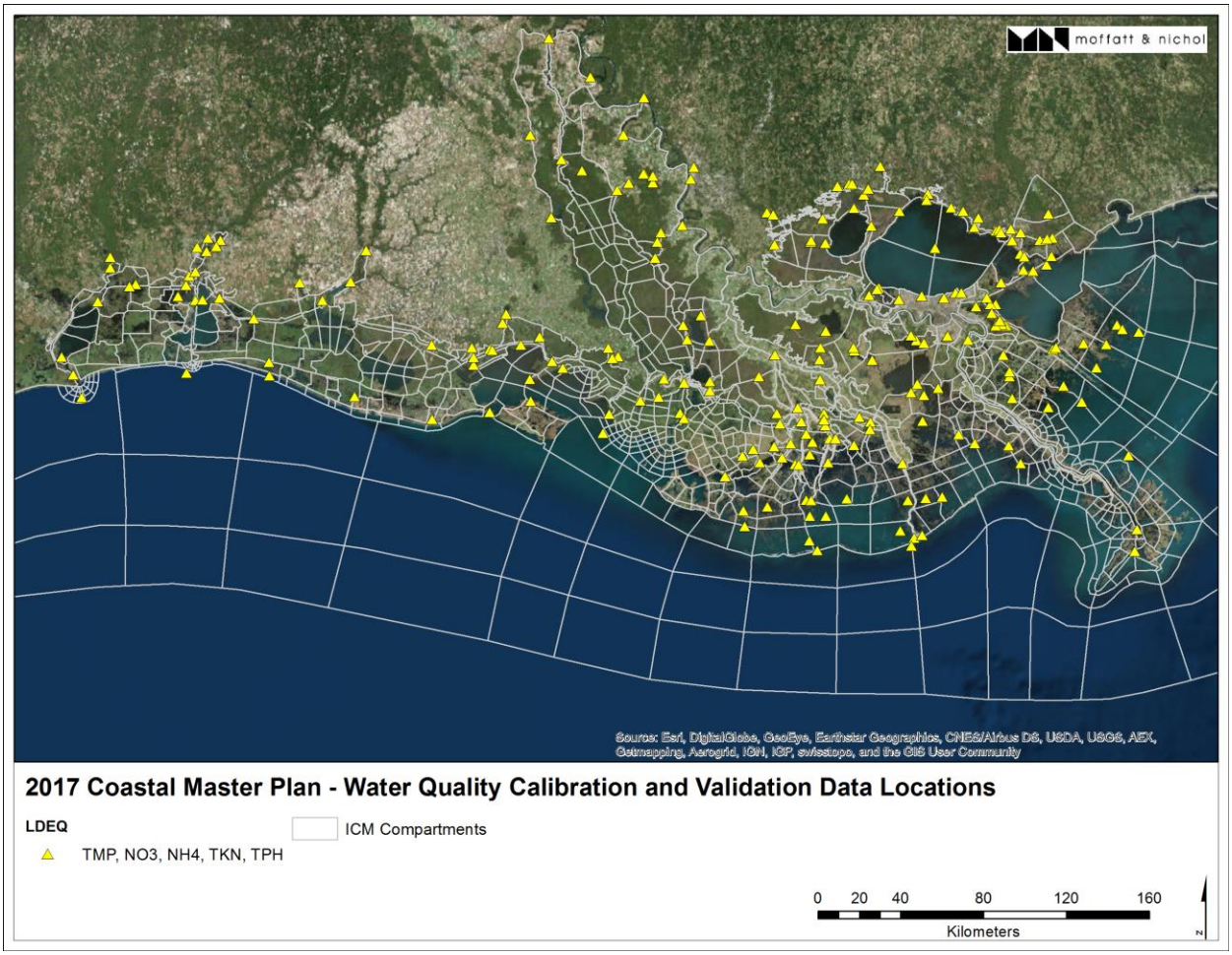

Figure 5: Temperature and Water Quality Calibration and Validation Stations.

2.2 Analysis

2.2.1 Stage

Time-series plots and the root mean square error (RMSE) were used to assess the model performance and to evaluate the level of agreement between the model and the observations. A goal to have 80% of the stations meet the target of 10-20% RMSE between modeled and observed stage (Table 2) was set. This goal was based on guidance of previous model calibrations (Meselhe & Rodrigue, 2013) with adjustments to accommodate the fact that the ICM utilizes a one-dimensional hydrodynamic model at a relatively course spatial resolution. To evaluate the level of agreement between the model results and field observations, time-series plots were generated following each model run for all compartments that contained observed data points for all model years. Initially, the level of agreement was defined as the percent of compartments that produced a RMSE of 10%-20%. However, due to water level values oscillating around 0.0 m NAVD88, this proved to be an inaccurate model statistic in assessing model performance. Fit was then defined as the percent of compartments that produced a bias of less than 0.15 m in the daily mean water level prediction. The magnitude of this bias corresponds approximately to the error in the underlying topographic DEM used in this analysis, which varies

from a RMSE of 0.07 to 0.3 m (see Attachment C3-27: Landscape Data for a discussion of this error). Link capacity and roughness were adjusted if the observed stage signal and amplitude were not in satisfactory agreement with the model results. If the modeled stage was being under-predicted, then the capacity was reduced or the roughness was increased. If the model stage was being over-predicted, then the capacity was increased or the roughness was decreased. Due to apparent datum inconsistencies in certain observed stations (as well as clear patterns of hydraulic controls influencing observed water levels); certain observed data were excluded when assessing overall model fit. These inconsistent datasets were still used to visually compare modeled and observed hydrographs, but they were excluded from any aggregate model performance statistics provided in this report. The excluded datasets and the model performance at each of these sites are provided in Attachment C3-23.2.

2.2.2 Flow

Time-series plots and the RMSE were used to evaluate the model performance as well as assess the level of agreement between the model results and the observations. The goal was to have 80% of the stations meet the target specified in Table 2. After each model run, time-series plots were generated using a post-processing script for all compartments that contained observed data points for all model years to check the fit and see if the fit improved over time. Link capacity and roughness were adjusted if the observed flow signal and amplitude were not matched by the model. If the modeled flow was under-predicted, the capacity was increased or the roughness was decreased. If the modeled flow was over-predicted, the capacity was decreased or the roughness was increased.

2.2.3 Salinity

Time-series plots and the bias were used to evaluate the model performance and assess if the model captured the observed patterns. A goal to have 80% of the stations meet the specified performance target of 20-30% RMSE (Table 2) was set. After each model run, time-series plots were generated for all compartments containing observed data points for all model years to check the fit and to see if the fit improved over time. The level of agreement was defined as the percent of compartments that produced a bias less than 1 ppt. The combined dispersion-diffusion coefficient, *Exy*, was adjusted if the observed salinity signal and amplitude were not matched by the model. To prevent model instabilities, a minimum value of 20 was used for this coefficient. Higher *Exy* values allowed for more exchange between compartments and lower values allowed for less exchange between compartments (Meselhe et al., 2013). Many values are not model-wide but vary by compartment (or even link); all values are included in the ICM input files. In addition to adjusting the dispersion-diffusion coefficient, salinity predictions were improved by the addition of a term in the hydrodynamic code that replaced the original central-difference method used for salinity convection with a first-order upwinding scheme (Patankar, 1980). Any link that experienced a flow velocity greater than 0.5 m/s was set to use the upwinding convection scheme for the timestep(s) exceeding this threshold velocity. The velocity threshold of 0.5 m/s was chosen during calibration to represent typical river/canal flows, where upwinding is an appropriate approximation, as compared to slower estuarine/marsh flow regimes. This addition of the upwinding technique greatly increased the stability of salinity predictions. Thresholds were selected based on the team's professional experience.

2.2.4 Sediment (TSS and Sediment Accumulation)

During the calibration process, model parameters were adjusted to ensure a reasonable estimation of the sediment sources, delivery to the water body, and transport behavior within the ICM's link system. Due to the extreme limitation of both spatial and temporal observed data needed to accurately calibrate all parameters for all compartments within the model domain, this effort focused on finding general values for most parameters. The objective was to ensure model results were statistically consistent with field observations and followed expected behavior and patterns.

Sediment calibration was done after the hydrologic calibration was completed. It is sensitive to the hydrology, particularly the predicted amount and timing of flows between neighboring compartments (connected via both open water channel links and overland/marsh flow links), within compartments (exchange flow between open water and marsh), as well as the sediment deposition and resuspension characteristics (as defined by model parameters). Refer to Attachment C3-1: Sediment Distribution for a full discussion. Table 3 provides an overview of the final sediment parameter values set during this calibration procedure.

Calibration of suspended sediments (TSS) was achieved primarily by adjusting α sc, the calibration coefficient for silt and clay particles (also referred to as the non-sand coefficient). The modeled TSS was relatively insensitive to adjustments to the parameters controlling sand transport due to the relatively low quantities of suspended sand in the riverine inflow data. Therefore, default values suggested for the sand transport equations were used (Attachment C3-1: Sediment Distribution).

In addition to adjusting the model parameter values, four other adjustments were made to the model code, with respect to sediment distribution. First, an initial source of bed sediments available for resuspension was defined at the open water bed boundary layer. Some knowledge of the bed depth and sediment characteristics of the open water bed was required; however, field data were limited during this calibration exercise and an assumption was made which limited the initial depth of an erodible sediment bed. The depth of the erodible sediment bed within each open water compartment was reset at the start of each model year to the calibrated value. Sediment either deposits on top of this initial bed, increasing the erodible bed depth, or it is removed from the erodible bed until the bed has completely eroded away. At the point when an open water compartment's erodible bed has a depth of zero, resuspension is deactivated; only deposition of sediment can occur within this compartment. The inorganic sediment grain size of the erodible bed was assumed to be 10% sand, 45% silt, and 45% clay. Distribution of organic sediments was not included in the hydrology subroutine, and organic content of the bed materials was therefore excluded from the modeled erodible bed.

The second adjustment made also dealt with deactivating the resuspension portion of the code. This was required due to the relatively rudimentary wave equations included in the hydrodynamic subroutine and the subsequent sensitivity of calculated TSS during energetic wave conditions. If the suspended concentration of an individual grain size class (e.g., sand, silt, clay, or floc) within an open water compartment is at or above 250 mg/L, only deposition of that grain size class is permitted to take place; resuspension of the bed is deactivated for the timestep for that grain size class.

The third adjustment included a new compartment-specific flag that allowed for deposition to be deactivated. This addition was important for accurate transferal of suspended sediments through the main stem of the Atchafalaya River. Due to the compartmentalization (and therefore simplification) of the actual channel geometries, the long reach of the Atchafalaya

River resulted in large deposits of sediment along the river, which in turn resulted in minimal sediment reaching the Wax Lake and Atchafalaya deltas. By reducing the number of main stem compartments that were allowed to receive sediment deposits, the ICM more accurately predicted the land building dynamics that are currently taking place in these areas. It should be noted that the ICM does not incorporate any dredging operations; the frequent dredging and maintenance of shipping channels further supports the limitation of sediment deposition in the model in these regions.

The first three adjustments discussed above generally dealt with calculations of suspended sediments and the deposition or resuspension of bed sediments within the open water areas of the model. The fourth adjustment made, however, dealt with the deposition of suspended sediments on the marsh surface. Suspended sediments in the water column were allowed to deposit on the marsh surface only if the marsh surface is inundated. The original attributes of the marsh portion of the compartment only defined the mean surface elevation of the marsh area. It was determined that using the mean elevation to initiate exchange flow resulted in an under-prediction of marsh sediment accumulation, due to the fact that no low-lying marsh areas were being inundated. To correct for this, an elevation adjustment was applied in the model that resulted in marsh exchange flow occurring at an elevation lower than the mean marsh elevation. The magnitude of this marsh elevation adjustment ranged from 0 to -0.6 m and varied spatially; however, the majority of the model domain initiated marsh exchange flow at an elevation adjustment of 0.4 m below the mean marsh elevation. This default value of -0.4 m was chosen based on a geospatial analysis that determined the median and mean of the standard deviation of marsh elevation across all model compartments was 0.32 m and 0.46 m, respectively. The default marsh elevation adjustment of -0.4 m therefore represents a condition in which exchange flow between the open water and marsh components of a compartment occurs when the water surface is at an elevation approximately one standard deviation below the mean marsh elevation. The ability to spatially adjust the inundation signal improved the model's ability to model inorganic sediment accumulation on the marsh surface.

Table 3: Sediment Parameter Values Set During Calibration. Refer to Attachment C3-1: Sediment Distribution for a full description of model parameters.

Parameter	**Definition**	**Recommended Values and Ranges**
CSS_{max}	CSS concentration threshold for bed resuspension (g/m^3)	250.0
D_{50}	Median particle diameters (m)	0.001 for sand, 0.00003 for silt, and 0.000001 for clay
n	Calibration exponent constant for silt and clay particles resuspension	1
α_{sc}	Calibration coefficient for silt and clay particles resuspension ($\alpha_{sc} = \frac{a_c}{T_{res}T_{con}{}^m}$)	$1e^{-9}$ global, $1e^{-7}$ on Chenier Plain

Parameter	Definition	Recommended Values and Ranges
dH_{marsh}	Marsh bed elevation adjustment (m)	0 - -0.6[8]
a_s	Sand particles resuspension coefficient	0.008
C_f	Bed shear stress coefficient	0.001
k_a	Wind-induced circulation current coefficient	0.023
C_1	Flocculation coefficient	0.1
C_3	Flocculation coefficient	4.38
$P_{floc, max}$	Upper limit to the fraction able to flocculate	0.5
erBedDepth	Depth of erodible bed in open water area (m)	0.01 – 0.05

2.2.5 Water Quality

Time-series plots and the RMSE were used to evaluate the model performance and assess its level of agreement with observations of temperature, TKN, and total phosphorus. It was found that water quality variable concentrations at the inflow tributaries were crucial in determining their distribution and fluctuation in the simulation domain. Due to the lack of continuous data at the boundaries, the water quality calibration focused on optimizing input time-series and finding general parameter values to ensure model results were statistically consistent with field observations and followed expected behavior and patterns.

2.3 Results

Model results for stage, flow, salinity, water temperature, TKN, and total phosphorus were plotted against field observations at several locations across the modeling area for both calibration (2010-2013) and validation (2006-2009) periods. Due to the large number of graphical plots, example calibration and validation results for only a few selected observation sites are shown in this section (Figures 6 – 34). A summary of the error across all sites is provided in Tables 4 and 5. The complete set of calibration and validation graphics as well as performance statistics (RMSE, absolute error/bias, R-squared) from model-to-observed comparisons at various timesteps for each of the calibration and validation sites are provided in Attachments C3-23.2, C3-23.3, C3-23.4, C3-23.5, C3-23.6, C3-23.7 and C3-23.8 and can be found online at http://coastal.la.gov/a-common-vision/2017-master-plan-update/technical-analysis/modeling/. A map of the ICM compartments is provided in Attachment C3-22: ICM Development.

[8] Global adjustment of -0.4; -0.6 on Mississippi River Delta; 0 on some compartments in the upper Atchafalaya Basin due to instability issues.

Table 4: Calibration Period (2010-2013) Mean Model Performance Statistics - Statistics are Aggregated Across All Model-Observed Pairs.

		No. Stns	Mean		Median		Standard Deviation		Root Mean Square Error			
Parameter	units		*Obs*	*Pred*	*Obs*	*Pred*	*Obs*	*Pred*	*Daily*	*2 week*	*Monthly*	*Annual*
Stage	m	*204*	0.24	0.24	0.24	0.24	0.17	0.14	0.12	0.10	0.10	0.08
Flow rate	m^3/s	*14*	968	1031	911	984	656	684	221	208	124	157
Salinity (0-1 ppt)	ppt	*55*	0.4	0.5	0.2	0.3	0.4	0.4	0.6	0.48	0.4	0.3
Salinity (1-5 ppt)	ppt	*51*	2.8	3.2	2.2	2.4	2.1	2.4	2.4	2.2	2.1	1.2
Salinity (5-20 ppt)	ppt	*74*	11.6	11.2	11.2	10.9	5.0	4.4	4.4	3.9	3.7	2.1
Salinity (>20 ppt)	ppt	*4*	22.0	23.8	21.8	24.4	6.2	3.9	6.4	5.84	5.6	4.0
TSS	mg/L	*146*	41	24	32	23	31	13	-	-	22	-
Temperature	mg/L	*144*	21.7	21.4	22.6	21.7	7.2	6.4	-	-	1.8	-
Total Kjeldahl N	mg/L	*144*	0.9	0.5	0.9	0.5	0.4	0.1	-	-	0.3	-
Total P	mg/L	*143*	0.2	0.1	0.2	0.1	0.3	0.0	-	-	0.2	-

Table 5: Validation Period (2006-2009) Mean Model Performance Statistics - Statistics are Aggregated Across All Model-Observed Paris.

		No. Stns	**Mean**		**Median**		**Standard Deviation**		**Root Mean Square Error**			
Parameter	*units*		*Obs*	*Pred*	*Obs*	*Pred*	*Obs*	*Pred*	*Daily*	*2 week*	*Monthly*	*Annual*
Stage	*m*	*204*	0.24	0.27	0.23	0.26	0.18	0.15	0.14	0.12	0.09	0.07
Flow rate	m^3/s	*14*	1088	1163	1042	1112	525	523	229	214	122	151
Salinity (0-1 ppt)	*ppt*	*47*	0.4	0.5	0.2	0.3	0.4	0.5	0.8	0.6	0.4	0.5
Salinity (1-5 ppt)	*ppt*	*59*	3.3	3.8	2.7	3.2	2.2	2.5	3.1	2.9	2.2	1.9
Salinity (5-20 ppt)	*ppt*	*74*	11.3	11.7	10.9	11.6	4.4	3.9	5.0	4.8	3.7	3.1
Salinity (>20 ppt)	*ppt*	*4*	21.7	23.8	22.0	24.3	5.4	3.1	6.6	6.0	4.2	3.2
TSS	*mg/L*	*148*	41.0	23.6	31.3	22.6	31.7	11.6	-	-	20.2	-
Temperature	*mg/L*	*145*	22.2	21.3	22.9	21.0	6.7	6.2	-	-	1.7	-
Total Kjeldahl N	*mg/L*	*145*	0.9	0.6	0.8	0.6	0.5	0.1	-	-	0.3	-
Total P	*mg/L*	*145*	0.2	0.1	0.2	0.0	0.1	0.0	-	-	0.1	-

2.3.1 Stage

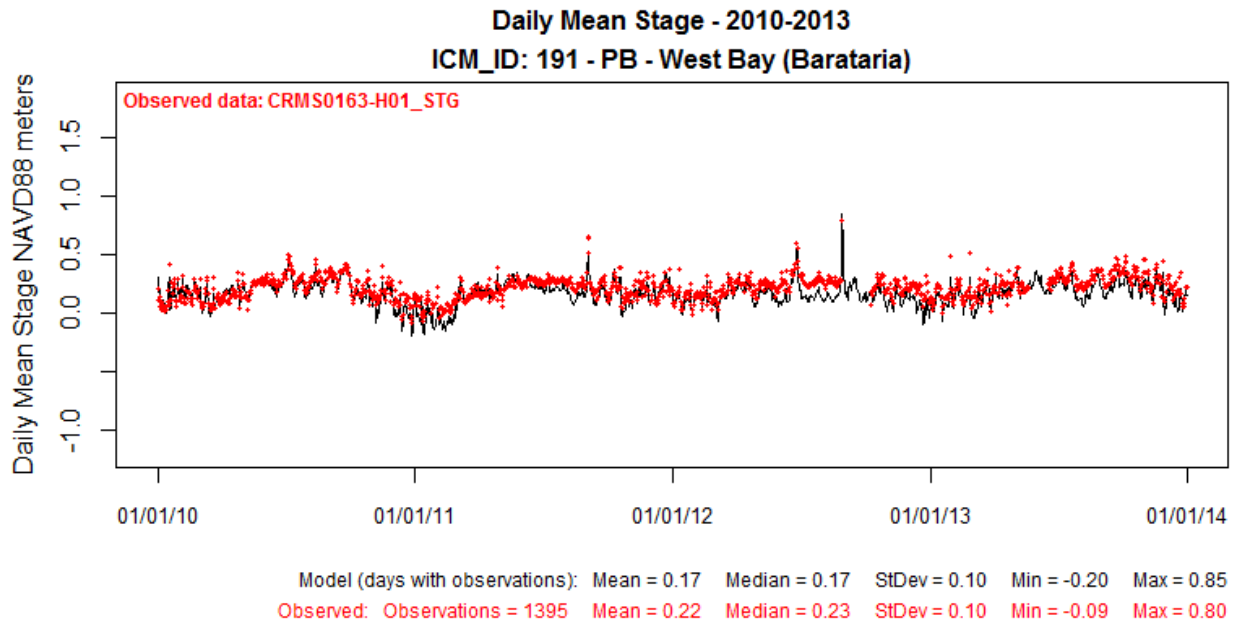

Figure 6: Modeled (black line) and Observed (red dot) Daily Mean Stage for ICM Compartment 191 in the Pontchartrain/Barataria Region for Calibration Period (2010-2013).

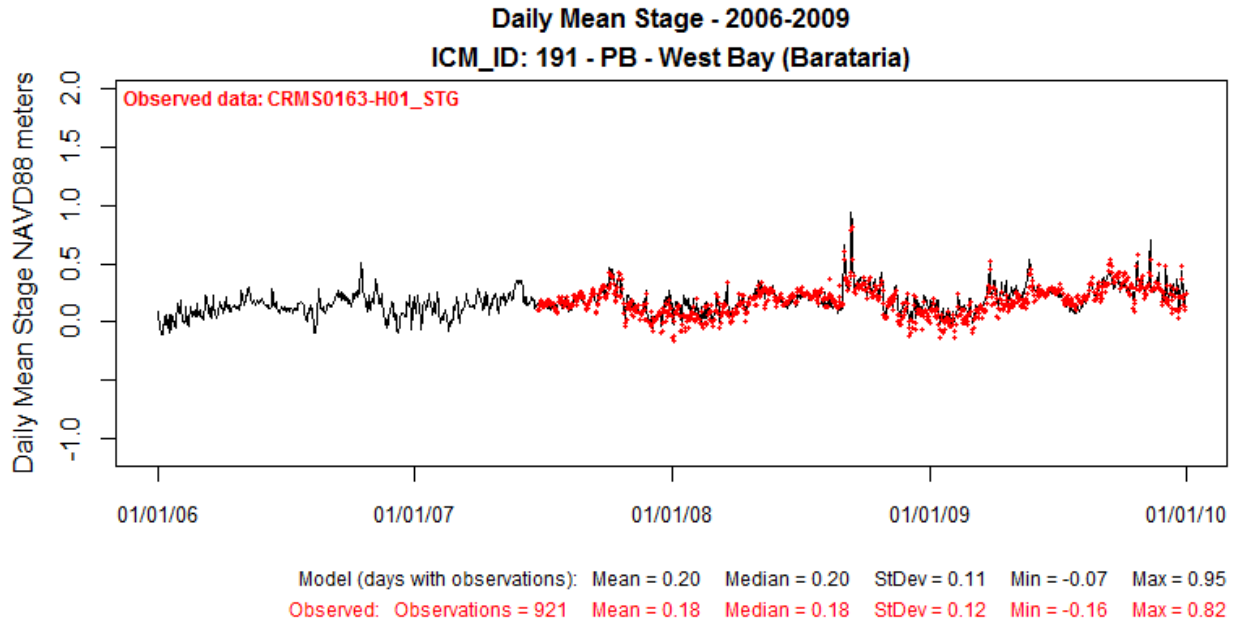

Figure 7: Modeled (black line) and Observed (red dot) Daily Mean Stage for ICM Compartment 191 in the Pontchartrain/Barataria Region for Validation Period (2006-2009).

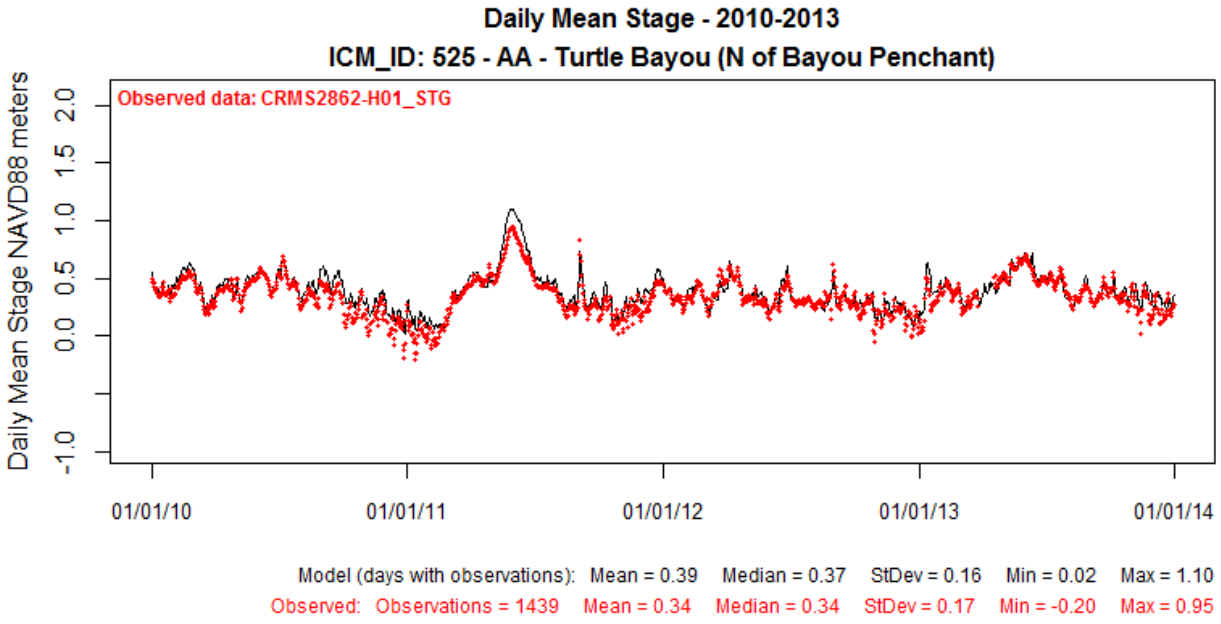

Figure 8: Modeled (black line) and Observed (red dot) Daily Mean Stage for ICM Compartment 525 in the Atchafalaya Region for Calibration Period (2010-2013).

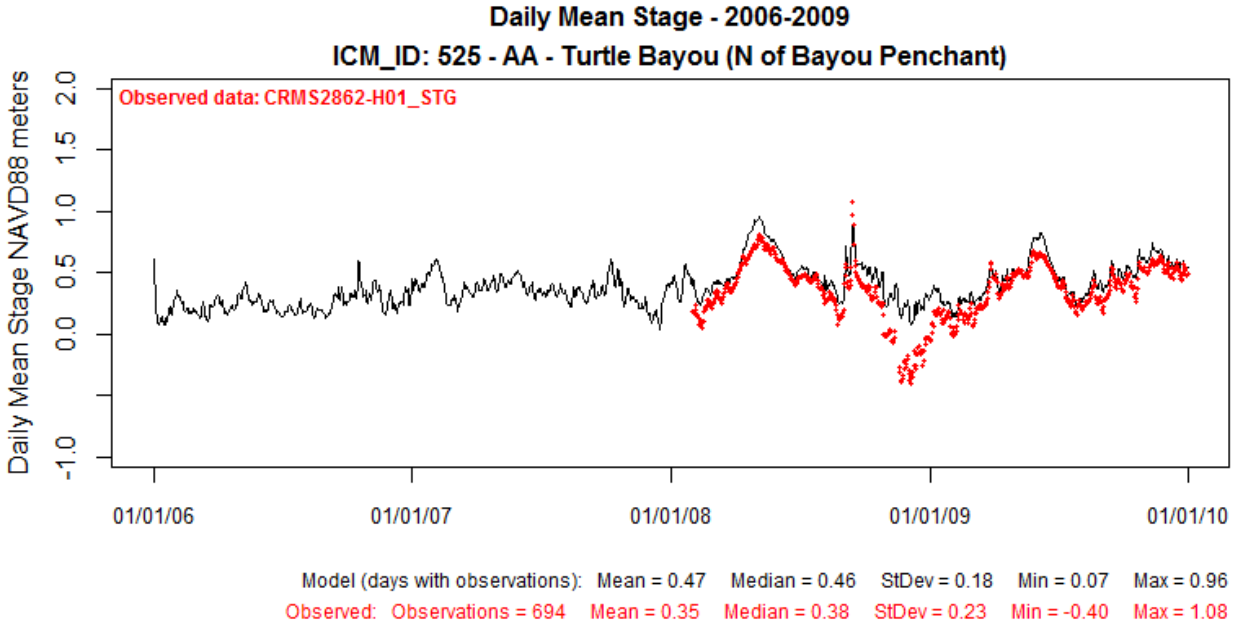

Figure 9: Modeled (black line) and Observed (red dot) Daily Mean Stage for ICM Compartment 525 in the Atchafalaya Region for Validation Period (2006-2009).

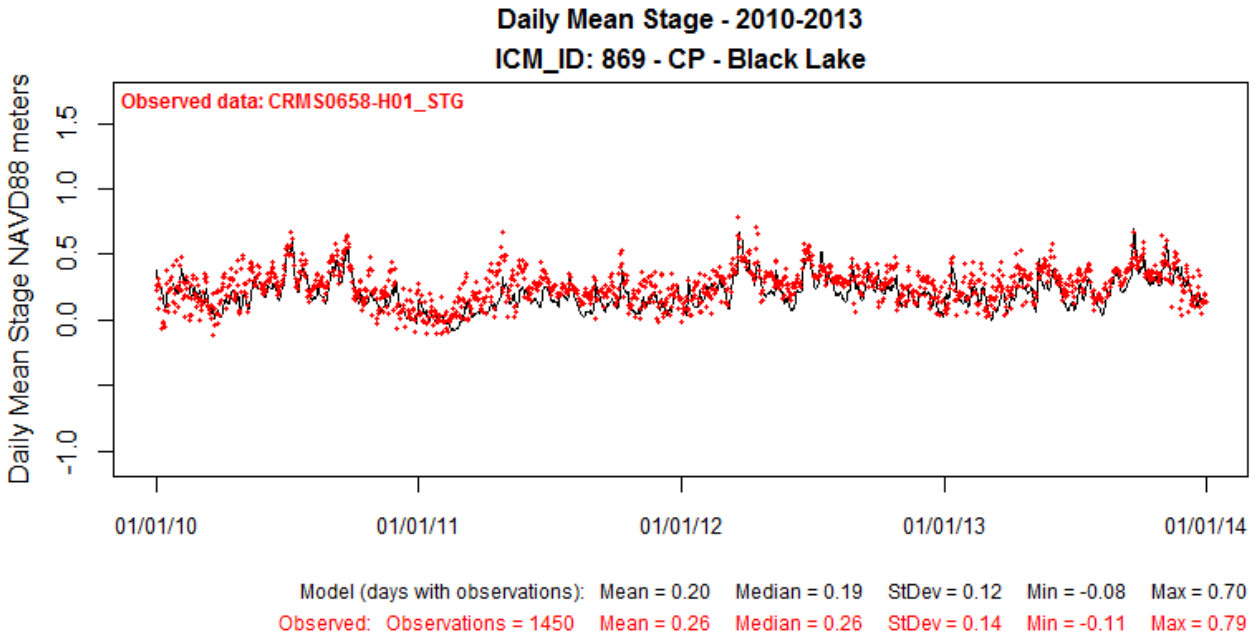

Figure 10: Modeled (black line) and Observed (red dot) Daily Mean Stage for ICM Compartment 869 in the Chenier Plain Region for Calibration Period (2010-2013).

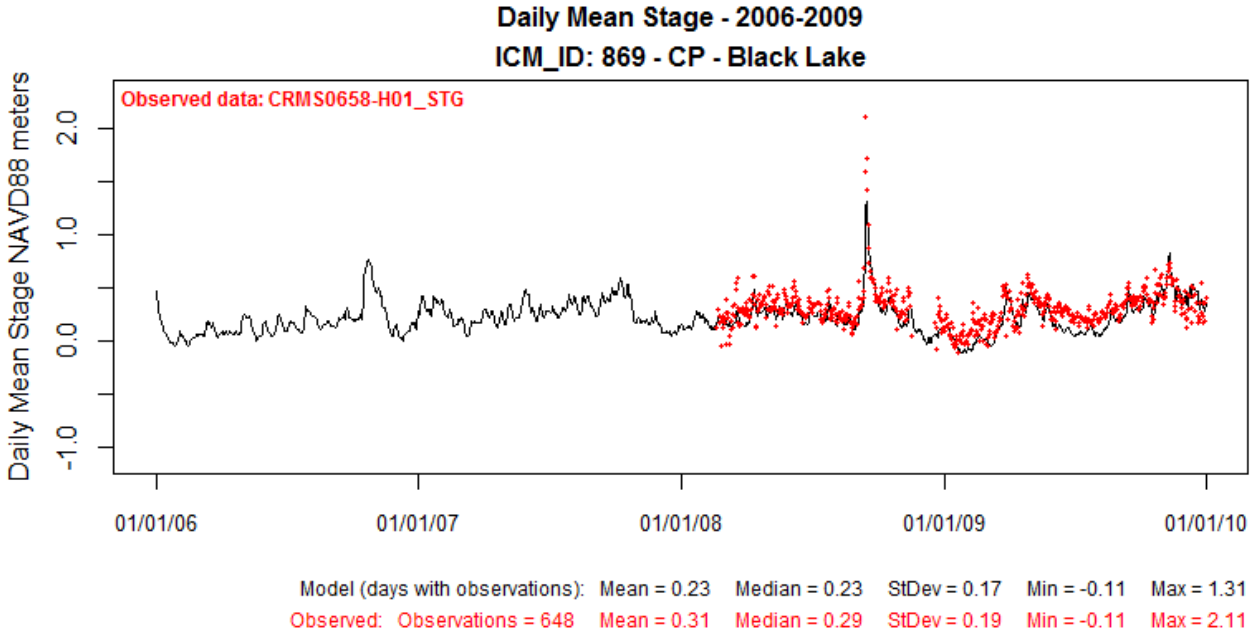

Figure 11: Modeled (black line) and Observed (red dot) Daily Mean Stage for ICM Compartment 869 in the Chenier Plain Region for Validation Period (2006-2009).

2.3.1 Flow

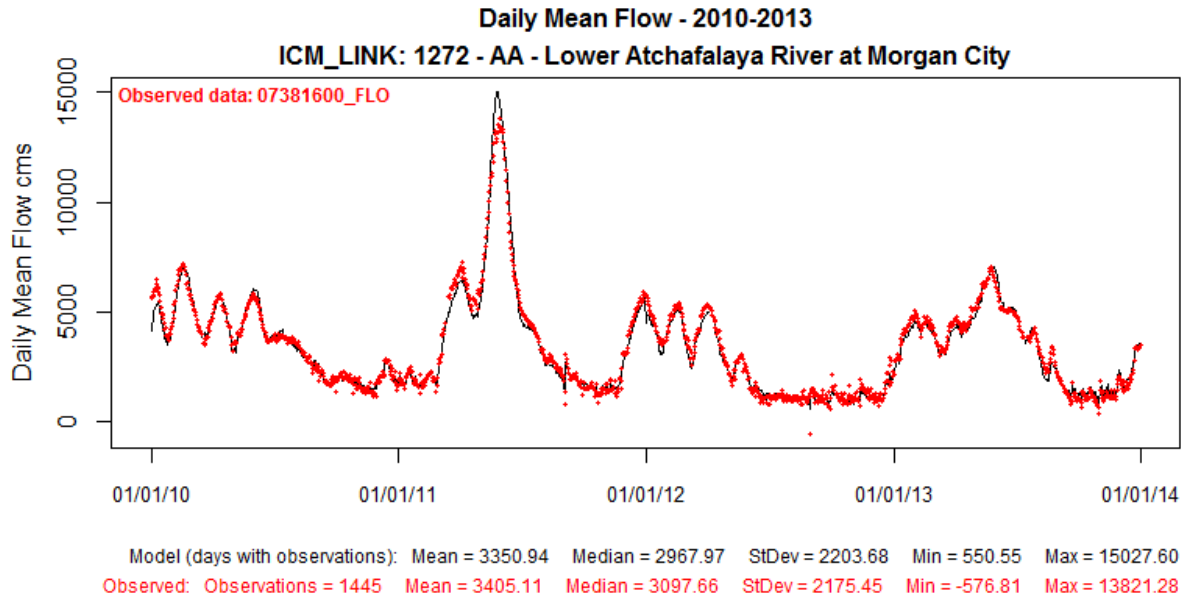

Figure 12: Modeled (black line) and Observed (red dot) Daily Mean Flow (cms) for ICM Link 1272 in the Atchafalaya Region for Calibration Period (2010-2013).

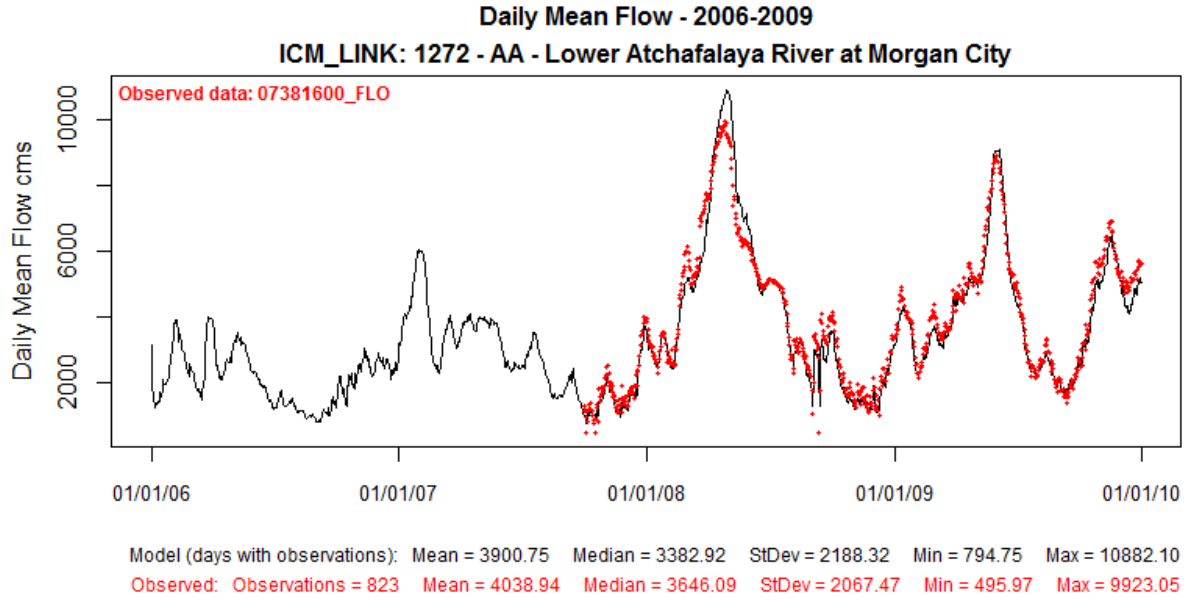

Figure 13: Modeled (black line) and Observed (red dot) Daily Mean Flow (cms) for ICM Link 1272 in the Atchafalaya Region for Validation Period (2006-2009).

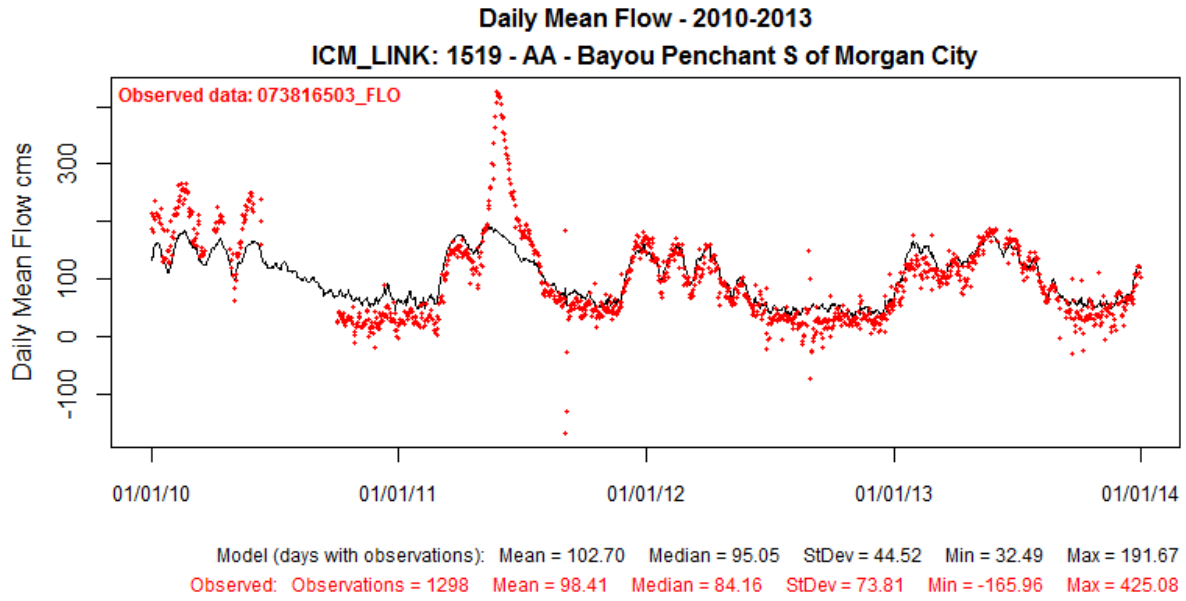

Figure 14: Modeled (black line) and Observed (red dot) Daily Mean Flow (cms) for ICM Link 1519 in the Atchafalaya Region for Calibration Period (2010-2013).

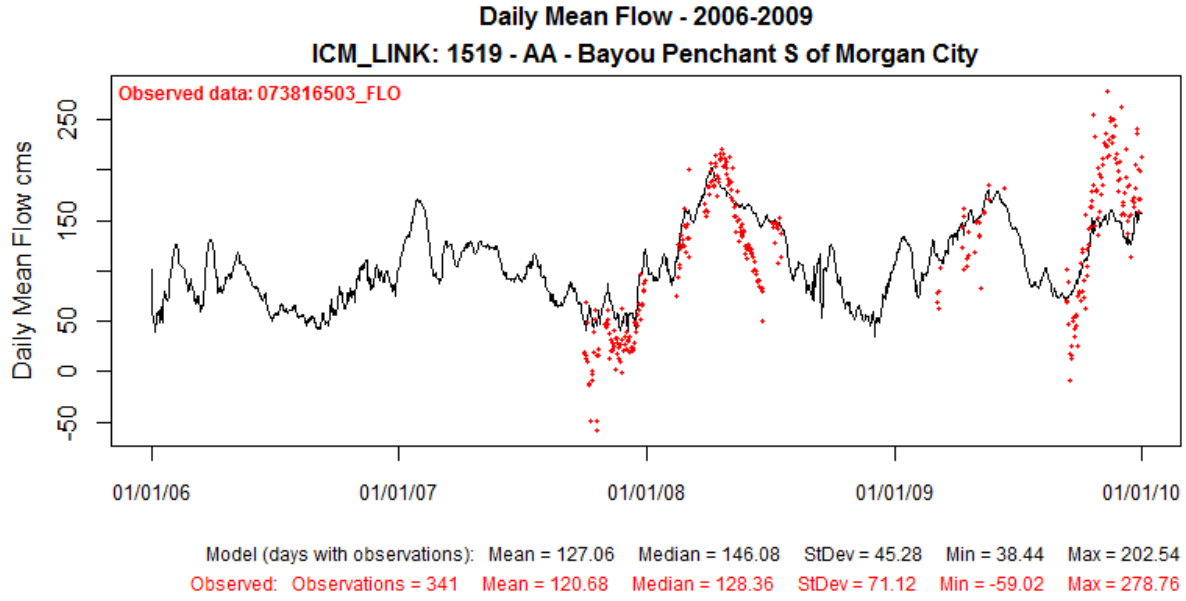

Figure 15: Modeled (black line) and Observed (red dot) Daily Mean Flow (cms) for ICM Link 1519 in the Atchafalaya Region for Validation Period (2006-2009).

2.3.2 Salinity

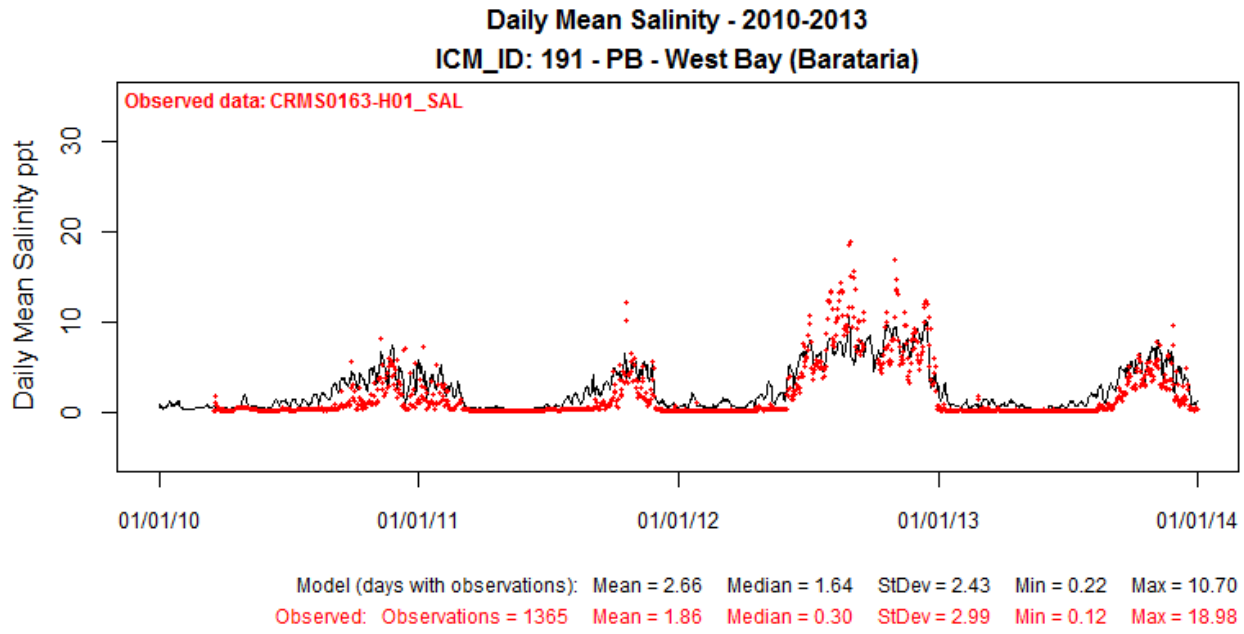

Figure 16: Modeled (black line) and Observed (red dot) Daily Mean Salinity for ICM Compartment 191 in the Pontchartrain/Barataria Region for Calibration Period (2010-2013).

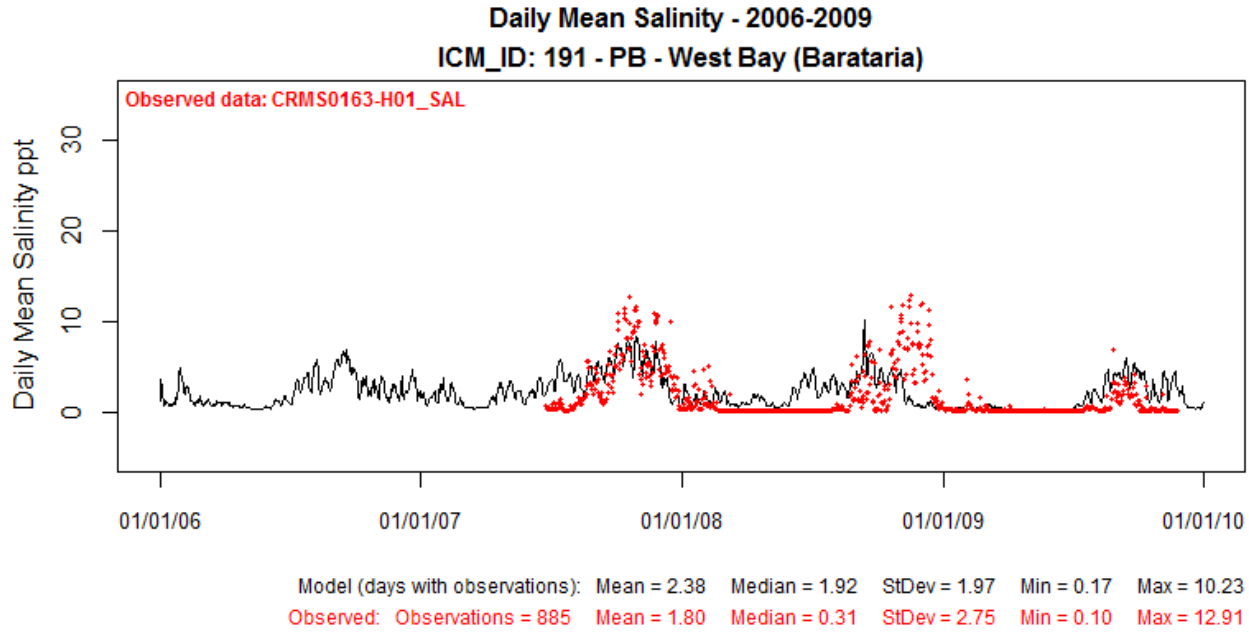

Figure 17: Modeled (black line) and Observed (red dot) Daily Mean Salinity for ICM Compartment 191 in the Pontchartrain/Barataria Region for Validation Period (2006-2009).

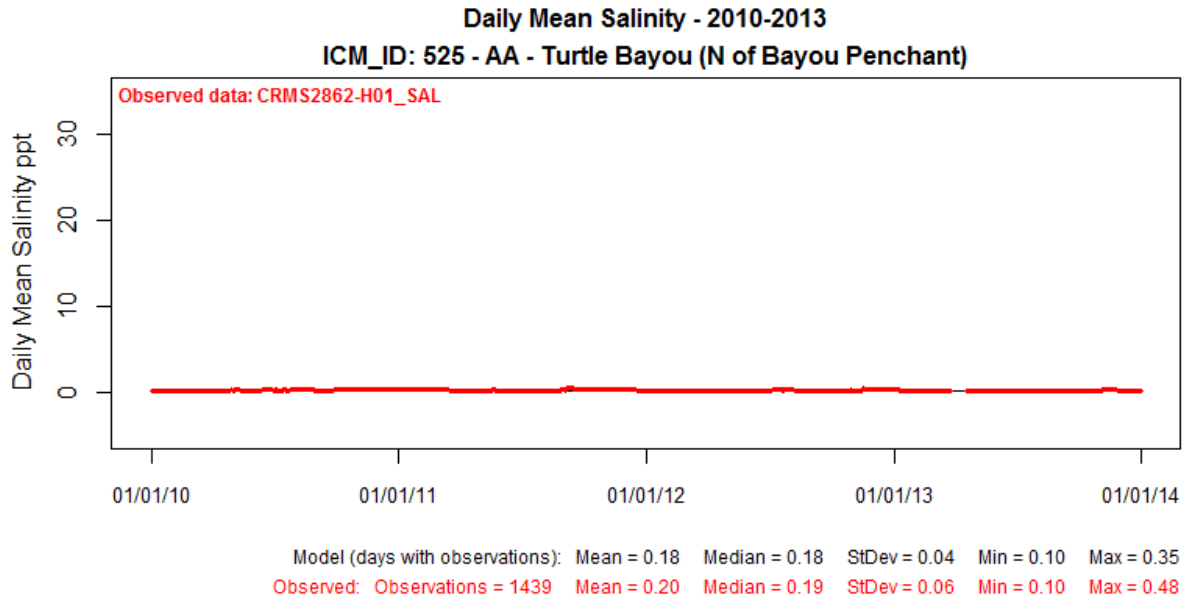

Figure 18: Modeled (black line) and Observed (red dot) Daily Mean Salinity for ICM Compartment 525 in the Atchafalaya Region for Calibration Period (2010-2013).

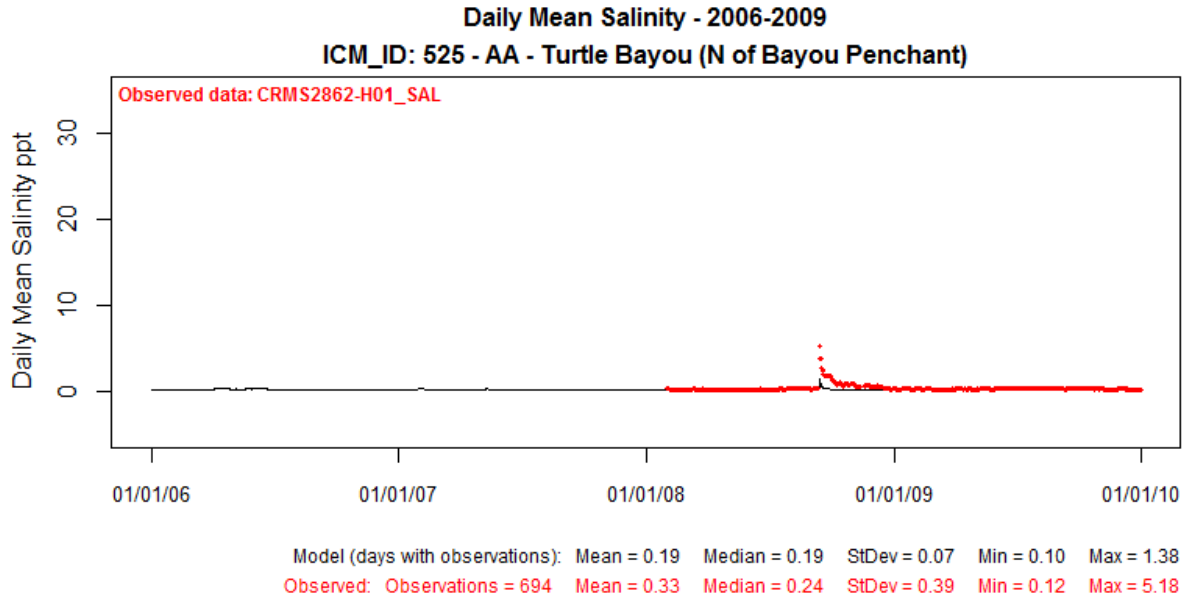

Figure 19: Modeled (black line) and Observed (red dot) Daily Mean Salinity for ICM Compartment 525 in the Atchafalaya region for Validation Period (2006-2009).

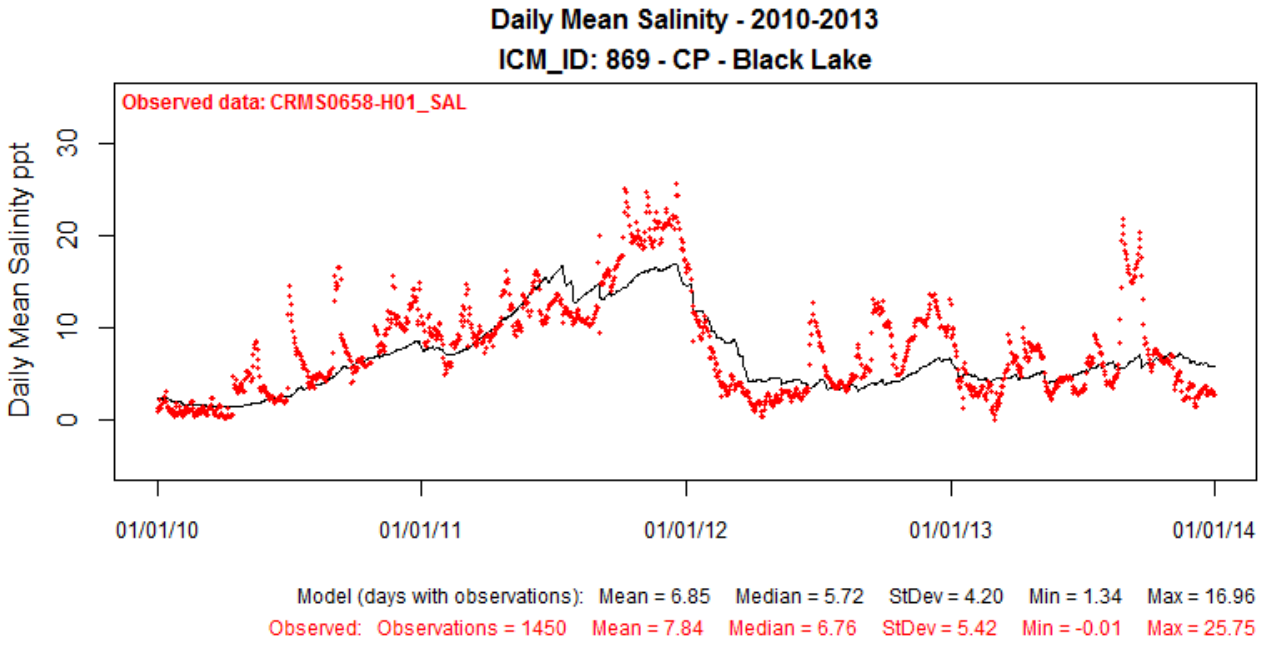

Figure 20: Modeled (black line) and Observed (red dot) Daily Mean Salinity for ICM Compartment 869 in the Chenier Plain Region for Calibration Period (2010-2013).

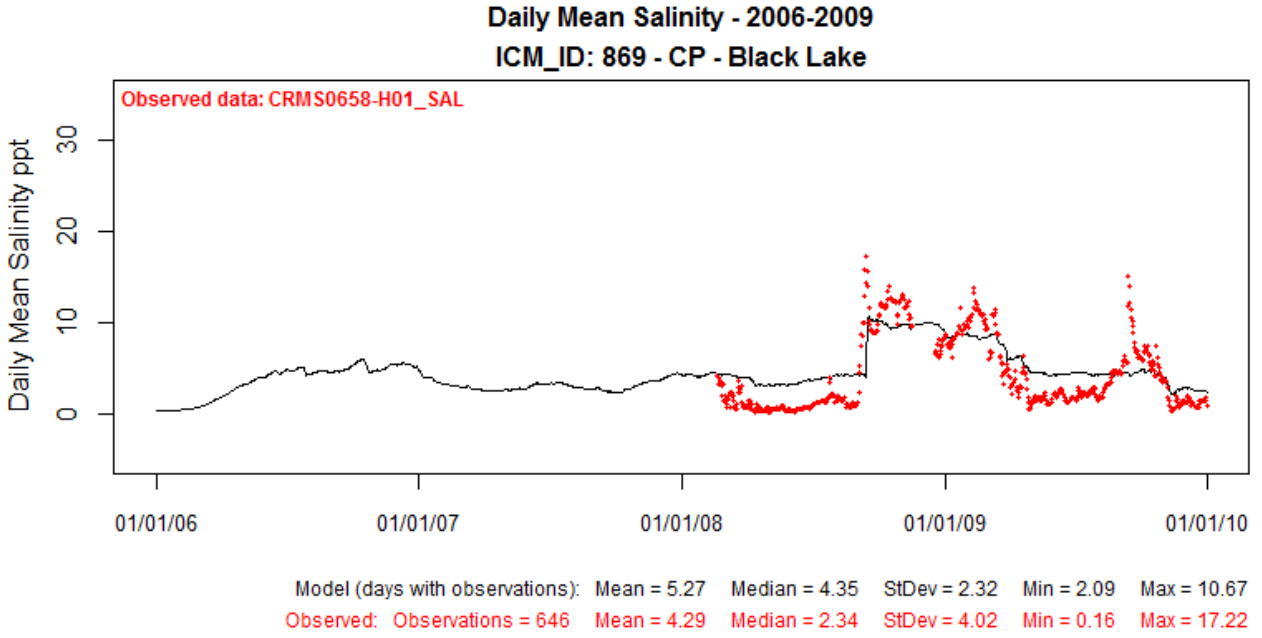

Figure 21: Modeled (black line) and Observed (red dot) Daily Mean Salinity for ICM Compartment 869 in the Chenier Plain Region for Validation Period (2006-2009).

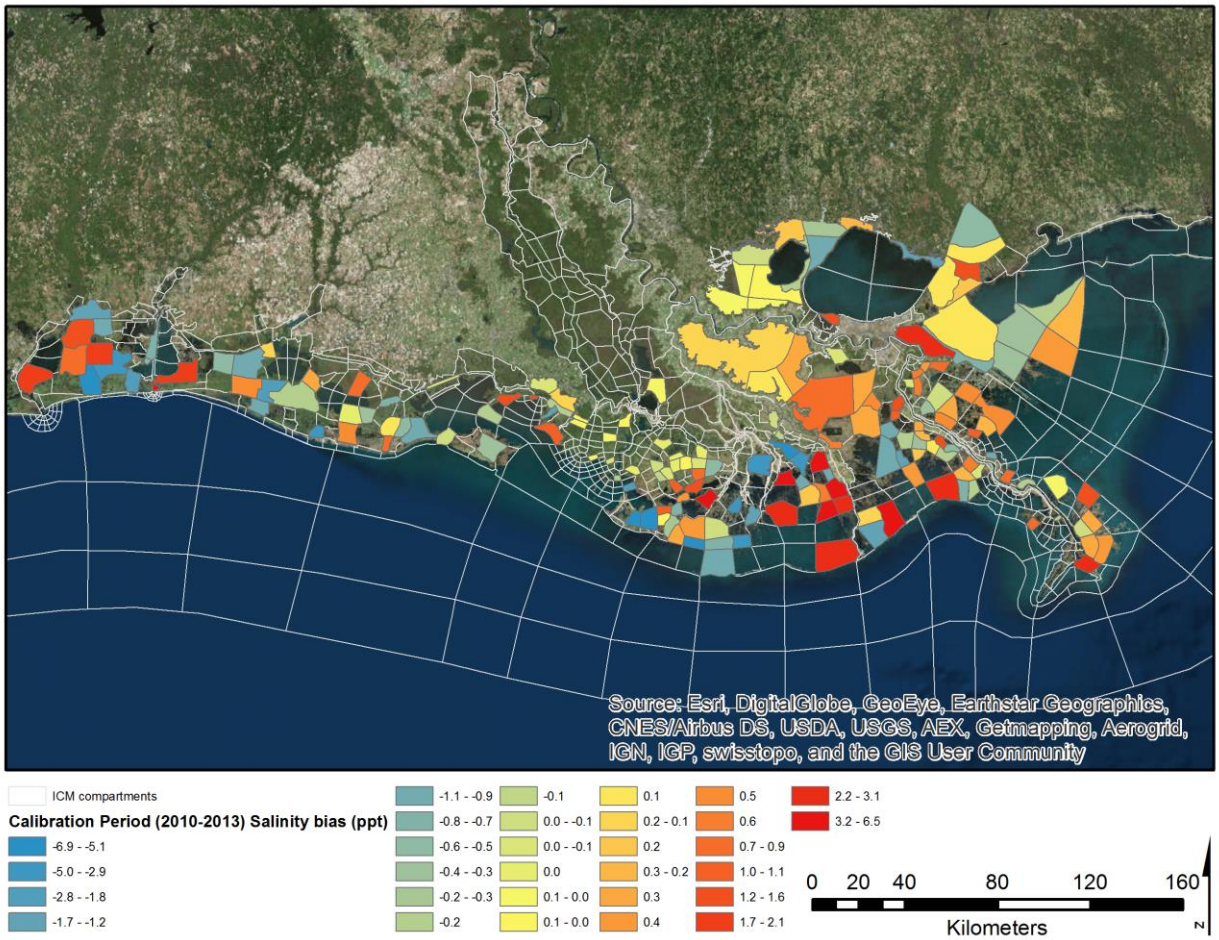

Figure 22: Map of Salinity Bias Terms from Calibration Period. Cool colors (blues) indicate the model tended to under-predict salinity (negative bias), warm colors (reds) indicate the model tended to over-predict salinity (positive bias).

2.3.3 Sediment

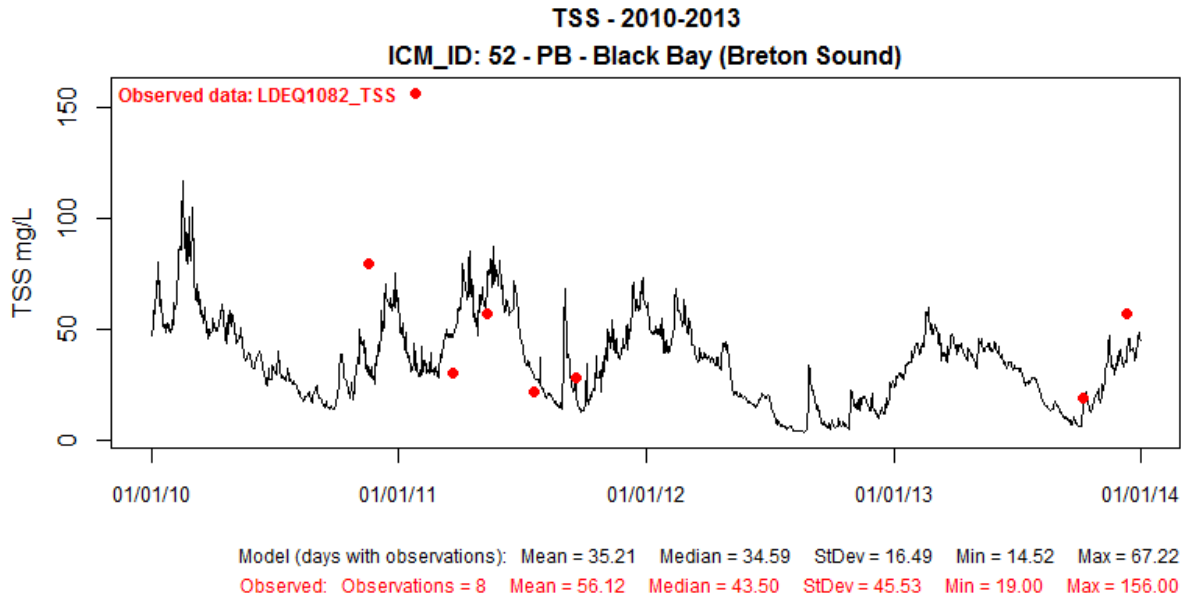

Figure 23: Modeled Daily Mean Inorganic Suspended Solids (black line) and Observed Total Suspended Solids (red dot) for ICM Compartment 52 in the Pontchartrain/Barataria Region for Calibration Period (2010-2013).

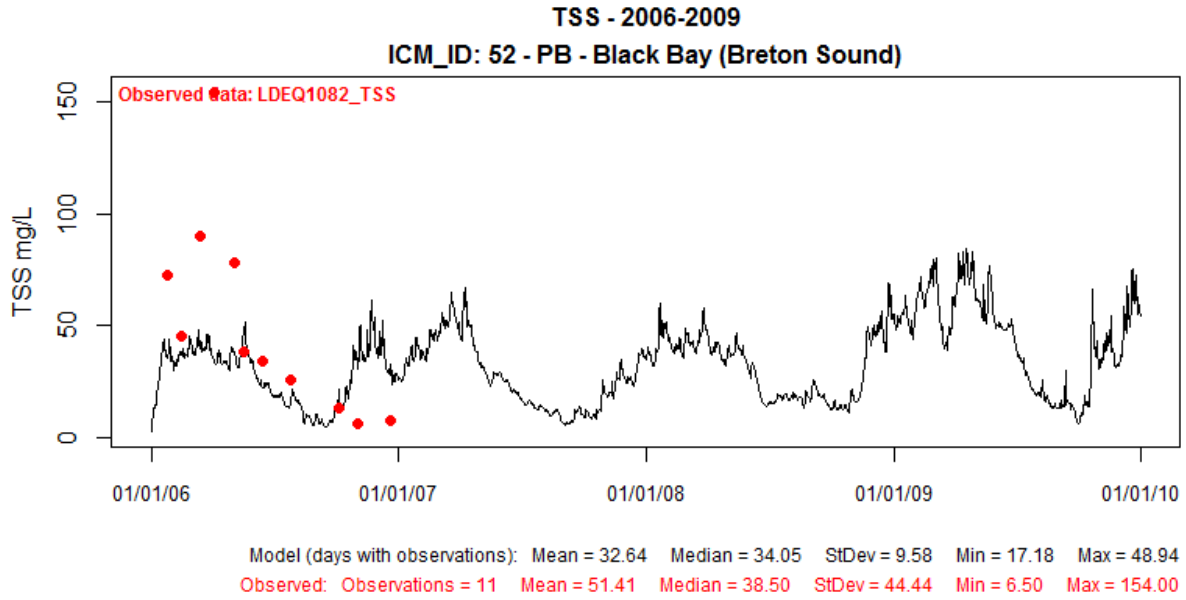

Figure 24: Modeled Daily Mean Inorganic Suspended Solids (black line) and Observed Total Suspended Solids (red dot) for ICM Compartment 52 in the Pontchartrain/Barataria Region for Validation Period (2006-2009).

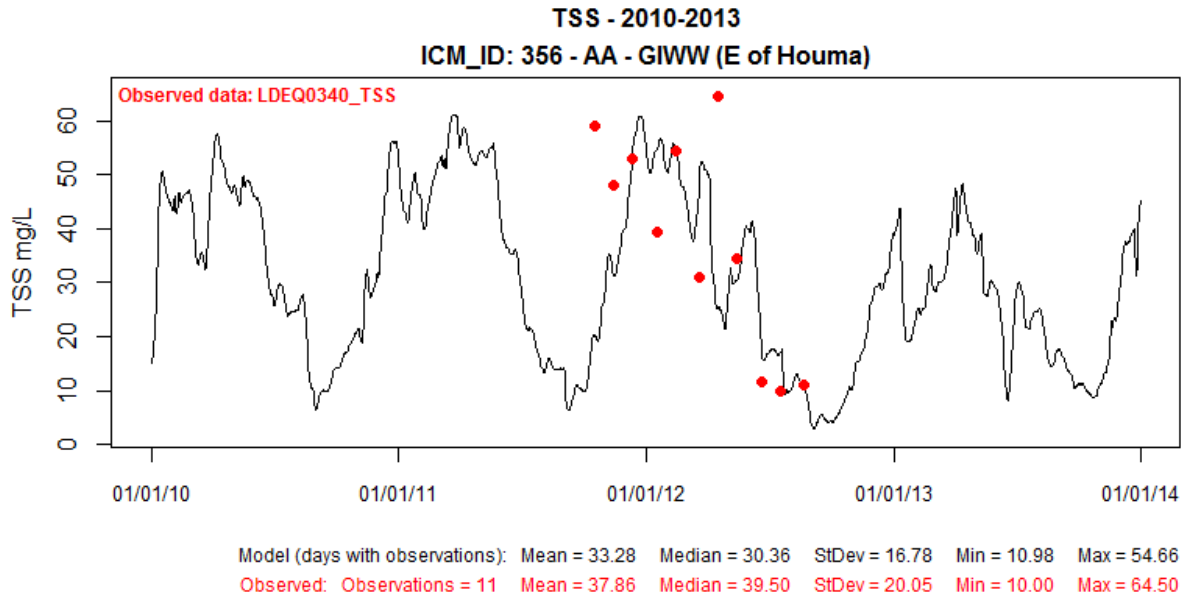

Figure 25: Modeled Daily Mean Inorganic Suspended Solids (black line) and Observed Total Suspended Solids (red dot) for ICM Compartment 356 in the Atchafalaya Region for Calibration Period (2010-2013).

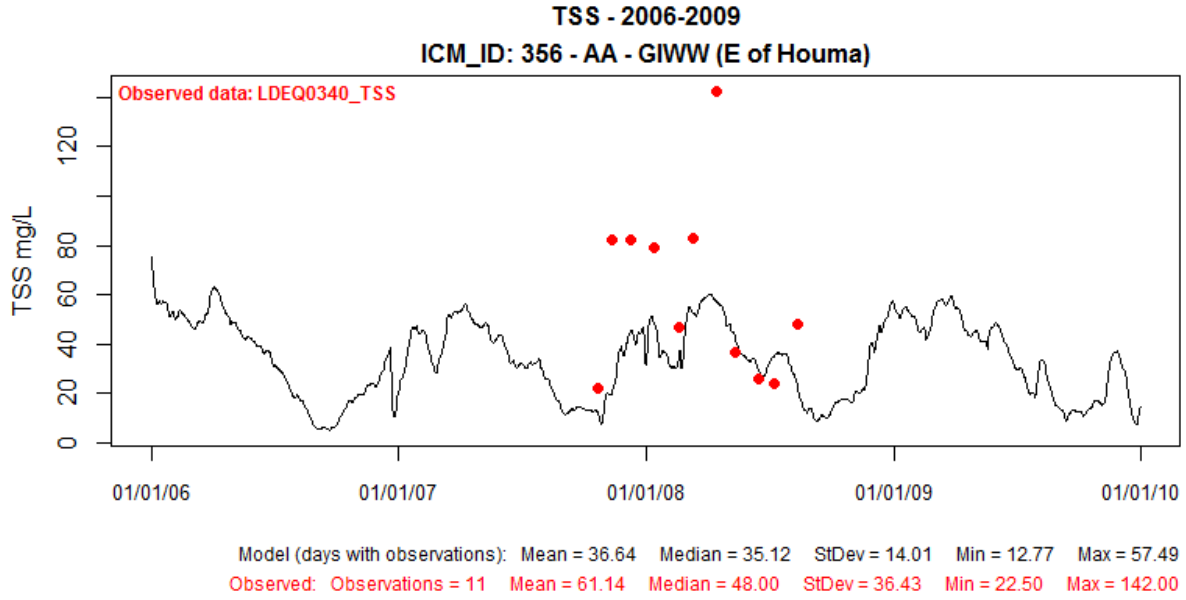

Figure 26: Modeled Daily Mean Inorganic Suspended Solids (black line) and Observed Total Suspended Solids (red dot) for ICM Compartment 356 in the Atchafalaya Region for Validation Period (2006-2009).

2.3.4 Temperature

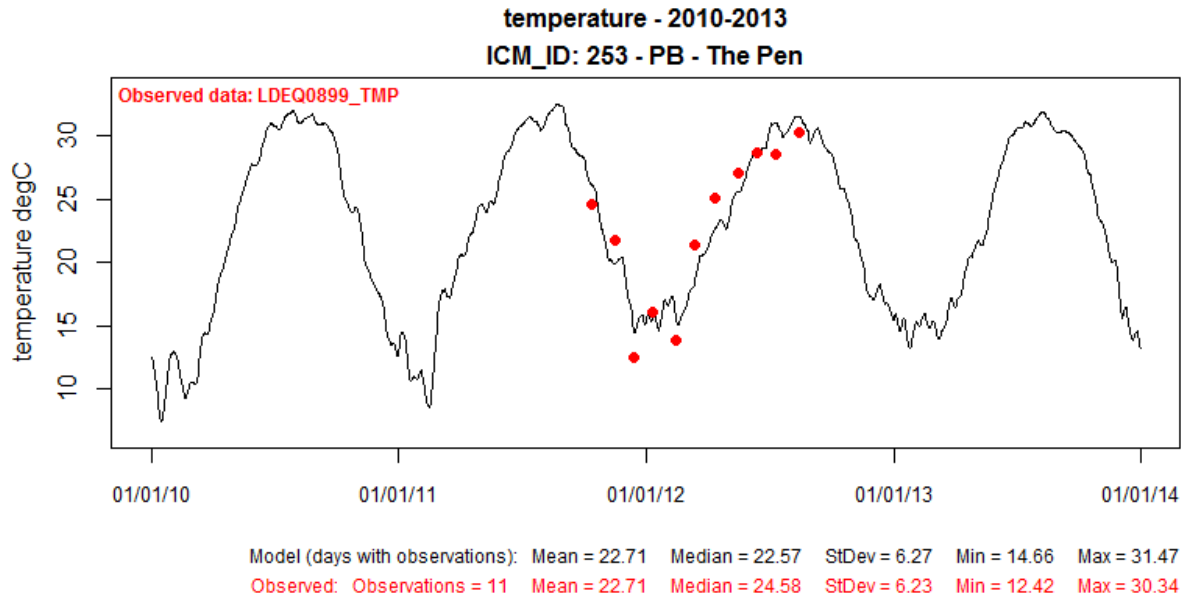

Figure 27: Modeled (black line) and Observed (red dot) Daily Mean Temperature (degrees Celsius) for ICM Compartment 253 in the Pontchartrain/Barataria Region for Calibration Period (2010-2013).

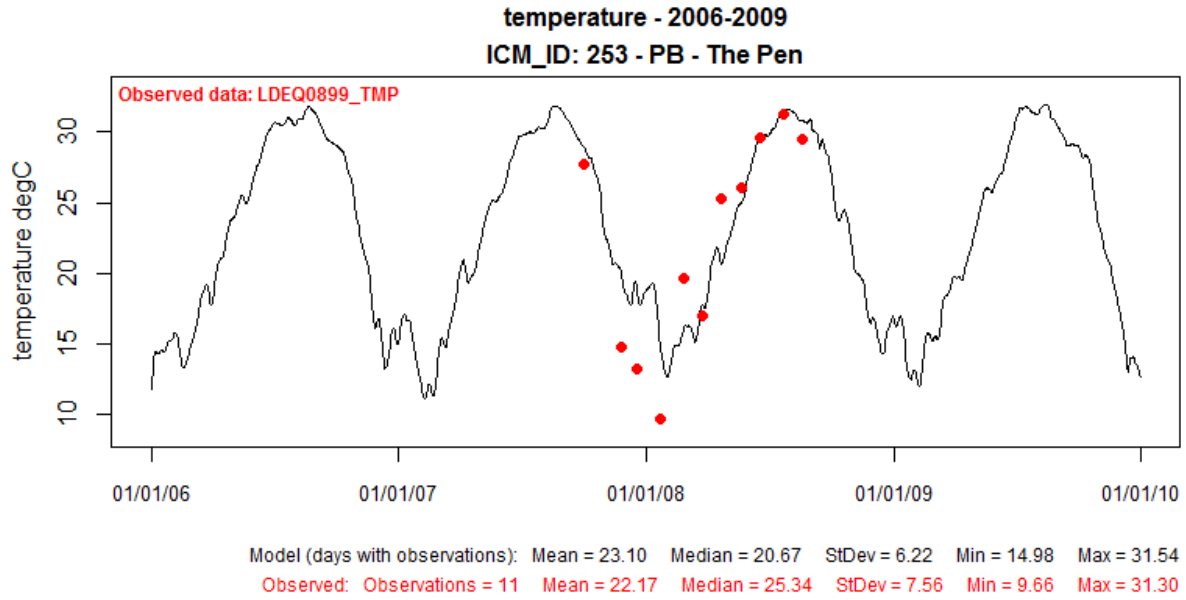

Figure 28: Modeled (black line) and Observed (red dot) Daily Mean Temperature (degrees Celsius) for ICM Compartment 253 in the Pontchartrain/Barataria Region for Validation Period (2006-2009).

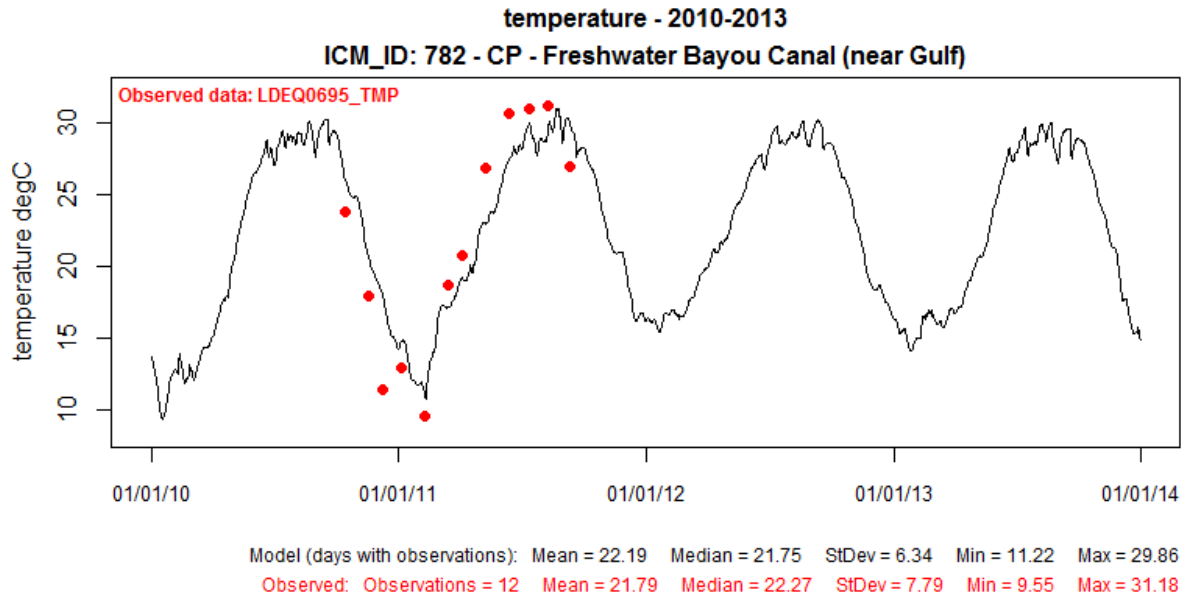

Figure 29: Modeled (black line) and Observed (red dot) Daily Mean Temperature (degrees Celsius) for ICM Compartment 782 in the Chenier Plain Region for Calibration Period (2010-2013).

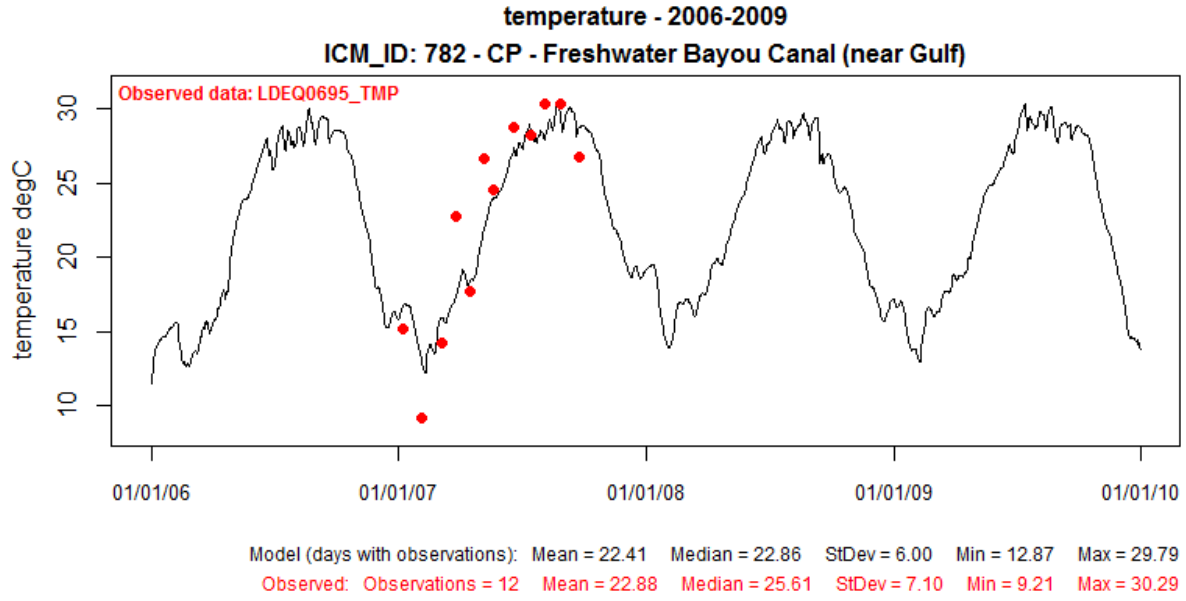

Figure 30: Modeled (black line) and Observed (red dot) Daily Mean Temperature (degrees Celsius) for ICM Compartment 782 in the Chenier Plain Region for Validation Period (2006-2009).

2.3.5 Water Quality

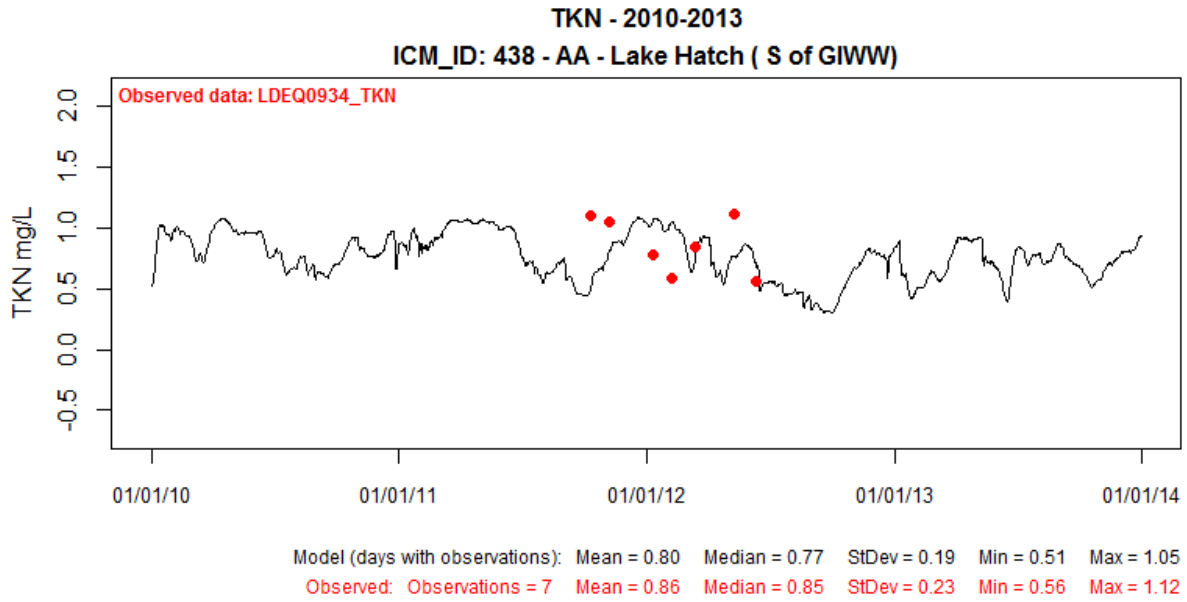

Figure 31: Modeled (black line) and Observed (red dot) Daily Mean Total Kjeldahl Nitrogen (mg/L) for ICM Compartment 438 in the Atchafalaya Region for Calibration Period (2010-2013).

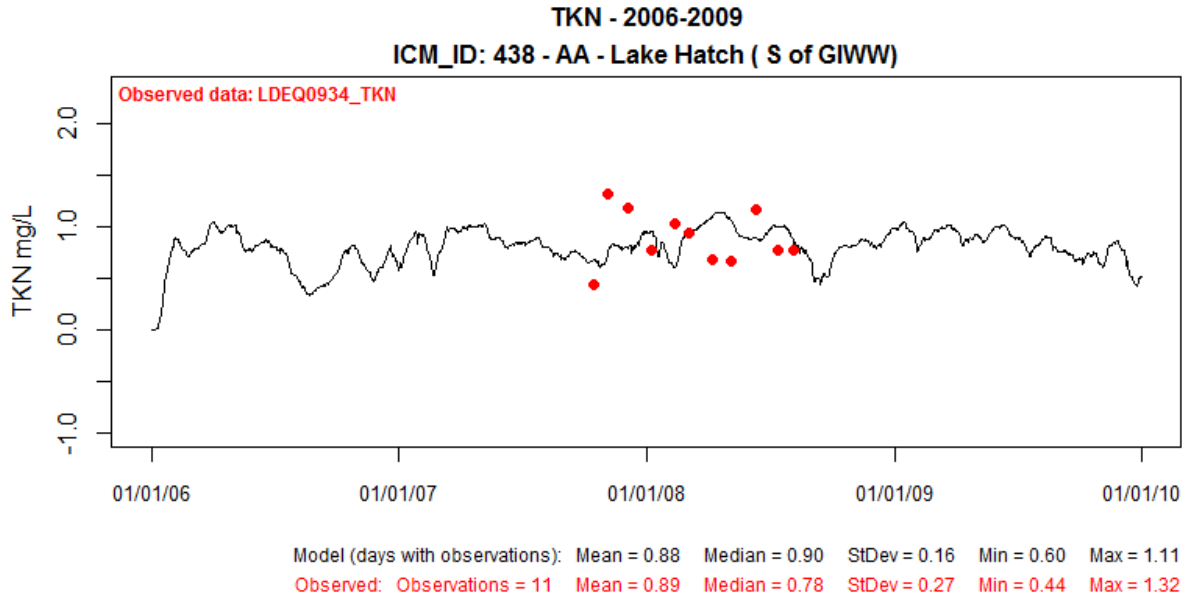

Figure 32: Modeled (black line) and Observed (red dot) Daily Mean Total Kjeldahl Nitrogen (mg/L) for ICM Compartment 438 in the Atchafalaya Region for Validation Period (2006-2009).

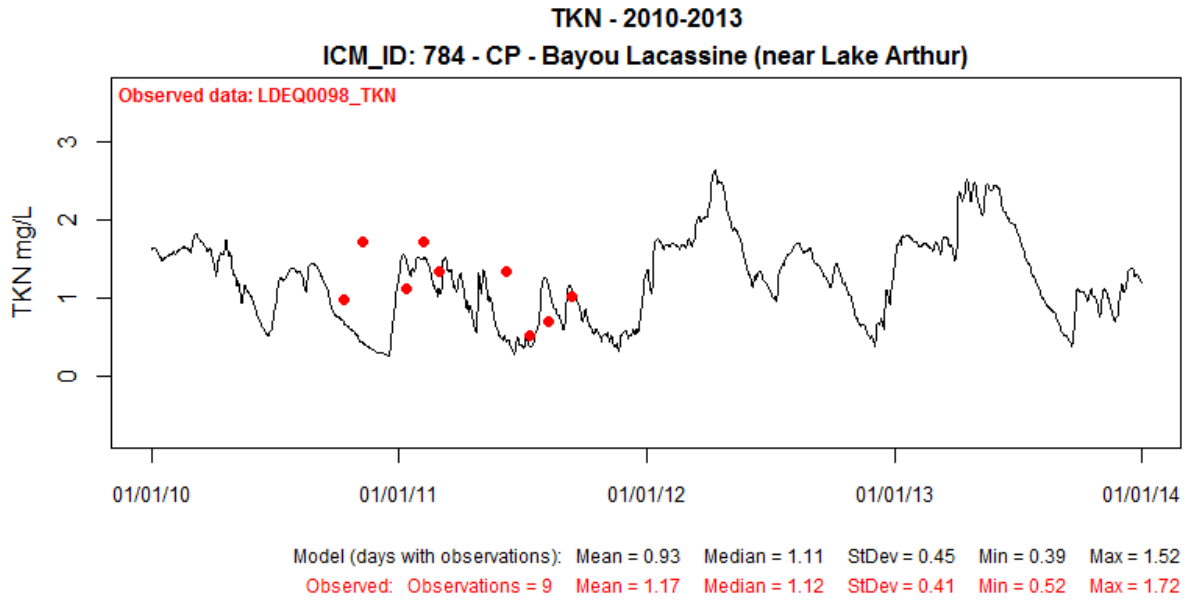

Figure 33: Modeled (black line) and Observed (red dot) Daily Mean Total Kjeldahl Nitrogen (mg/L) for ICM Compartment 842 in the Chenier Plain Region for Calibration Period (2010-2013).

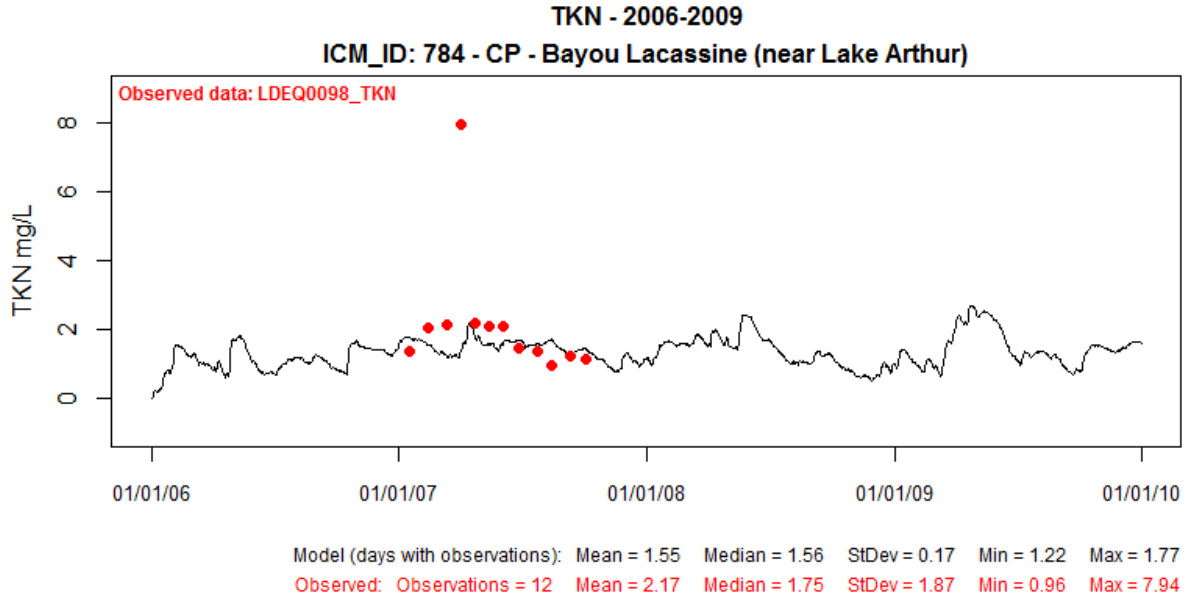

Figure 34: Modeled (black line) and Observed (red dot) Daily Mean Total Kjeldahl Nitrogen (mg/L) for ICM Compartment 842 in the Chenier Plain Region for Validation Period (2006-2009).

2.4 Discussion

2.4.1 Stage

In general, the model results show a strong agreement between the modeled and measured stage, as 99% of compartments with measured stage produced a bias of less than 0.3 m (Figures 6 – 11). Spatially, the model shows no persistent over- or under-prediction compared to the measured stage with an average bias over the model domain of 0.00 m. In areas where stage is strongly influenced by the operation of water control structures and the operation/schedule of these structures were limited or incomplete (i.e., in the Chenier Plain), the model was limited in its ability to replicate the measured stage. As the surveying of gauged elevations to a vertical datum and geoid becomes more accurate, the stages used to develop the offshore tidal boundary conditions and to compare to model results will allow for more accurate model calibrations.

The model statistics for mean stage during the validation period (Table 5) are not substantially different than during calibration, indicating that the model is capable of accurately predicting mean water level at a variety of timescales (daily through annually).

2.4.2 Flow

In general, the model results predicted measured flow well (Figures 12 – 15) as 50% of links with measured flow produced an RSME of less than 20%, and 93% of the links produced an RSME of less than 30%. The model link in the Gulf Intracoastal Waterway across the Bayou Sale Ridge near Franklin, LA, shows a consistent over-prediction compared to the measured flow at USGS 07381670. During calibration, when the link was reduced to replicate the measured flow across the ridge, the stage on the west side of the ridge no longer showed a correlation to the stages in the Wax Lake Outlet, particularly during the 2011 flood peak. The measured stages on the west side of the ridge do show a correlation to the Wax Lake Outlet; therefore, matching the stage on the west side of the ridge was used to calibrate this link rather than the measure flow. The inability of the model to capture both variables simultaneously is perhaps due to the complex flow dynamics of this area that could not be reproduced by a simplified mass-balance model.

2.4.3 Salinity

In general, the model results predicted measured salinities well (Figures 16 – 22), as 74% of compartments with measured salinity produced a bias of less than 1 ppt – with a mean bias of 0.25 ppt and -0.39 ppt for sites with mean salinities of less than 5 ppt and less than 20 ppt, respectively (Table 4). Spatially, there are areas showing a cluster of under- or over-predicted salinity; however, there were no widespread under- or over-predictions (Figure 22). For these clustered areas, the gauge(s) are located in a portion of the compartment that is not very representative of the hydrology for the majority of the compartment. Since the compartment is limited to one daily-averaged salinity value, the modeled salinity did not compare well to the measured where large spatial variation in salinity occurs at the sub-compartment scale.

The model statistics for mean salinity during the validation period (Table 5) are not substantially different than during calibration. The error does increase slightly across all timescale comparisons, indicating, that the model suffers some degree of accuracy loss when operated outside of the calibration period. However, the increase in mean error is relatively small (~ 0.5

ppt) and capable of accurately predicting mean salinity at a variety of timescales (daily through annually).

2.4.4 Sediment

Simulation results show that the model captured the general trends of TSS and sediment accumulation patterns in coastal Louisiana reasonably well (Figure 23 – 26). For a simplified, compartment model, which assumes fully mixed flow at a coarse spatial compartment resolution, the general agreement in TSS concentration is acceptable. The model performance further indicates that its ability in predicting sediment distribution in the coastal zone is adequate.

Admittedly, the hydrodynamic and sediment distribution routines are simplified as compared to more advanced modeling suites employing full representation of coastal and deltaic processes. However, the current limiting factor in increasing model performance is the paucity of suspended and bed sediment data. It was found during the calibration process that the model is largely sensitive to bed sediments available for resuspension, and simplifying assumptions were required to be made during TSS calibration. Additionally, time-series of TSS at tributary inflow boundaries are lacking at almost all of the streams and rivers at the boundaries of the ICM. Compounding the lacking boundary condition data, there were little to no continuous TSS data within the interior of the model domain at a high temporal resolution. Grab samples of TSS were the only available data to guide the calibration. It was challenging to accurately parameterize sediment distribution equations that are highly sensitive to fluctuations in flow rates when there are only a few samples at each location to be used in model calibration. Due to the scarcity of TSS data, it was difficult to thoroughly and quantitatively assess the model performance. Accordingly, the focus was to ensure that the TSS calibration and surface inorganic sediment accumulation were analyzed in a holistic manner.

2.4.5 Temperature

In general, the model results agreed well with the temperature measurements, as illustrated in Figure 27 – 30. The model captured the seasonal temperature variations across the domain. There are few locations where the predicted temperature appeared to be shifted from the observations. These mainly occur in compartments with a collectively large water body; a site specific heat exchange coefficient may improve the delay in response to the air temperature in future versions of the model.

2.4.6 Water Quality

As illustrated in Figure 31 – 34 for TKN, the model reproduced general water quality constituents level at most locations. Due to the lack of continuous data at the tributary inflow, long-term averaged values were used as model input. Data scarcity greatly hinders the ability of the model to accurately predict water quality patterns (both temporal fluctuations and spatial distributions). In addition, all water quality constituents are coupled by chemical kinetic processes and interactions (Meselhe et al., 2013), which expand the impacts of missing individual input parameters at the tributary inflow boundaries. Nevertheless, the model results capture the magnitude of observed water quality concentrations reasonably and are considered satisfactory to represent the general spatial distribution and concentration. Of all water quality constituents in the water quality subroutine, only one is used by another component of the model; the EwE model relies on TKN simulations to predict primary production for the fishery food webs (De Mutsert et al., 2015).

3.0 Morphology

3.1 Data and Methods

The morphology subroutine is a relative elevation model, and as such its projections depend upon a wetland's ability to maintain or build to an elevation capable of supporting wetland establishment or persistence. Accretion is the mechanism by which wetlands can maintain that elevation; therefore, accretion was selected as the primary parameter upon which to conduct calibration. Accretion is a function of both inorganic and organic components, and this subroutine of the ICM therefore relies on both inorganic sediment accumulation rates as calculated by the hydrodynamic subroutine and the organic soil properties associated with the vegetative communities predicted by the vegetation subroutine.

Although accretion is the primary parameter in determining elevation changes through time, the master plan modeling effort is not only focused on elevation, but also land area. Therefore, in addition to the focus on accretion, the long-term land change rates are also included in this analysis to ensure that the general trends of land change through time are captured by the ICM.

The calculations of accretion (Equation 1) contain three parameters of interest.

$$H = \frac{Q_{sed}+Q_{org}}{10{,}000*BD} \quad (1)$$

Where H is the rate of vertical accretion (cm/yr), Q_{sed} is mineral sediment accumulation rates ($g/m^2/yr$) calculated by the hydrology subroutine; Q_{org} is soil organic matter (OM) accumulation rates ($g/m^2/yr$); and BD is soil bulk density (g/cm^3). The constant 10,000 is a conversion factor from cm^2 to m^2.

Q_{sed} is an output of the hydrology subroutine and was calibrated in that portion of the calibration effort. The two remaining parameters Q_{org} and BD were chosen for manipulation during the calibration of the accretion rates projected by the morphology subroutine. Data related to these parameters were obtained for different combinations of hydrologic basins and vegetation types using soil data collected from CRMS and supplemented with Soil Survey Geographic Database (SSURGO) soil data where CRMS data were unavailable.

Statistics were developed for BD and OM% for a total of 50 observed ecoregion[9]-vegetation groups (from 10 of the 12 ecoregions and five vegetation types). Mean and standard deviations were calculated for each group. Organic matter percent was converted to OM loading (Q_{org}). For ecoregion-vegetation groups in which data were unavailable, representative values were assigned from similar groups. Initial calibration efforts used the mean values for each ecoregion-vegetation group. This initial calibration effort focused on comparing accretion rates as predicted during the same time period as the TSS calibration effort for the hydrodynamic subroutine; average accretion rates were calculated for each group and those values were compared to long-term sediment accumulation and vertical accretion field data described in the following section. The time period used for model calibration (4 years) did not match the decadal patterns measured by the field data; therefore, upon completion of calibration, a

[9] Ecoregions are geographic subunits (e.g., upper Barataria basin). There are 12 ecoregions in the ICM.

separate, long term, model run was conducted that best represented historical conditions. A description of this process is provided in section 3.3 – Results.

3.1.1 Calibration Data

All available long-term sediment accumulation and vertical accretion (Cesium) field data collected from the Louisiana Coastal Area Science and Technology (LCA S&T) Program were used to calibrate the subroutine (Piazza et al., 2011). This dataset contains 178 Cesium cores (Figure 35).

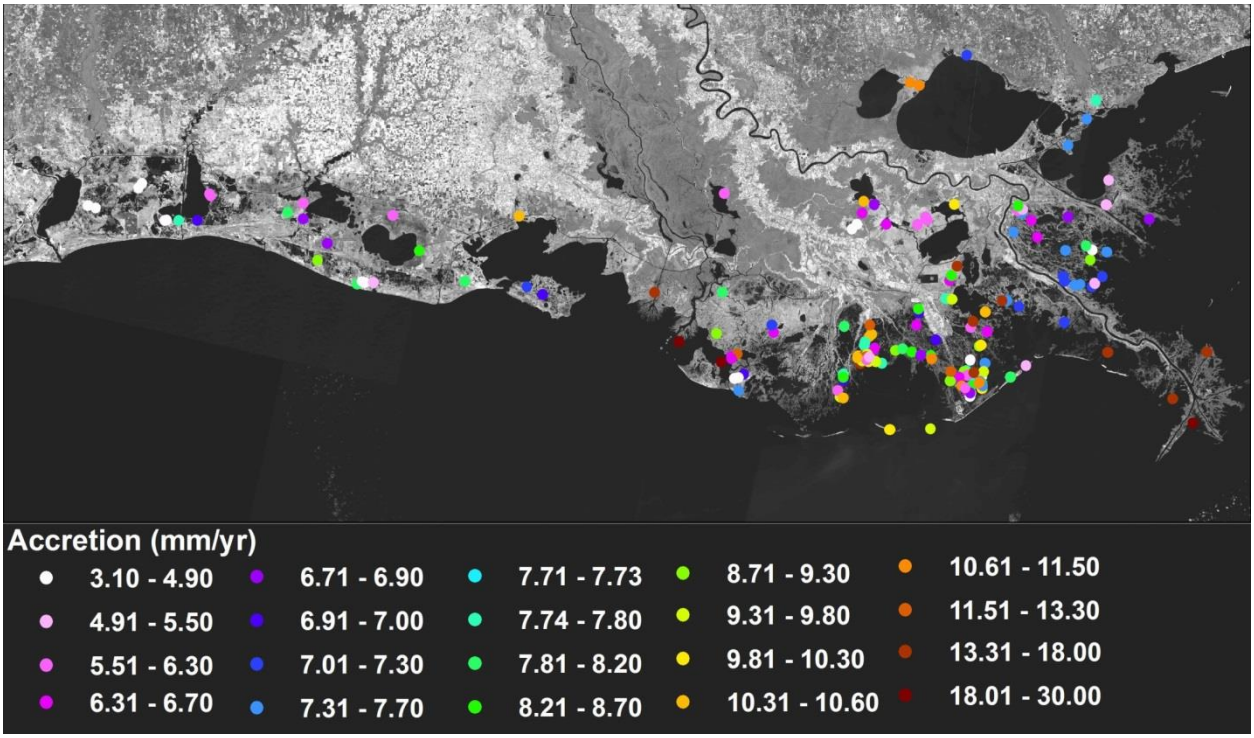

Figure 35: Map of Available Cesium Cores.

3.2 Analysis

3.2.1 Comparison to Measured Accretion Rates

The estimated vertical accretion rates at sites in basin-vegetation groups were then compared with the observed accretion rates to calculate the RMSE using Equation 1. After each model run, the RMSE was assessed to evaluate the performance and to determine if agreement with historical data and trends improved over time. If adjustments were needed, BD and Q_{org} values were altered according to standard deviations from the mean of observed data. For example, if modeled accretion values were, on average, lower than observed values, a new run was conducted with bulk density values 0.25 standard deviations lower than the mean. This process was repeated until values for BD and Q_{org} were obtained that resulted in an acceptable model performance.

Upon completion of OM and BD input value adjustments, it was determined that vertical accretion rates were still slightly under-predicted by the model (Figure 36). To improve model

performance, a background vertical accretion rate of 2 mm/yr was added to all accretion calculations. This 2 mm value was determined by fitting a regression line through the data shown in Figure 36. With this addition in place, it was determined that using the mean BD and Q_{org} values for each ecoregion-vegetation group resulted in the best model performance.

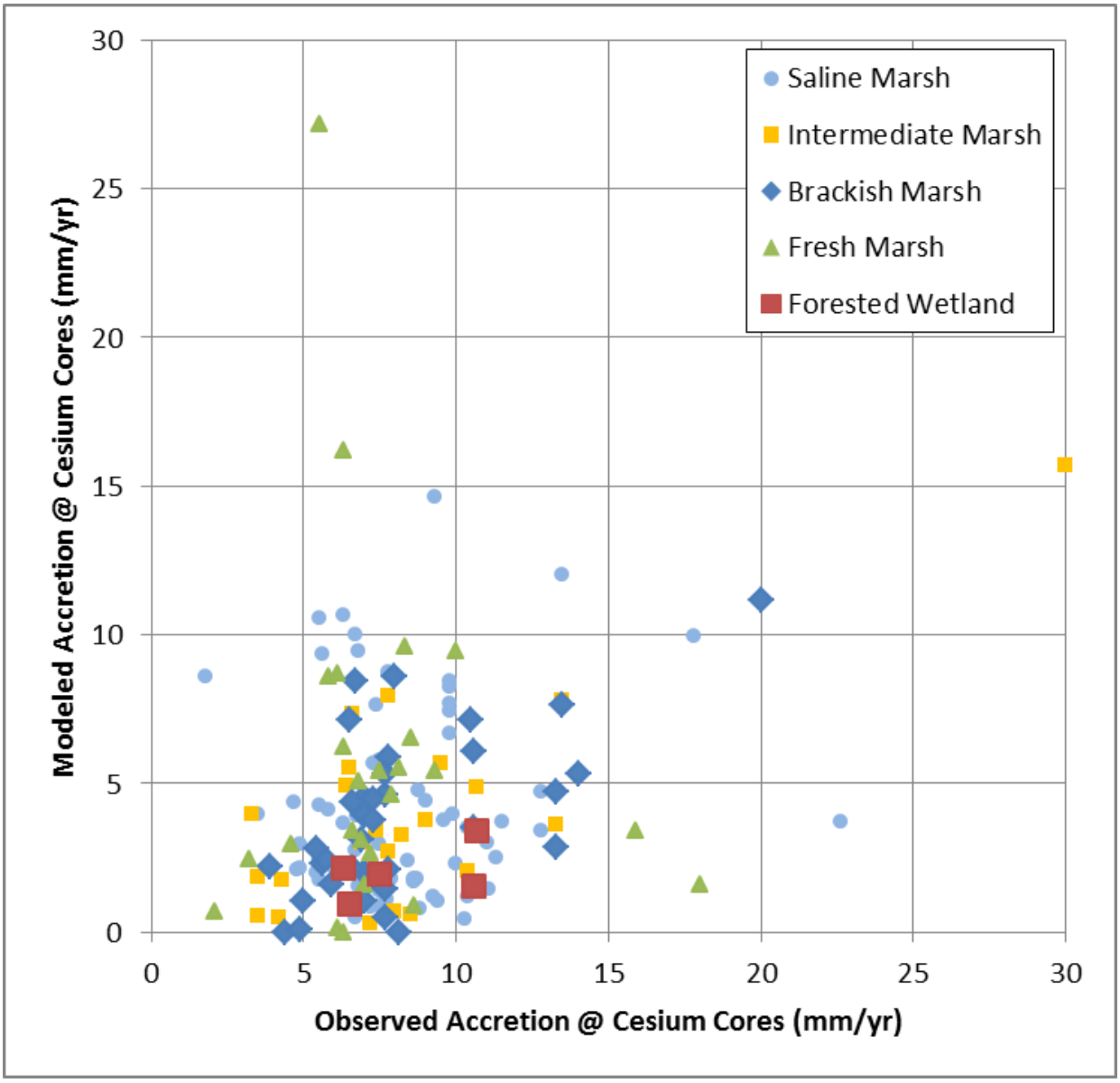

Figure 36: Modeled Versus Observed Accretion Rates Averaged by Marsh Type for Calibration Period 2010-2013.

3.2.2 Comparison to Historical Land Area Change Rates

The output of this subroutine includes land area change, which is utilized in the formulation of restoration and protection planning. As such, a comparison of modeled land area change rates to historical rates was conducted to provide relevant information regarding how well the

subroutine reflects this parameter. Land area change rates were calculated for each ecoregion-vegetation group initially during a 2010-2013 observation period. Example comparisons are shown in Figure 37.

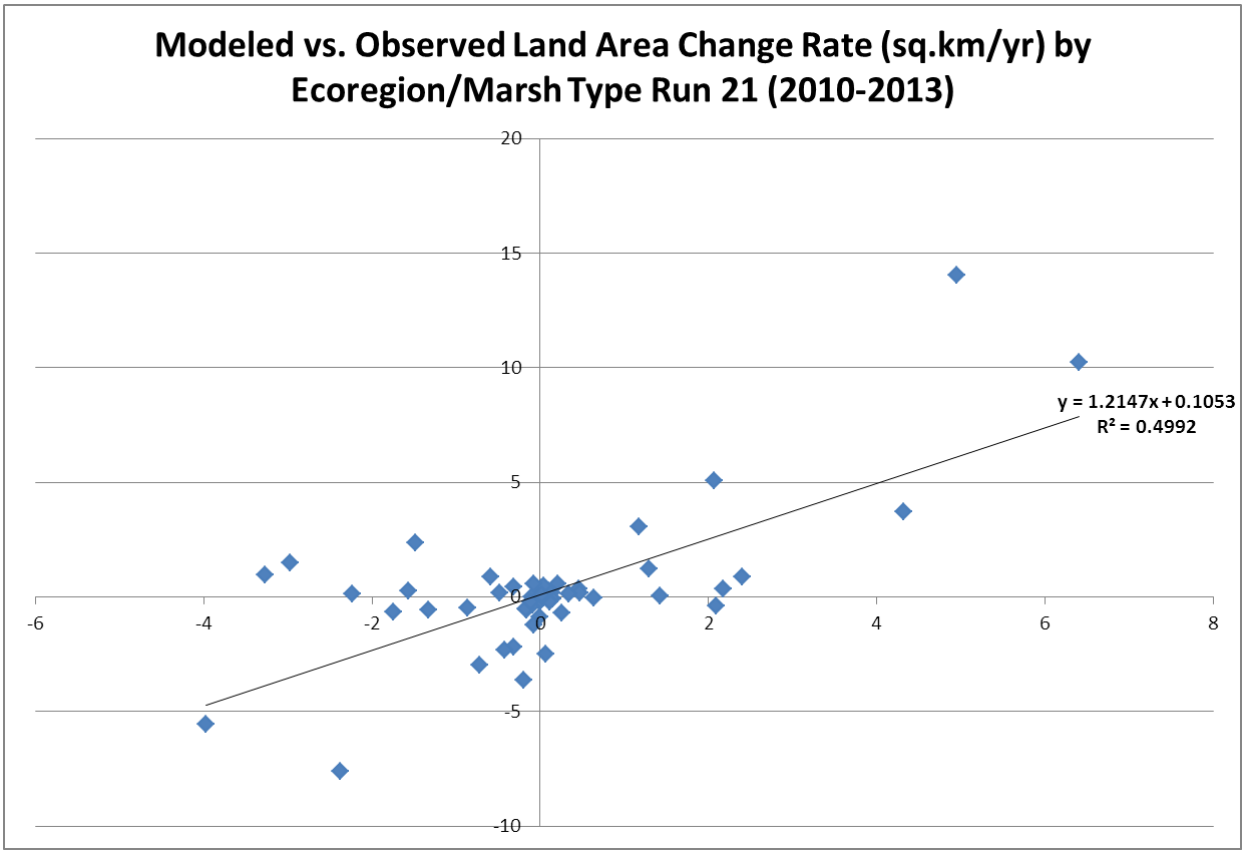

Figure 37: Modeled Versus Observed Land Area Change Rates by Ecoregion During a 2010-2013 Observation Period.

In addition to being dependent on accurately calculated vertical accretion rates, the land area change rate was also sensitive to elevation thresholds used to define land collapse and gain. Fresh forested and fresh marsh areas are subjected to collapse within the morphology subroutine due to short-term salinity spikes. For this modeling effort, the salinity value used to define a short-term spike was the maximum of two week mean salinity experienced during a model year. Salinity-tolerant species are subjected to collapse if they experienced long periods of inundation. Conversely, land was gained in the model if a water area had an elevation frequently above the calculated mean water surface. Values used to calculate these loss and gain occurrences were based on Couvillion and Beck (2013) and are provided in Table 6. Thus, the model land loss outputs shown in Figure 37 are not only influenced by accretion but also by elevation and salinity regimes.

Table 6: Collapse and Gain Thresholds Used in the Morphology Subroutine (based on Couvillion & Beck, 2013).

Land Type	Collapse threshold	Land Type	Land Gain Threshold
Fresh Forested Wetlands	Land will convert to water if it is at, or below, the annual mean water level for the year and the maximum two week mean salinity during the year is above: 7 ppt	Water	Water will be converted to land if the mean water level for two consecutive years is at least 0.2 m lower than the bed elevation of the water area
Fresh Marsh	Land will convert to water if it is at, or below, the annual mean water level for the year and the maximum two week mean salinity during the year is above: 5.5 ppt		
Intermediate Marsh	Land will convert to water if the annual mean water depth over the marsh for two consecutive years is greater than: 0.36 m		
Brackish Marsh	Land will convert to water if the annual mean water depth over the marsh for two consecutive years is greater than: 0.26 m		
Saline Marsh	Land will convert to water if the annual mean water depth over the marsh for two consecutive years is greater than: 0.24 m		

3.3 Results

Vertical accretion rates and land area change can be highly variable over short time periods, and rates during short time periods modeled during calibration may not be representative of longer term trends. Therefore, to validate the modeled accretion and land area change rates, a full 50-year model run was completed and compared to historical wetland change rates as assessed from USGS Scientific Investigations Map 3164 (Couvillion et al., 2011).

Observed datasets to drive the full 50-year ICM run do not exist for this length of time. Therefore, to assess the long-term land change rates predicted by the ICM, the environmental uncertainty scenario (Appendix C: Chapter 2 Future Scenarios) which most closely resembled historical conditions, scenario S20, was used to provide the best comparison with historical data.

The modeled accretion and land area change rates, as compared to historical datasets are shown in Figures 38 and 39.

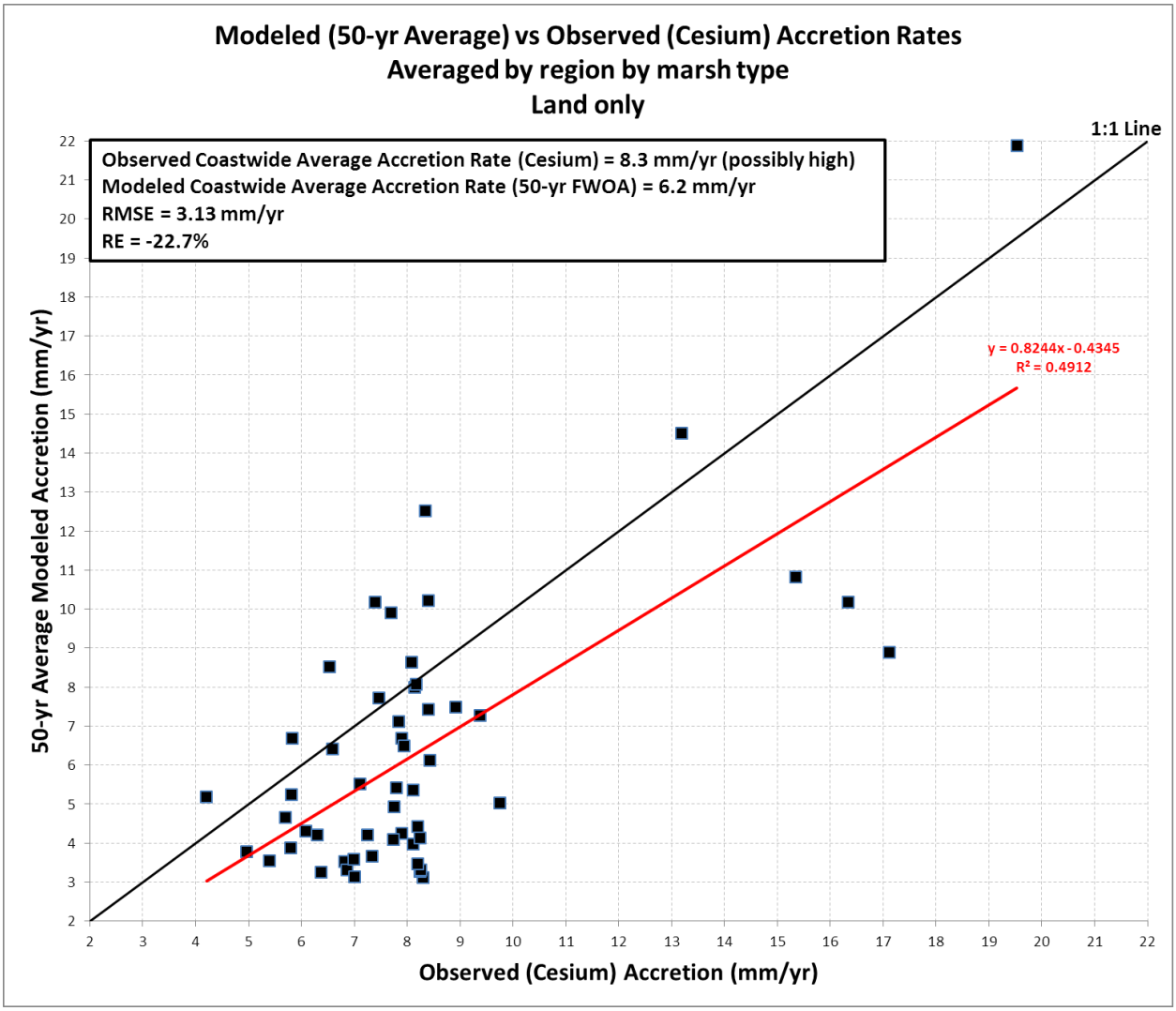

Figure 38: Modeled Versus Observed Average Accretion Rates (mm/yr) by Region and Marsh Type for 50-Year Historical Scenario.

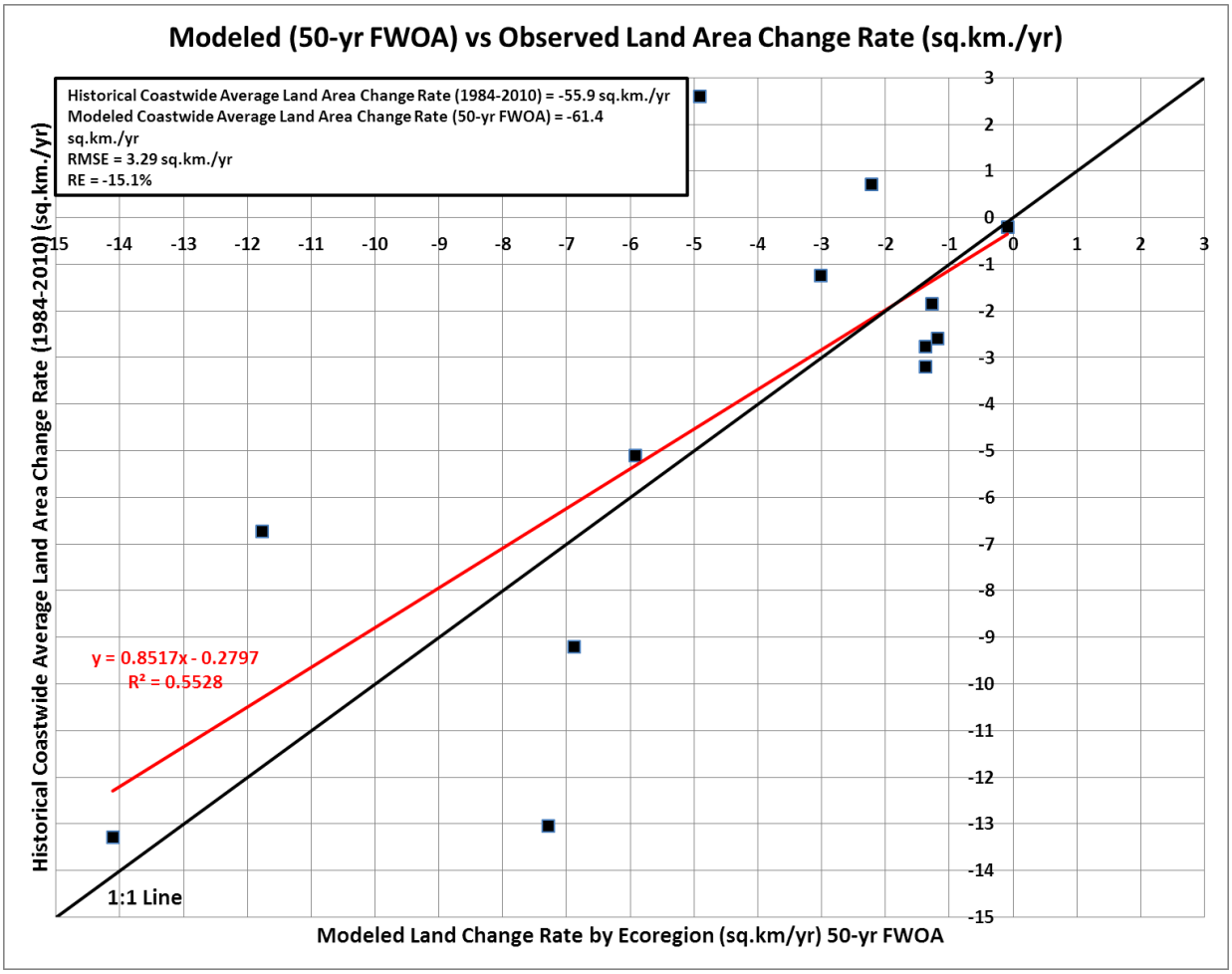

Figure 39: Modeled Versus Observed Land Area Change Rates by Ecoregion Under the 'Baseline' Scenario Intended to Represent Historical Conditions (S20; Appendix C: Chapter 2).

3.4 Discussion

The results of the morphology calibration effort indicate that the vertical accretion and long-term land change trends match observed data fairly well. There are a few underlying data deficiencies that impede a thorough quantitative analysis of model error. First, there are large disparities of both spatial and temporal scales of modeled and observed accretion. Modeled accretion is calculated from a sediment accumulation value that is calculated annually at a resolution equal to the hydrodynamic compartments (dozens of km^2 in size). This is then compared to vertical accretion as measured in soil cores that are many orders of magnitude smaller in spatial extent (several cm^2 in size). Furthermore, the soil core data are used to measure long-term accretion, which inherently captures many physical processes (e.g., compaction) that are not included in the ICM. The data deficiencies that impart uncertainty and error to the TSS calibration in the hydrodynamic subroutine (previously discussed), similarly impact the long-term accretion and land change results. Improved datasets for use in both driving the model and for validation against observed data, would improve modeled TSS and subsequent accretion/land change rates.

4.0 BIMODE

Because substantial changes were made to the 2012 Coastal Master Plan barrier island model (discussed in full in Attachment C3-4: Barrier Island Model Development), it was necessary to recalibrate the new barrier island model (referred to as the BIMODE subroutine) for use in the ICM.

The model calibration period was 2006-2011. The Breton Island region could not be calibrated within this time period because it was almost completely submerged during the early part of this timeframe. Breton Island began to re-emerge with approximately 0.48 km of shoreline visible by December 2009 and 2.6 km by May 2014. This is a cross-shore recovery process, which the BIMODE subroutine is incapable of replicating.

Similarly, the Chandeleur Islands were substantially disintegrated following Hurricane Katrina and had not recovered by the start of the 2006 calibration period. Recovery of the Chandeleur Islands has been observed and could be a function of natural rebuilding and the construction of the Louisiana Emergency Berm Project. There were sufficient continuous stretches of shoreline along the Chandeleur Islands to facilitate a quasi-calibration of the long-shore transport rate but not enough to provide a truly calibrated model in that area.

4.1 Data and Methods

The initial conditions for the calibration model runs were based on 2005 and 2006 Light Detection and Ranging (LiDAR) survey data (BICM, 2006) and hydrographic surveys offshore. Post-construction survey data from the following projects were inserted into the model to account for recent project construction. These were inserted in a single month nearest to the end of beach construction:

- Chaland Headland Barataria Barrier Island Restoration Project (BA-38-2) – December 2006
- Pass Chaland to Grand Bayou Pass Barrier Shoreline Restoration Project (BA-35) – May 2009
- Whiskey Island Back Barrier Marsh Creation Project (TE-50) – March 2010
- East Grand Terre Island Restoration Project (BA-30) – June 2010
- West Belle Pass Barrier Headland Restoration Project (TE-52) – September 2012
- Pelican Island Restoration Project (BA-38-1) – November 2012
- Scofield Island Restoration Project (BA-40) – March 2013
- Raccoon Island Shoreline Protection and Marsh Creation Project (TE-48) – April 2013
- Shell Island East Berm Barrier Restoration Project (BA-110) – August 2013

At the time the 2006 LiDAR data were collected, there was a very shallow bar feature across the mouth of Bay Champagne, but the bay was essentially open. The BIMODE subroutine therefore read the shoreline to be the north edge of Bay Champagne almost 914 m to the north. Within a year, the spit had regrown such that Bay Champagne was closed. BIMODE is not designed to be able to replicate re-emergence of the shoreline; therefore, pre-construction survey data (September 2010) from the Caminada Headland Phase 1 restoration project were used as a proxy for the starting shoreline location and cross-section in the Bay Champagne area along the Caminada Headland.

The wave climate was based on Wave Information Studies (WIS) data (http://wis.usace.army.mil/) from January 2006 through December 2012 for the stations shown in the BIMODE report (Attachment C3-4). Wave data from January 2013 to December 2014 were acquired from WAVEWATCH (http://polar.ncep.noaa.gov/waves/download.shtml).

Storms were inserted into the model using six proxy storm events (i.e., synthetic storms from the FEMA/USACE synthetic storm suite). These proxy storms were used to represent the impact of hurricanes Humberto, Gustav, Ike, Ida, Lee, and Isaac.

The SBEACH model was independently calibrated. Pre- and post-Hurricane Isaac survey data for Pelican Island and West Belle Pass Barrier Headland were used to calibrate the SBEACH model along with measured wave, wind, and water level data. The wave and wind data were extracted from the WIS data, and water level data were acquired from the NOAA tide gauge located at the eastern end of Grand Isle.

4.1.1 Cross-Shore Model Component

An independent calibration of the SBEACH model was performed. A root mean square difference in elevation between the modeled post-storm profile and measured post-storm profile was developed. This was performed for a single profile on West Belle Pass and three profiles on Pelican Island (this project was under construction, and there were three distinctly different initial profiles). Calibration parameters within SBEACH (Table 7) included the transport rate coefficient, overwash transport rate coefficient, coefficient for slope dependence, decay multiplier, grain size, landward surf zone depth, and maximum slope prior to avalanching. The set of parameters having the lowest root mean square difference was selected.

Table 7: SBEACH Calibration Parameters.

Calibration Parameters	
Landward surf zone depth (D_{SURF} - m)	0.12
Grain size (mm)	0.10
Maximum slope prior to avalanching	45
Transport rate coefficient (K - m^4/N)	2.5x10-6
Overwash transport parameter (C_o)	0.006
Coefficient for slope dependent term (ε m^2/s)	0.005
Transport rate decay coefficient (λ)	0.1
Water temperature (^oC)	27

4.1.2 Long-Shore Transport

The first step for calibrating the BIMODE subroutine was to calibrate the long-shore transport rates. The long-shore transport component was calibrated by modifying the "K" value within the Coastal Engineering Research Center (CERC) equation. The default "K" value is 0.39. The "K" value was altered until the modeled long-shore transport rate was within the reported range of long-shore transport. A different "K" value was applied in each barrier island region. The "K" values applied in the various model grids are shown in Table 8. The calculated long-shore transport was then compared to the reported long-shore transport rates for each region. The modeled sediment transport rate was then divided by a sediment transport calibration factor to approximate the reported values. The transport calibration factors ranged from 5 to 13 for the four regions west of the Mississippi River. A transport rate calibration factor was not developed for Breton Island. A transport calibration factor of 0.75 was used for the Chandeleur Islands. The calibration factor was held to a full unit (no decimal point) for the model region west of the Mississippi River to avoid over calibrating the model to the reported values, which also have variability in their range and accuracy.

Table 8: CERC Equation "K" Value Calibration Factor for Long-Shore Transport.

Grid Sub-Domain	"K" Factor
Isles Dernier	0.047
Timbalier	0.030
Caminada Headland/Grand Isle	0.078
Barataria Bay	0.039
Breton Island	0.390
Chandeleur Island	0.513

The second calibration factor within the BIMODE subroutine was the shoreline retreat caused by silt loss. Once the sediment transport rate was calibrated, BIMODE was run to provide a shoreline output. The shoreline location at the end of the calibration period was compared to the most recent aerial image available (January 24, 2015). A shoreline retreat parameter was then applied to the shoreline to better match the location of the shoreline. This value was changed on an island by island basis during calibration to match the overall shoreline location. Some localized differences along each island were also incorporated to account for changes in shoreline retreat, primarily at the ends of the islands where retreat rates were higher.

4.2 Analysis

Calibration was performed through visual comparison of the modeled shoreline with January 24, 2015 aerial images in Google Earth. BIMODE outputs the shoreline location point for each subaerial profile during a simulation. The shorelines were then drawn according to these points. The initial and post-calibration shorelines were converted to kmz format and loaded into Google Earth. This analysis was performed for both the Gulf-side and bay-side shorelines. Specifically, the

post-calibration shorelines were compared with the existing shorelines in aerial images. If post-calibration shorelines retreated more than the existing shorelines, the calibration parameters were adjusted to reduce retreat rates. If the opposite was noted, the calibration parameters were adjusted to increase shoreline retreat. The distance between the two shorelines was used to quantify the amount of adjustment.

Final cross-section profiles were also reviewed; however, there was limited profile data with which to compare the final calibration runs.

4.3 Results

The results of the calibration are shown in Figures 40-51. These figures show the modeled shoreline at the end of the calibration, overlaid on the January 24, 2015 aerial images.

The calibration results for Isle Dernieres area are shown in Figures 40-42. The eastern end of Raccoon Island was limited by a starting shoreline that did not extend to the eastern terminal groin in the January 2006 starting condition (Figure 40). Overall, BIMODE was able to replicate the shoreline retreat. It could not replicate the separation and rollover of the island to the west or the western end of the breakwater field.

The calibration for Whiskey Island shows again that the general trend of the shoreline could be replicated (Figure 41). There were two areas where instability in the shoreline occurred, which was mitigated through the shoreline retreat calibration factor. Due to limitations in the physical processes included, BIMODE could not replicate the spit growth observed on the western end of the island.

BIMODE showed good general agreement on Trinity and East Island (Figure 42). Again, spit growth on the eastern end of the island could not be replicated due to model limitations. The bay and Gulf shorelines crossed at the eastern end, which was addressed in BIMODE by allowing northward bay shoreline movement through overwash.

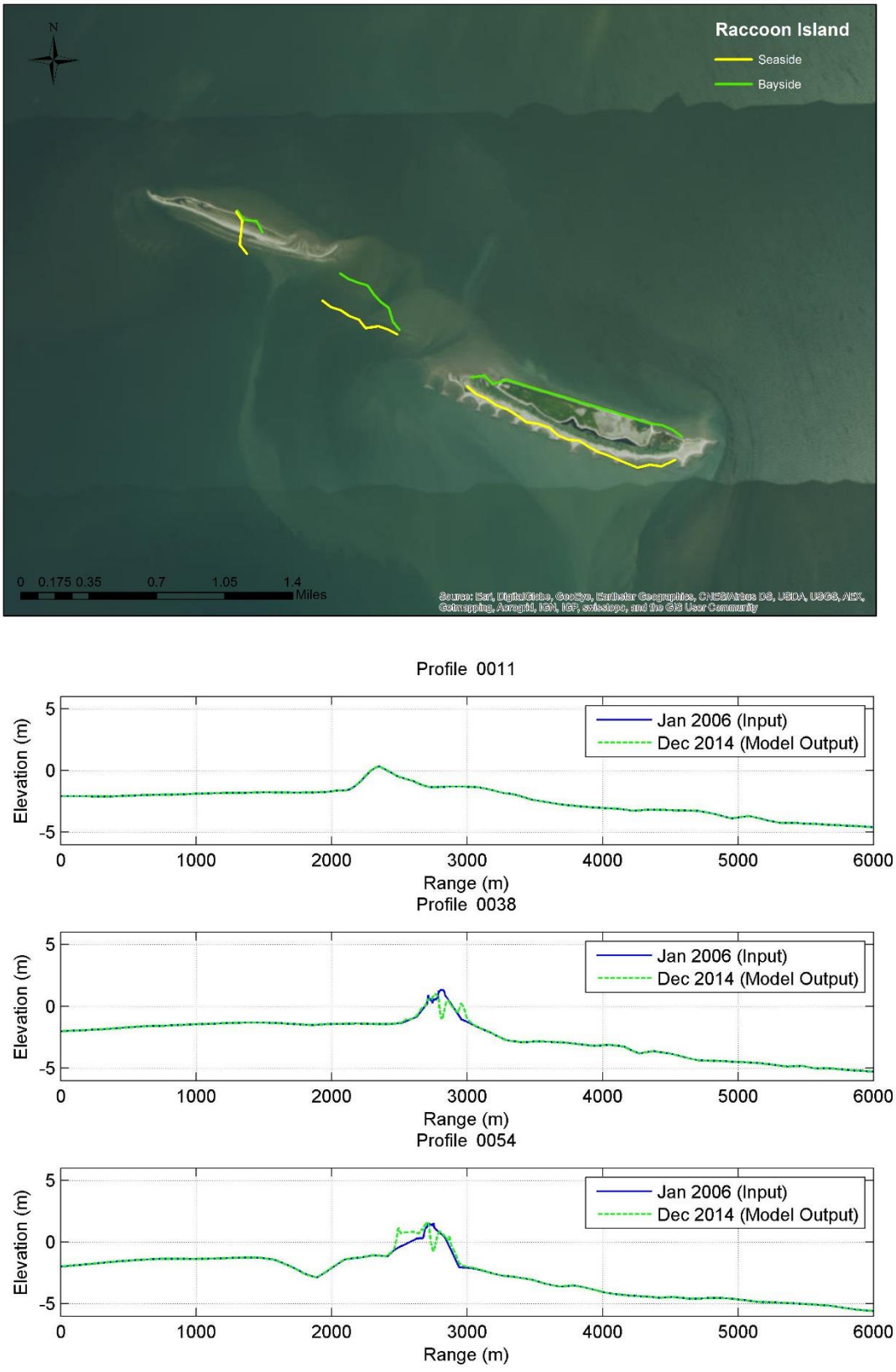

Figure 40: Calibration Results for Raccoon Island.

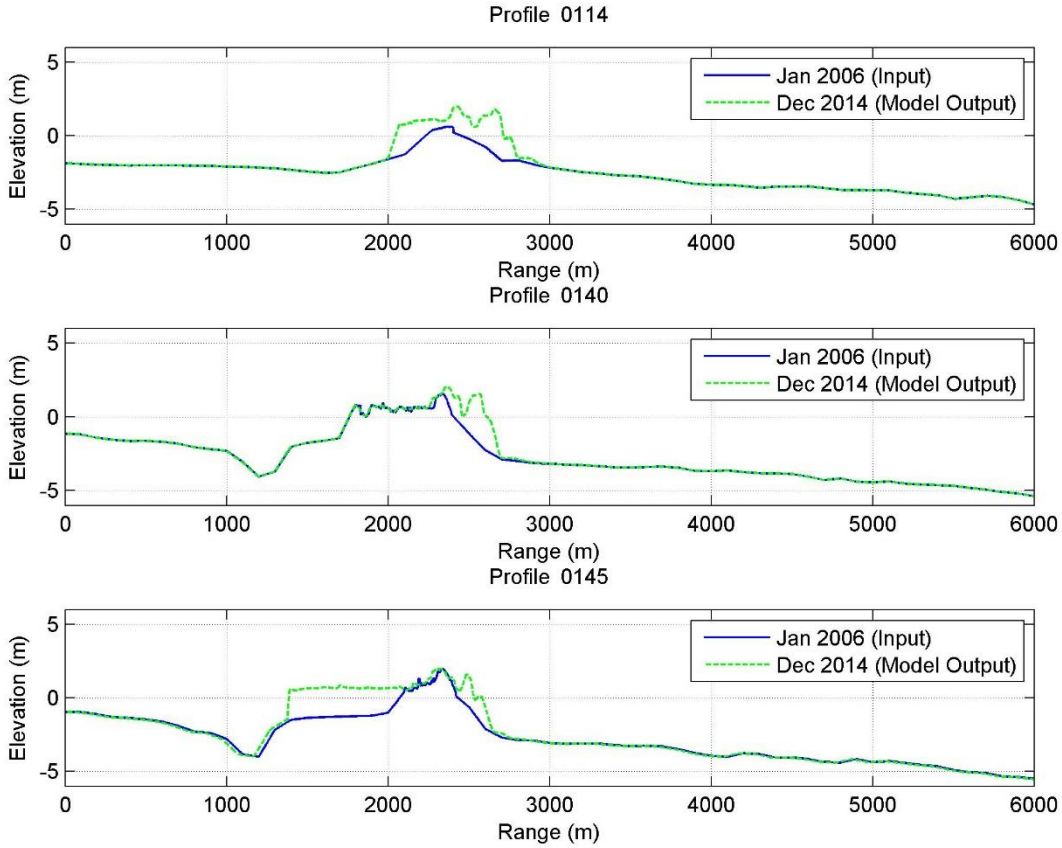

Figure 41: Calibration Results for Whiskey Island.

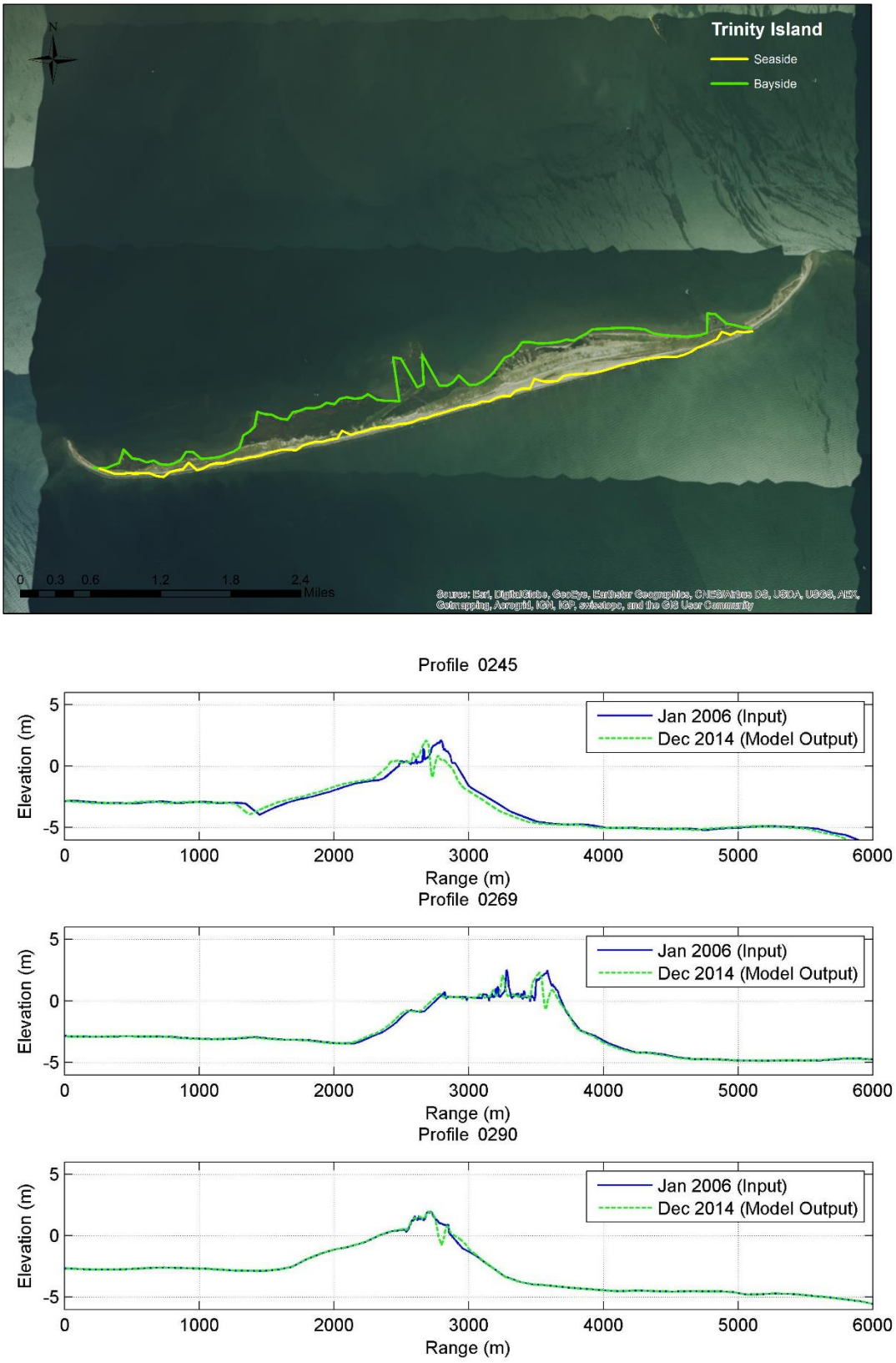

Figure 42: Calibration Results for Trinity Island and East Island.

The calibration results for Timbalier area are shown in Figures 43-44. BIMODE was run both including and excluding the revetment on the eastern end of Timbalier Island (Figure 43). It was determined that a better calibration was obtained by excluding it from the model. Additional calibration simulations were performed using the shoreline retreat calibration factors to replicate the eastern end of the island. The eastern remnants of East Timbalier Island were rolled backwards, but BIMODE suggested their continued existence. They were actually transformed into shoal features and moved northward more rapidly than seen in the BIMODE output (Figure 44). The western section of the island was fairly well replicated.

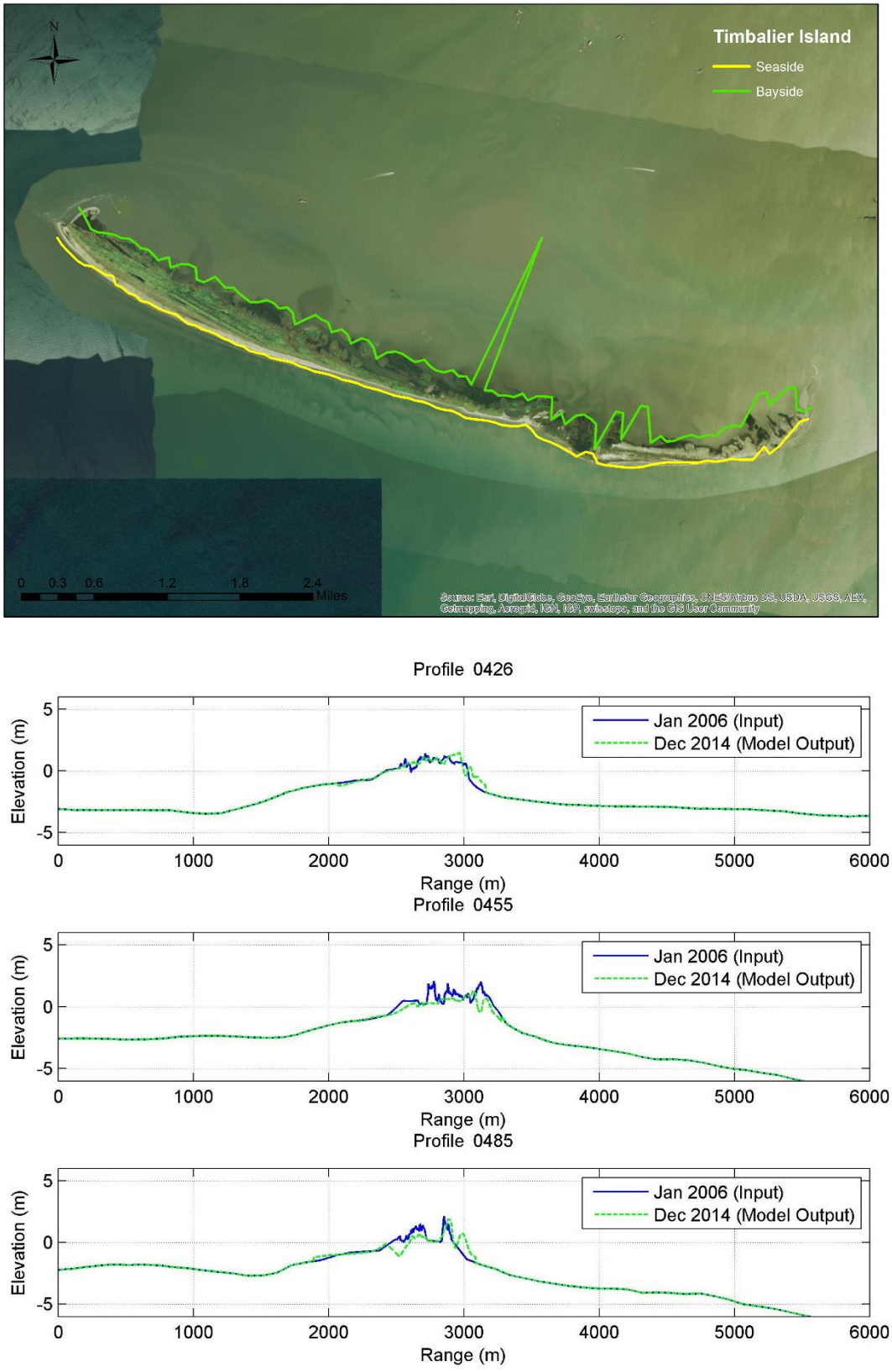

Figure 43: Calibration Results for Timbalier Island.

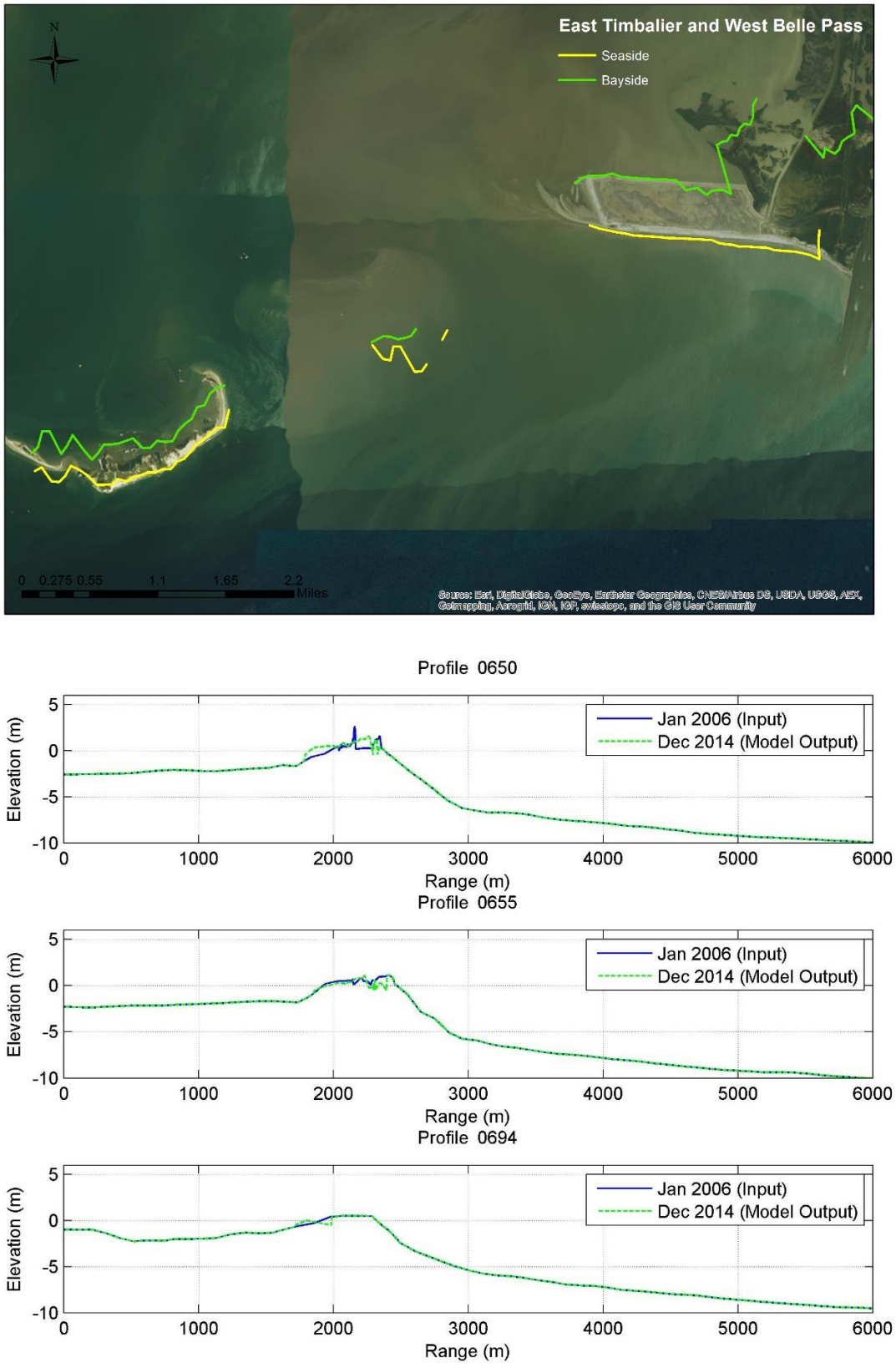

Figure 44: Calibration Results for East Timbalier Island and West Belle Pass Barrier Headland.

The calibration results for Caminada and Grand Isle are shown in Figures 44-47. As with other spit features, the spit feature at the western end of the West Belle Pass Barrier Headland was not replicated in BIMODE (Figure 44). The profile azimuth of the jetties also provided a challenge in calibrating the eastern end of the headland, though this was later improved. The western half of Caminada Headland was well replicated (Figure 45). The cross-shore profiles indicate that the restoration project was constructed during the calibration period.

Some revisions to the shoreline retreat calibration factor were required to calibrate the shoreline at the eastern end of the Caminada Headland (Figure 46). Calibration was attempted with and without the structures, and the final calibration excluded the effect of the breakwaters. The eastern end of Caminada Headland also required some revisions to the silt content/shoreline recession calibration in order to replicate the shoreline changes. Breaching of Elmer's Island was predicted in BIMODE, but natural breach closure, which occurred on Elmer's Island, could not be replicated. Therefore, there is a shoreline offset in the vicinity of the closed breach.

BIMODE over-predicted shoreline retreat on the western side of Grand Isle (Figure 47). Repeated attempts to obtain better calibration through the shoreline retreat factor were not successful; in fact they appeared to make BIMODE unstable. The effect of the breakwaters was significantly muted within BIMODE (less than 5% effect), compared to an expected effect of 30-50% based on the breakwater configuration, but they were ultimately left within the model. Fluctuations in shoreline location at the eastern end of the island could not be controlled without extensive modification of the shoreline retreat factor, and it was not deemed appropriate to over calibrate BIMODE. Thus, care must be taken when interpreting the results of a 50-year model run.

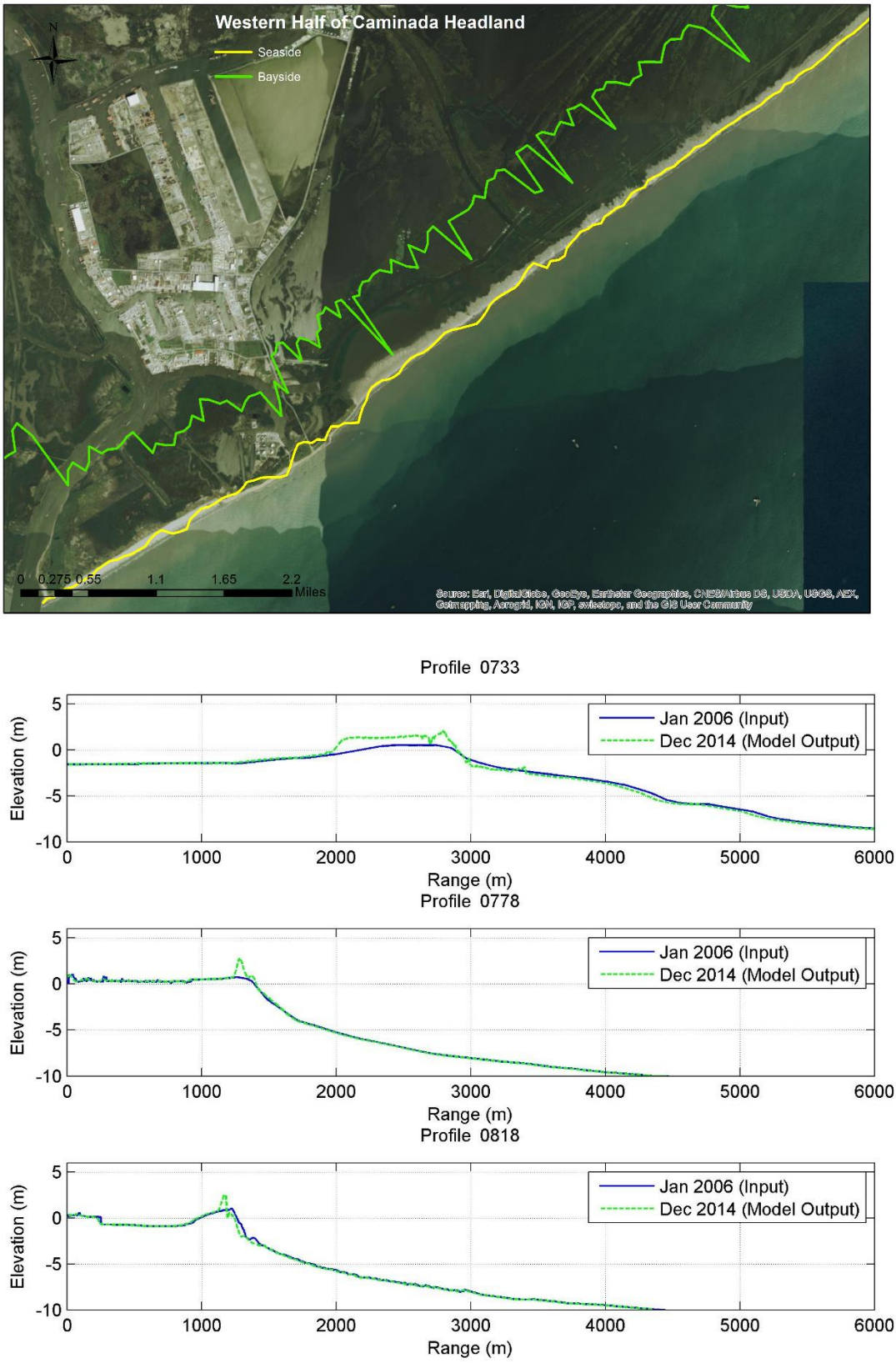

Figure 45: Calibration Results for the Western Half of Caminada Headland.

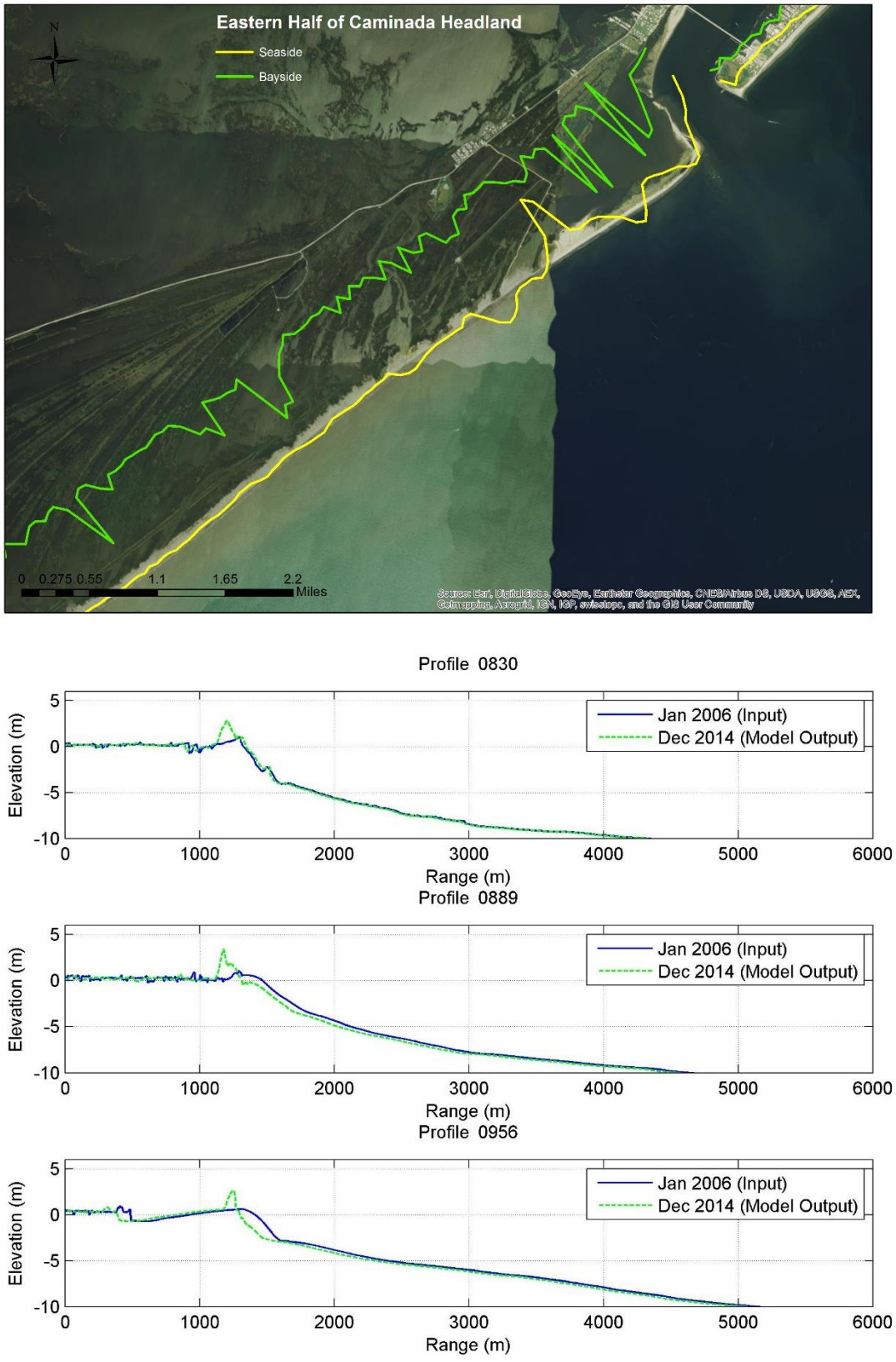

Figure 46: Calibration Results for the Eastern Half of Caminada Headland.

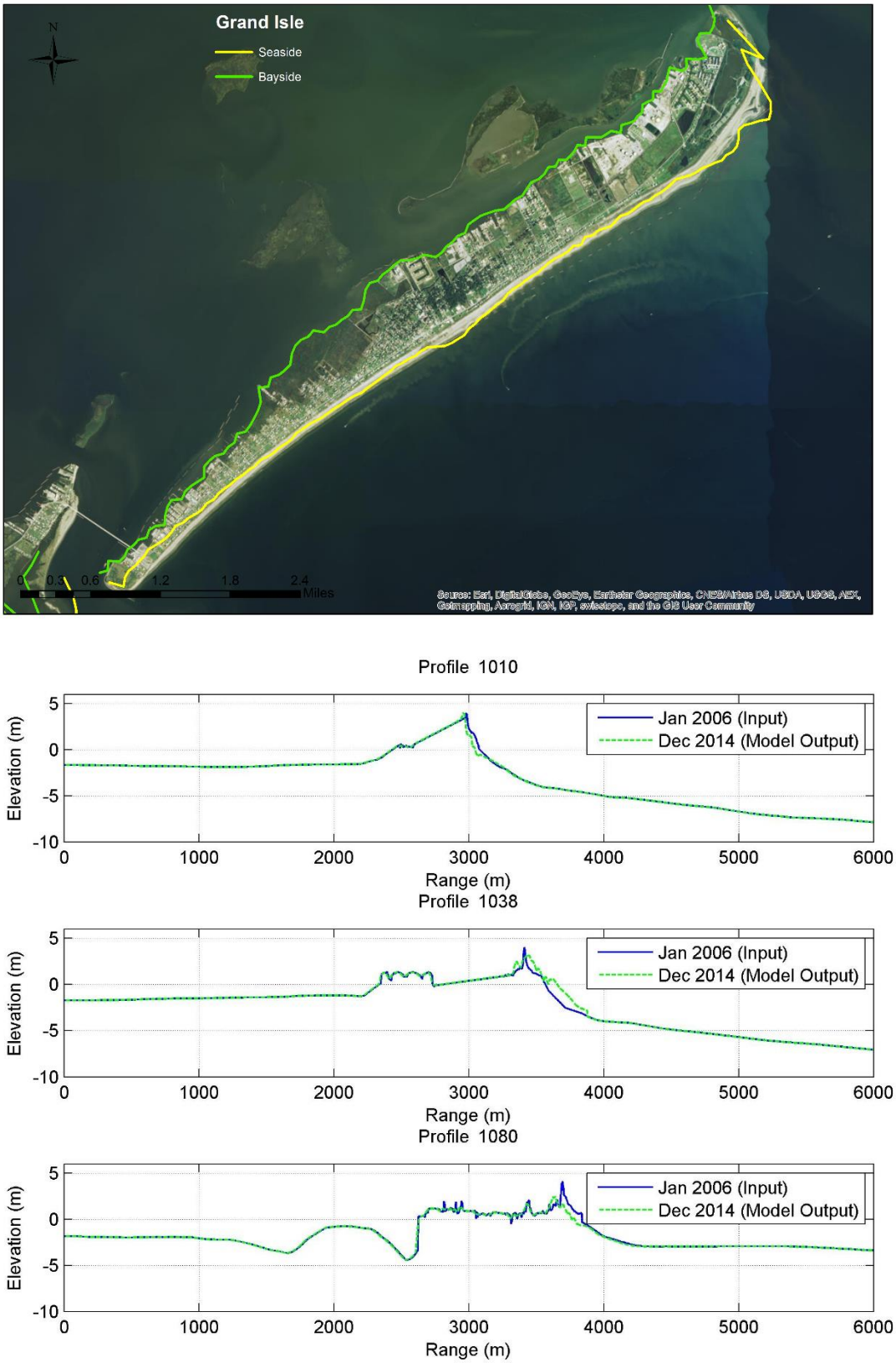

Figure 47: Calibration Results for Grand Isle.

The calibration results for Barataria area are shown in Figures 48-51. The western end of West Grand Terre proved challenging to model (Figure 48). BIMODE does not appear to replicate the effect of the Barataria Pass ebb shoal and the terminal groin effect of the Fort Livingston protective breakwater. Thus, the longer 50-year simulations may be problematic in this area. Although BIMODE replicated the general shape of the shoreline along East Grand Terre, it underestimated shoreline retreat on the eastern end (Figure 48). Attempting to increase this retreat resulted in a greater advancement of the western half of the island.

BIMODE appeared to replicate the overall trend of shoreline retreat along Grand Pierre (Figure 49) and Chenier Ronquille (Figure 49). Sediment transport across Pass La Mer had to be set within BIMODE rather than assuming no sediment transport. This assumption is supported by the literature and observations (Thomson et al., 2011). BIMODE predicted greater shoreline retreat on the Chaland Headland side of Pass la Mer, but overall the trend of the shoreline was adequately replicated, especially considering the construction of the Chaland Headland project and subsequent impacts by all six storm events.

As with Pass La Mer, BIMODE was set to allow sediment transport across Pass Chaland (Figure 50). Therefore, the shoreline is continuous in this area. The Pass Chaland to Grand Bayou Pass project was included in the calibration, so this function is working properly; however, it limits the actual calibration period of the model.

Construction of Shell Island East was completed in 2013 (Figure 51). It was included in BIMODE, but the island was only exposed to two years of wave conditions and no storms. Although the calibration looks promising, additional data could improve future calibration efforts. The Emergency Berm project could have been inserted into BIMODE, but since it was only two years until construction of the Berm to Barrier project, it was excluded from the modeling effort. Prior to the Emergency Berm project, there were only two very small island fragments that could not be effectively incorporated into BIMODE and were thus excluded. Prior to the Pelican Island restoration project, the island was significantly deteriorated such that it was not an effective starting condition upon which to base the model effort. Given that the restoration project was designed for a two-decade design life, it was decided to calibrate BIMODE for the reconstructed condition. Similarly, construction of Scofield Island followed completion of the Pelican Island project. Sediment transport across Scofield Pass was allowed.

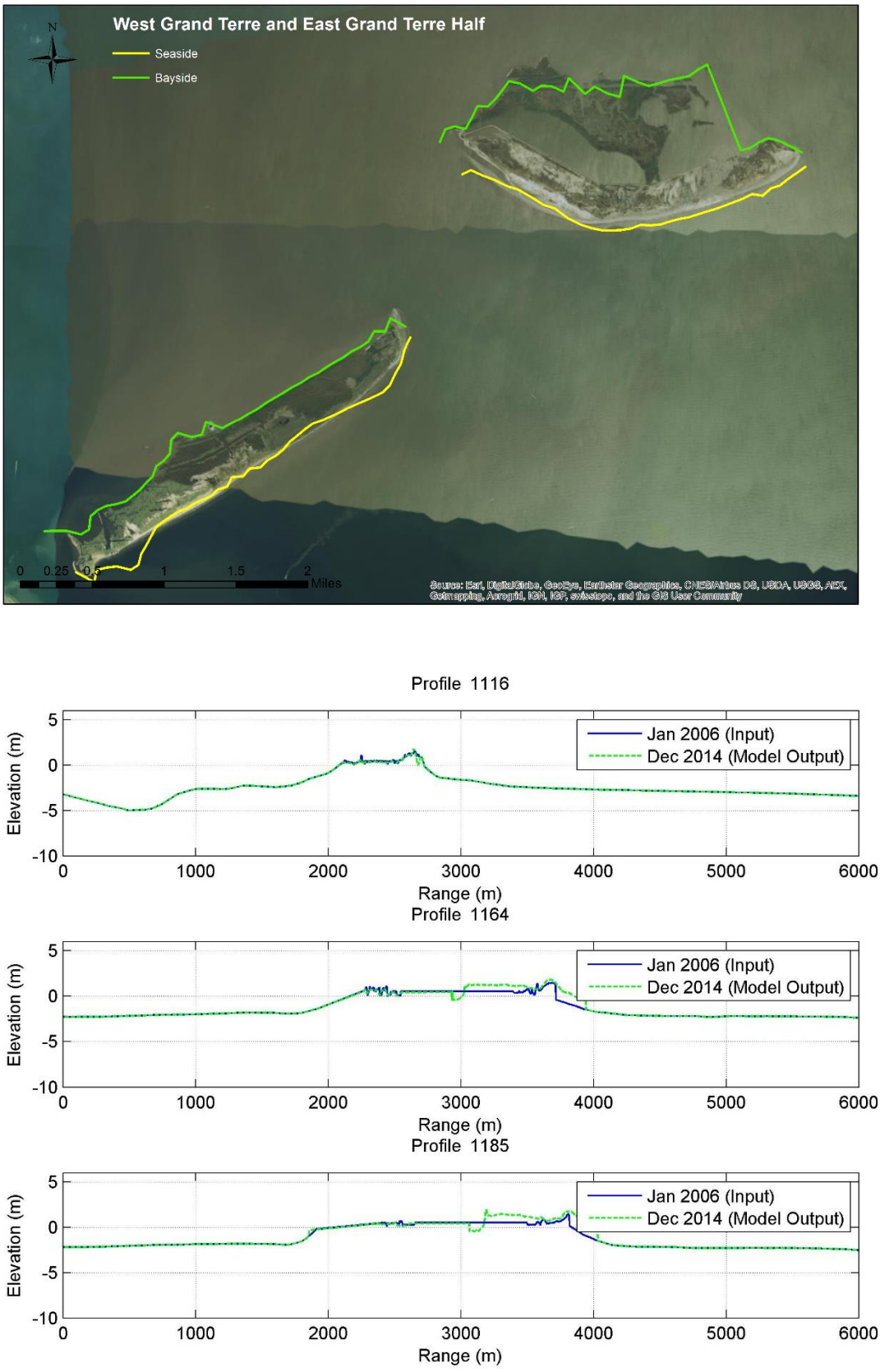

Figure 48: Calibration Results for West Grand Terre and East Grand Terre.

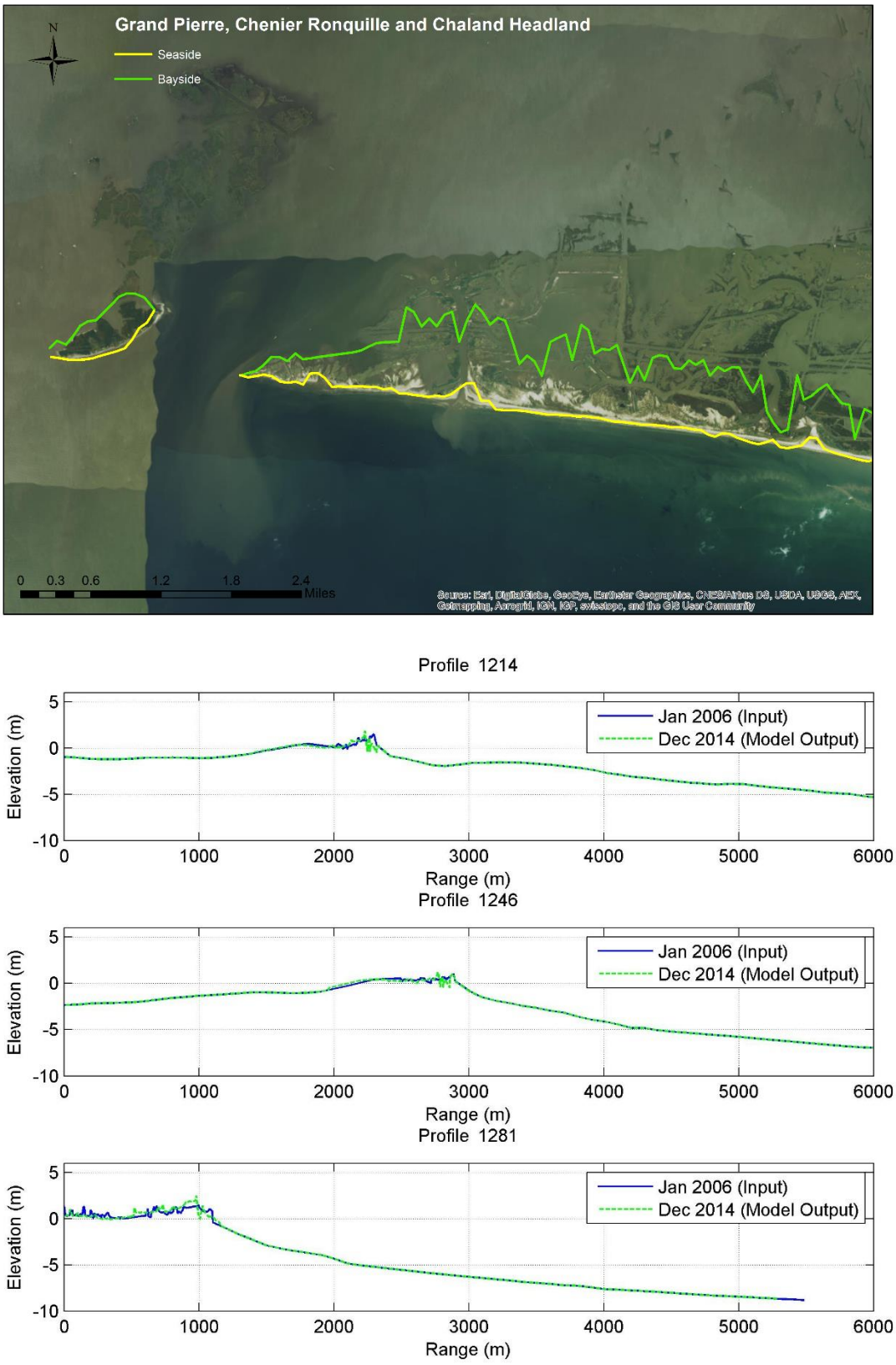

Figure 49: Calibration Results for Grand Pierre, Chenier Ronquille and Chaland Headland.

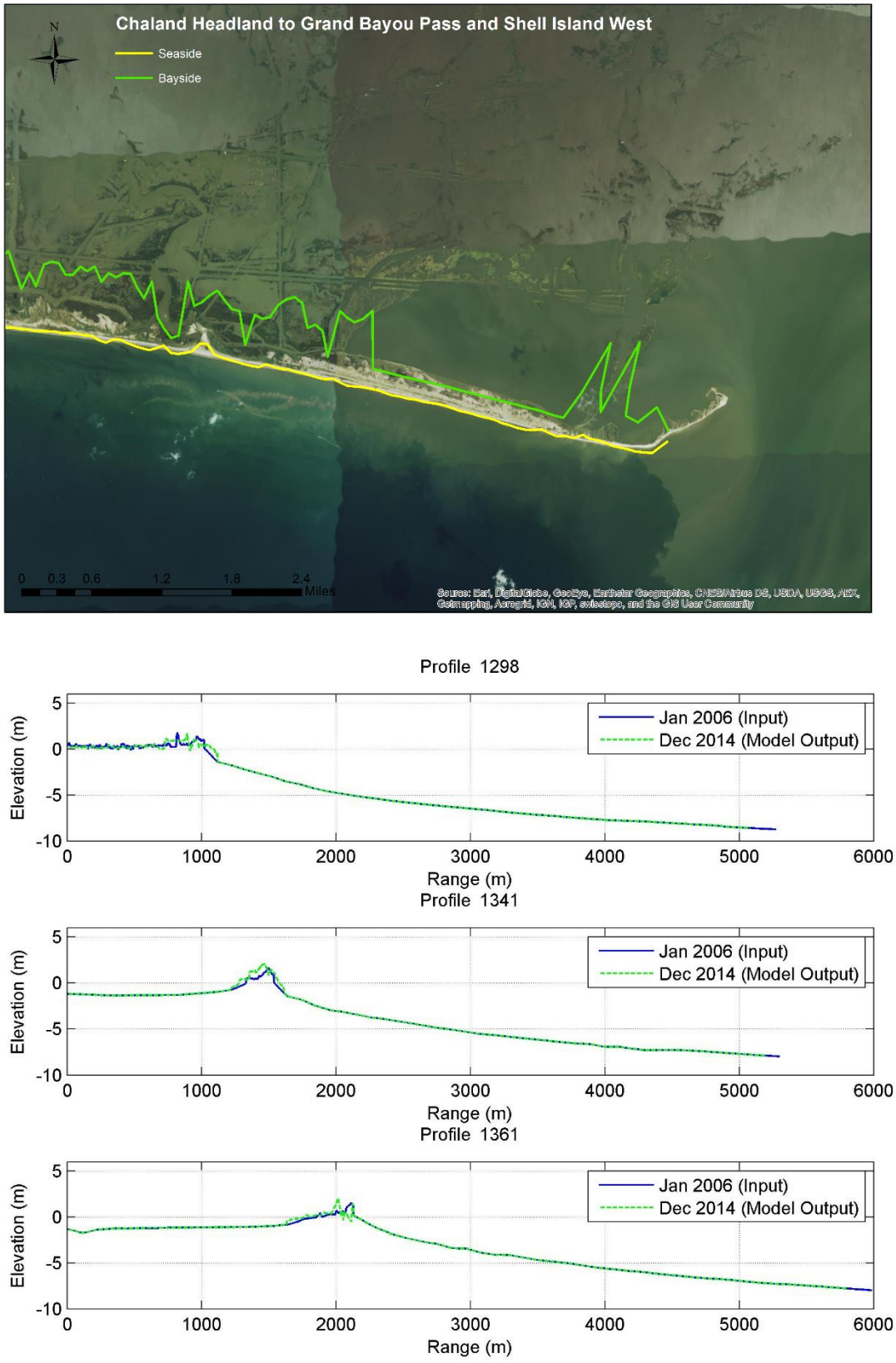

Figure 50: Calibration Results for Chaland Headland to Grand Bayou Pass and Shell Island West.

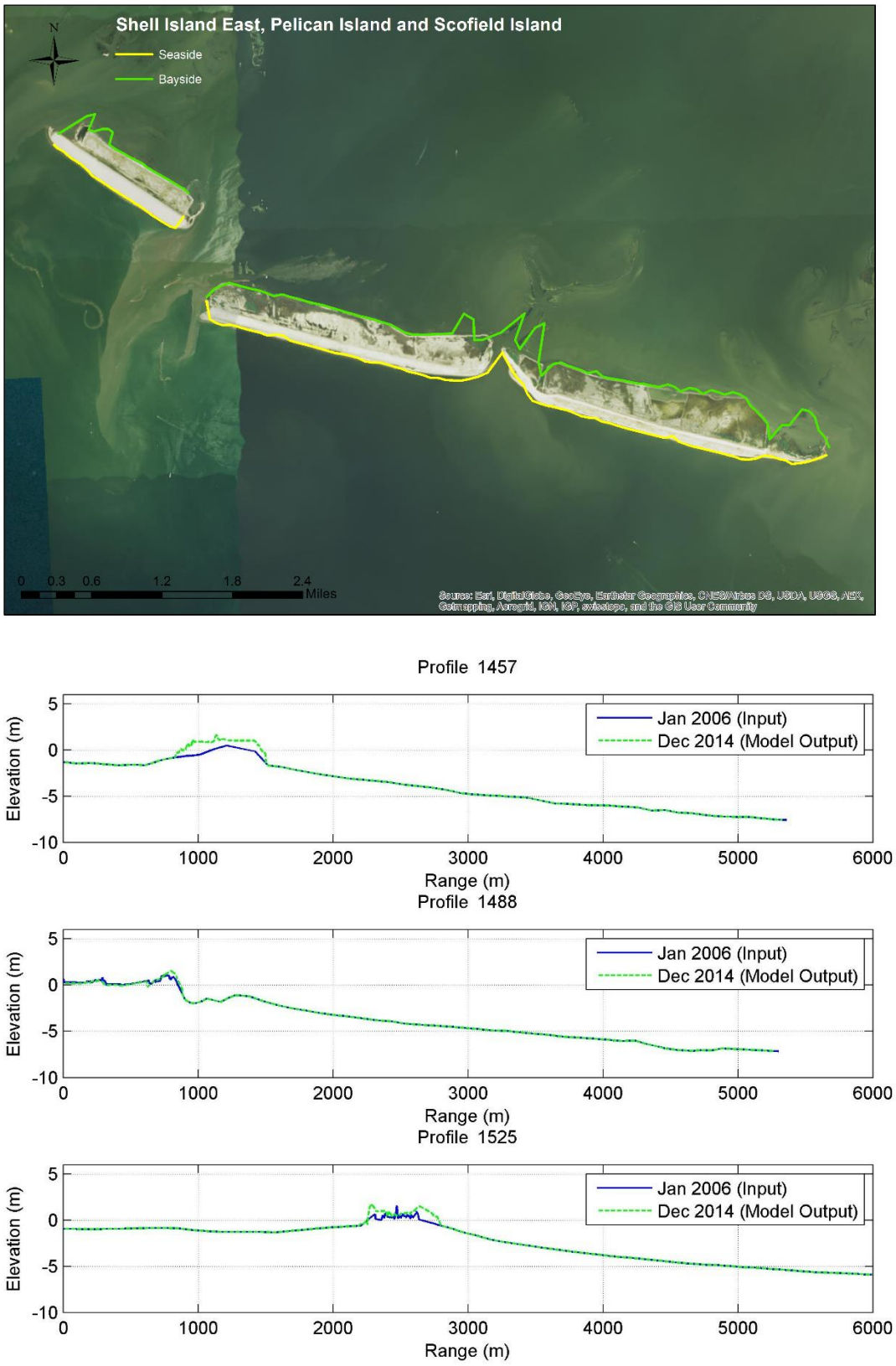

Figure 51: Calibration Results for Shell Island East, Pelican Island and Scofield Island.

4.4 Discussion

As the results show, BIMODE performed better along some sections of the model domain than others. Overall, BIMODE was able to replicate the trends of shoreline retreat. The cross-shore profiles give the comparison between initial bathymetry and BIMODE output at the end of the simulation. Some profiles reflect restoration project construction during the calibration period.

The lack of comprehensive shoreline data throughout the model domain in 2015 limits the ability to quantify the shoreline response. Thus, only a graphical comparison could be performed. Although BICM data were available for 2006, there were still areas that had to be adjusted to better match initial conditions. There were also limited profile data with which to compare the final modeled profile. Future efforts could possibly use alternate (earlier) time periods to assess and improve BIMODE performance.

5.0 Vegetation

5.1 Data and Methods

The CRMS vegetation data from 2010-2014 (Folse et al., 2012) were used to calibrate the most recent version of the Louisiana Vegetation Model (LAVegMod 2.0). This dataset contains 336 marsh stations and 56 swamp forest stations (Figure 52). Marsh stations consist of ten 2 x 2 m plots that are surveyed annually during the late summer (August-September) for plant species cover (Folse et al., 2012). The 56 swamp stations consist of three 20 x 20 m canopy plots, in which the basal area of the trees was determined in 2012. It is important to note that these data are not exactly the same as the data produced by LAVegMod 2.0 (Table 9). The observed (CRMS) data cover a relatively small area that is targeted to represent the wetland vegetation, while LAVegMod 2.0 includes all vegetation areas including ridges and open water. LAVegMod 2.0 is restricted to species that dominate significant parts of the coastal area, while the observed includes all species. Because of these differences, the presence/absence of the modeled species was used as an approach to calibrate LAVegMod 2.0. To avoid some of the inherent noise of the data, a species was considered present if it had greater than 5% cover.

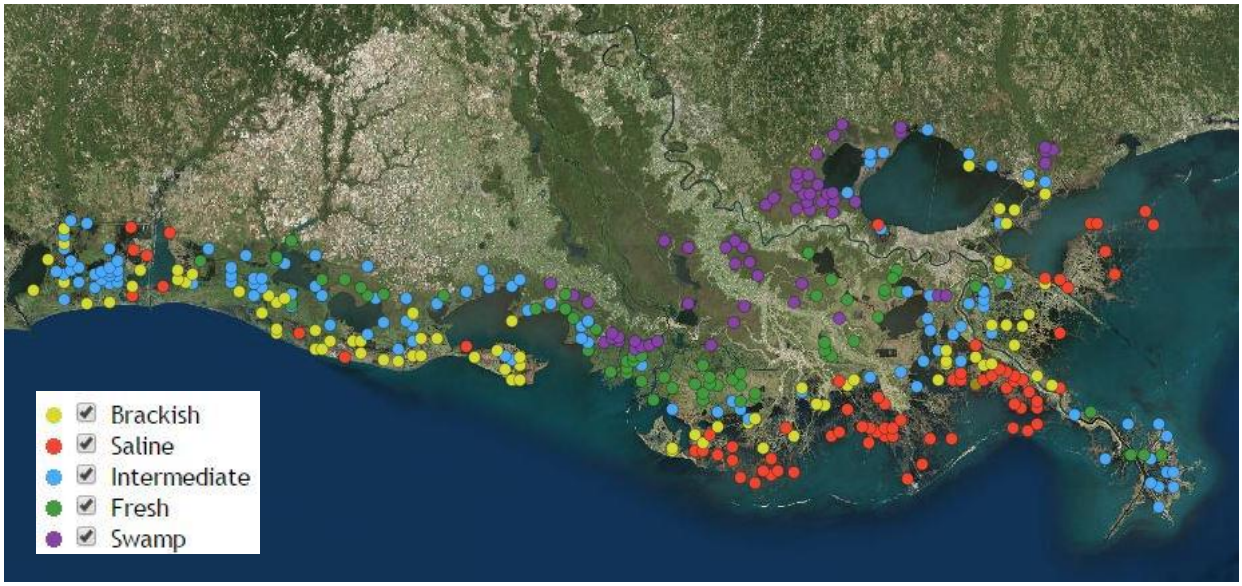

Figure 52: Map of the Distribution of CRMS Stations Across the Louisiana Coast.

Table 9: Differences Between Observed (CRMS) and Modeled (LAVegMod 2.0) Vegetation Data.

	LAVegMod 2.0	**CRMS**
Area	500 x 500 = 250,000 m^2	10 x 2 x 2 = 40 m^2
Represents	All habitat Includes ridges	Target habitat Marsh or swamp
Cover	Dominants	All species
Presence	> 5% cover	> 5% cover in one of the plots

5.2 Analysis

A Chi-square analysis was conducted to evaluate LAVegMod 2.0 performance (Table 10), testing if the modeled and observed represented the same plant community (Kent & Coker, 1995). A goal of 80% was set for the stations correctly classified for the fully calibrated model. That goal was set based on the professional experience of the team. After each model run, chi-squares were prepared for all species in all model years to evaluate the performance and determine if the level of agreement between the modeled and observed data improved. Agreement was defined as the percent of stations that were correctly classified by LAVegMod 2.0 (present when observed + absent when not observed). Establishment matrices were adjusted if the species observed increase was not matched by LAVegMod 2.0. Mortality matrices were adjusted if the species observed decline was not matched by the model. It took 11 calibration trials to arrive at a fully calibrated model.

Table 10: Chi-Square Analysis Used for LAVegMod 2.0 Calibration.

	Modeled	
Observed	Absent	Present
Absent	Correctly classified	Model over-predicts
Present	Model under-predicts	Correctly classified

5.3 Results

Some of the lowest agreements were observed in the saline marsh species (Table 11). For *Spartina alterniflora* (SPAL) LAVegMod 2.0 showed a decline at the CRMS stations, while the observed was relatively stable (Figure 53). When examining the spatial distribution (Figure 54), it became apparent that LAVegMod 2.0 captures the distribution of the area where this species is most prevalent (>25% cover observed). For *Distichlis spicata* (DISP), the initial modeled condition had significantly lower DISP at the CRMS stations than was observed. Although LAVegMod 2.0 showed increases in DISP over time, they never reached the observed values (Figure 53), and only 69% were classified correctly at the end of the simulation (Table 11). The results for *Avicennia germinans* (AVGE) reflect that this species was only observed at one of the CRMS stations, and LAVegMod 2.0 predicted no occurrence at any of the CRMS stations.

Table 11: Summary of Model Fit by Marsh Type and Species. Numbers represent the percentage of CRMS stations where there is agreement or discrepancy between the predictions of the model and the observations reported in the CRMS data. For example the first column of numbers represent the percentage of CRMS stations where the model predicts the species/marsh type to be absent and the field observation confirms that the species/marsh type is absent. The presence or absence of the marsh type is defined by the presence of species that make up that marsh type in the model.

Marsh Type	**Species**	**Model Prediction: Observed:**	**Absent Absent**	**Present Present**	**Absent Present**	**Present Absent**
Fresh			**71.60**	**7.10**	**19.14**	**2.16**
	MOCE2		97.32	0.00	2.68	0.00
	PAHE2		92.56	0.30	7.14	0.00
	ELBA2		95.54	0.30	0.00	4.17
	HYUM		94.94	0.00	5.06	0.00
	SALA2		98.21	0.00	1.79	0.00

Marsh Type	Species	Model Prediction: Observed:	Absent Absent	Present Present	Absent Present	Present Absent
	ZIMI		96.13	0.00	3.87	0.00
	CLMA10		97.62	0.00	2.38	0.00
	TYDO		78.57	2.68	13.10	5.65
	SCCA11		96.43	0.00	3.57	0.00
			59.34	**8.30**	**30.71**	**1.66**
	SALA		78.56	3.27	17.86	0.60
Intermediate	PHAU7		87.80	0.89	11.01	0.30
	IVFR		91.07	0.00	3.87	5.06
	BAHA		91.37	0.00	2.98	5.65
			25.00	**67.89**	**18.83**	**16.36**
Brackish	SPPA		28.87	37.80	17.86	15.48
	PAVA		89.58	0.60	5.95	3.87
			50.00	**20.37**	**27.47**	**2.16**
	JURO		87.20	0.89	11.31	0.60
Saline	DISP		64.58	7.14	20.54	7.40
	SPAL		70.24	8.33	20.54	0.89
	AVGE		99.70	0.00	0.30	0.00

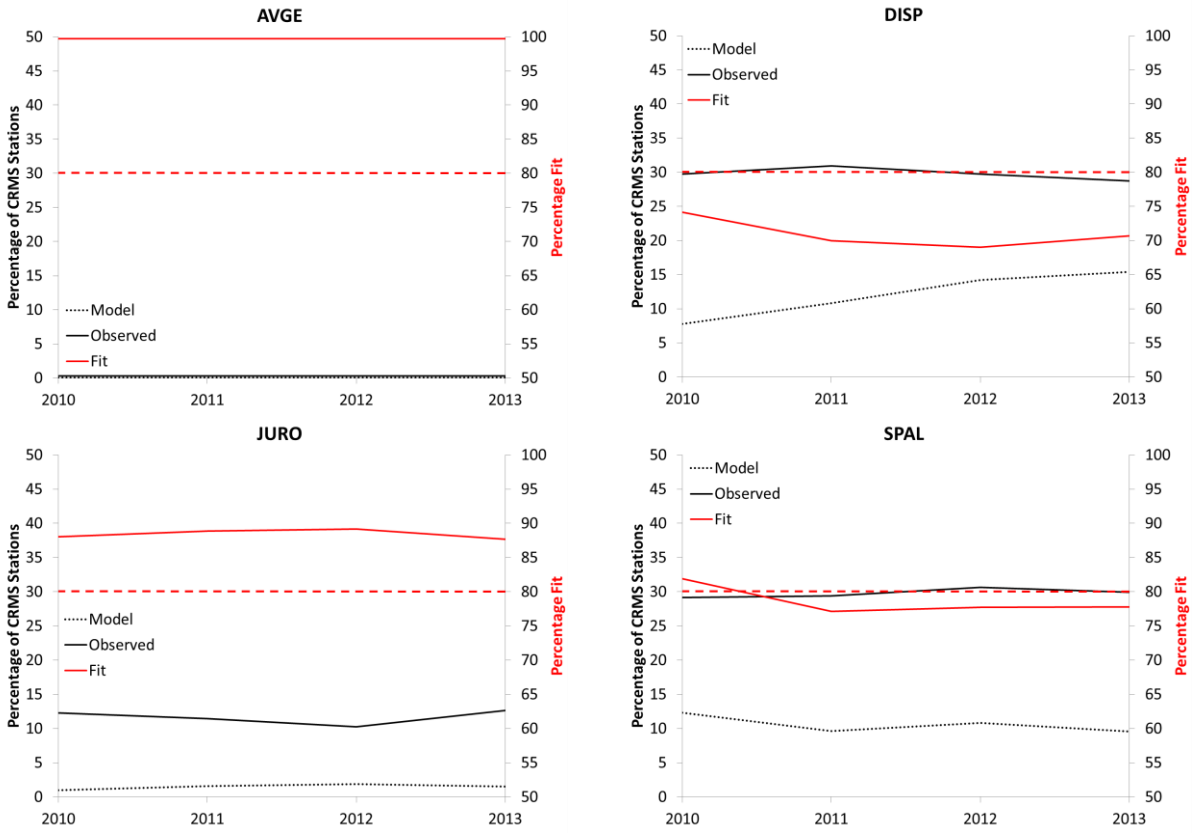

Figure 53: Calibration Results for the Saline Marsh Species. The red dashed line represents the goal of at least 80% fit of the model. Model fit (solid red line) below this line indicates a failure to attain the ambitious goal.

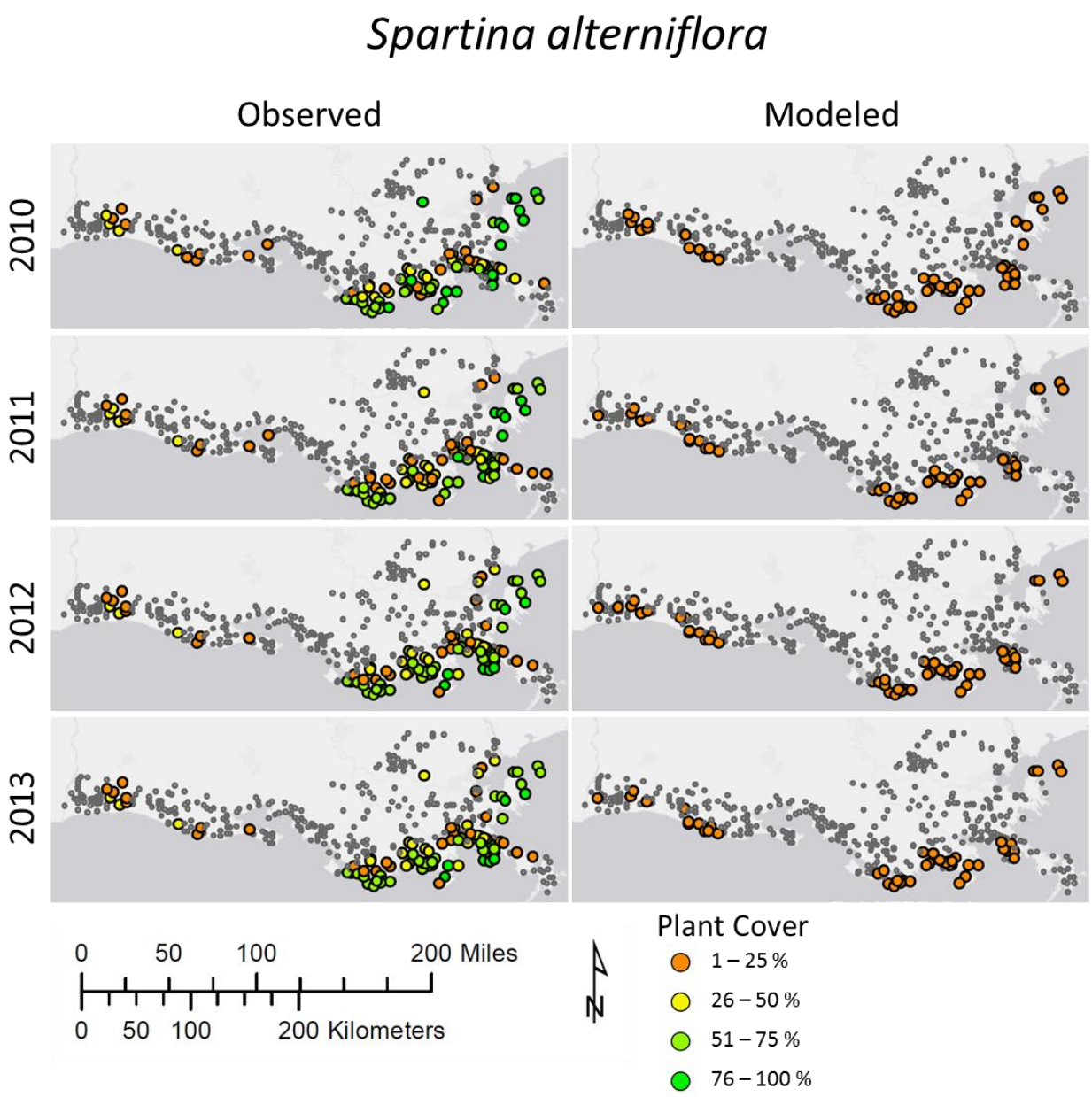

Figure 54: Spatial Distribution of Spartina Alterniflora as Observed at CRMS Sites and as Predicted for Those Same Sites by the Calibrated LAVegMod 2.0.

Spartina patens (SPPA) showed the worst level of agreement of all species (Table 11). Even though the percentage of stations occupied in LAVegMod 2.0 and the observed were similar (Figure 55), LAVegMod 2.0 predicted presence at 17% of the stations where it was not observed and absence at 20% of the stations where it was observed. Spatial distribution shows that LAVegMod 2.0 captures the spatial distribution reasonably well (Figure 56), but it over-estimates the presence of *Spartina patens* in what are currently saline marshes (e.g., Barataria Bay rim) as well as intermediate marshes (e.g., Bird's Foot Delta). Some of this is an artifact of the cover of this species being over-estimated in the initial condition.

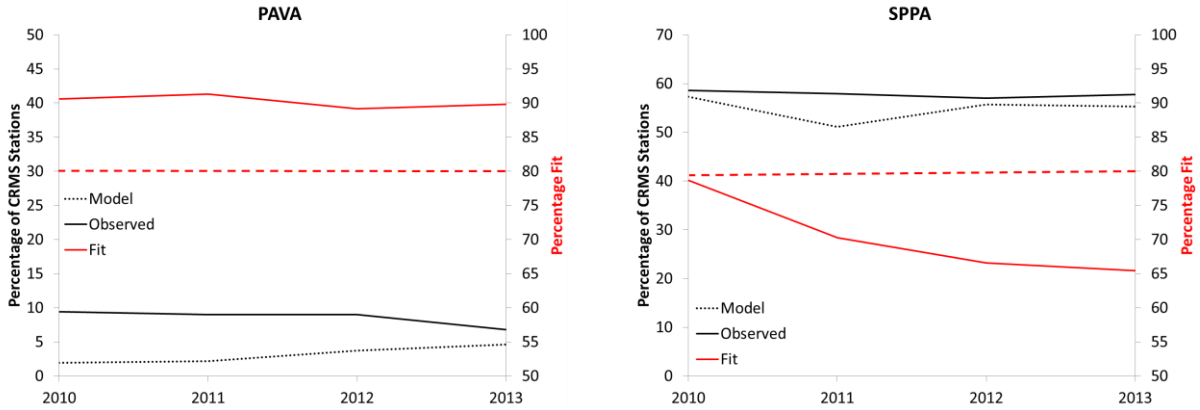

Figure 55: Calibration Results for the Brackish Marsh Species. The red dashed line represents the goal of at least 80% fit of LAVegMod 2.0. Model fit (solid red line) below this line indicate a failure to attain the ambitious goal.

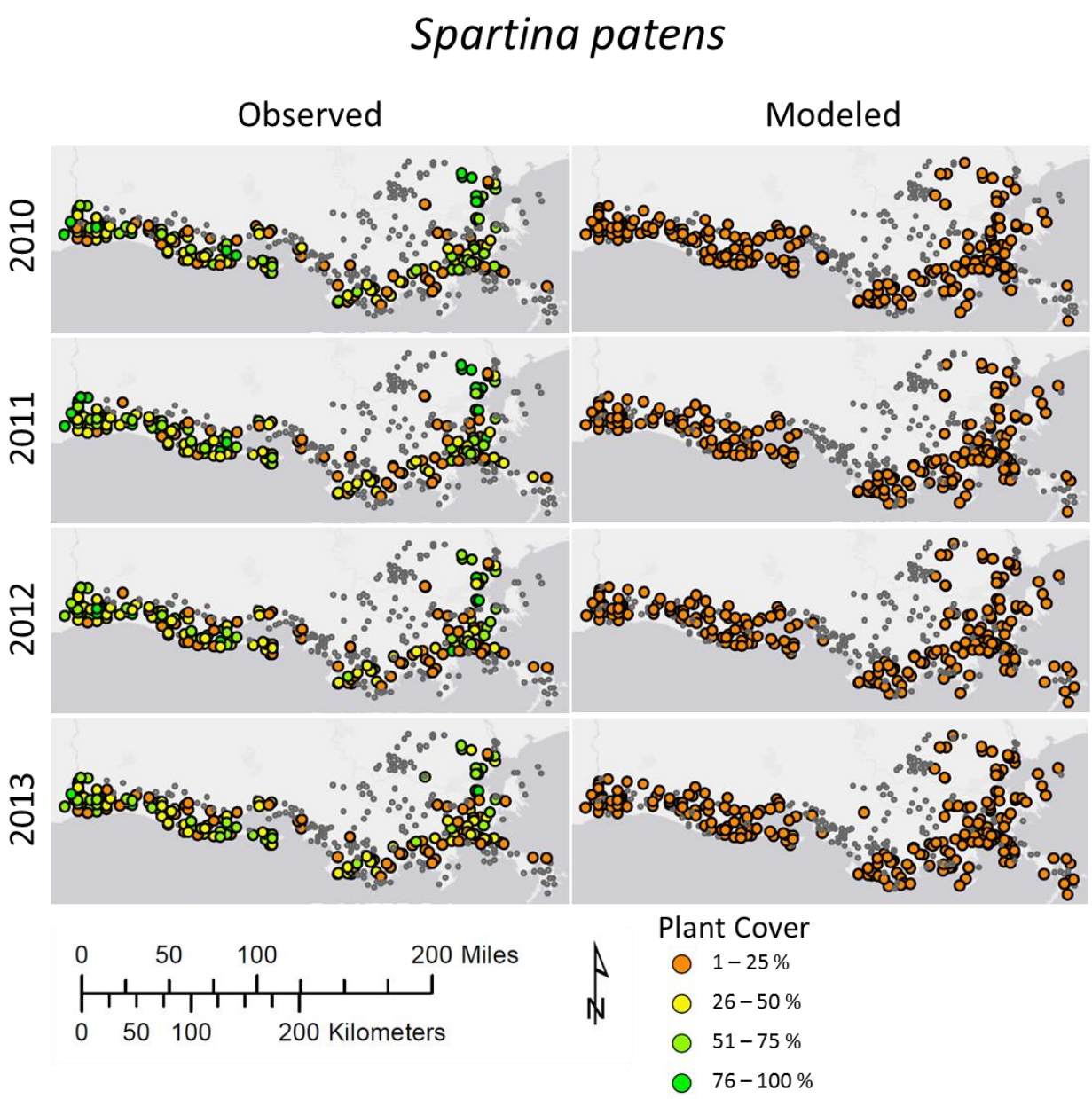

Figure 56: Spatial Distribution of Spartina Patens as Observed at CRMS Sites and as Predicted for Those Same Sites by the Calibrated LAVegMod 2.0.

The intermediate and fresh marsh species all were above the 80% agreement goal (Figures 57 and 58). These species all have relatively small footprints, and the agreement is mostly the result of the model correctly classifying the stations where the species are absent. When examining the spatial distribution of these species (e.g., *Sagittaria lancifolia* Figure 59), LAVegMod 2.0 generally captures the distribution of the areas where the species are most prevalent.

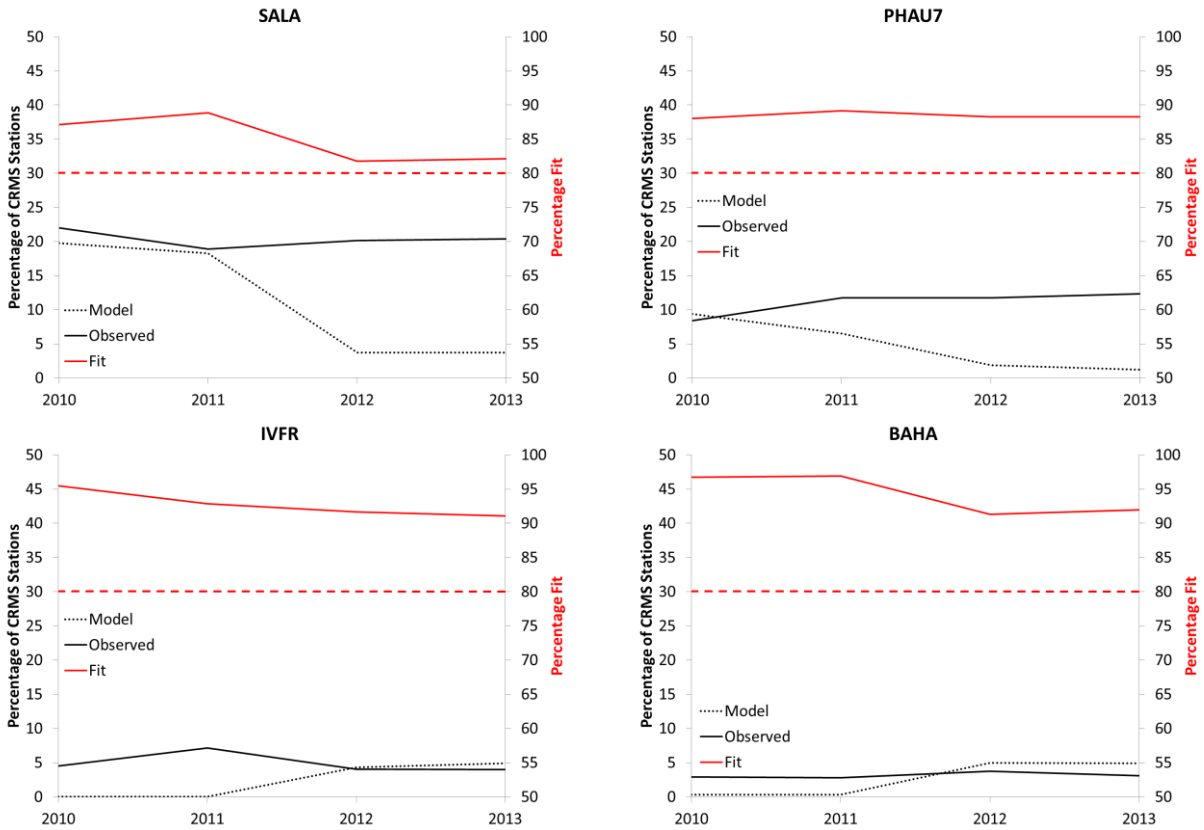

Figure 57: Calibration Results for the Intermediate Marsh Species. The red dashed line represents the goal of at least 80% fit of LAVegMod 2.0. Model fit (solid red line) below this line indicate a failure to attain the ambitious goal.

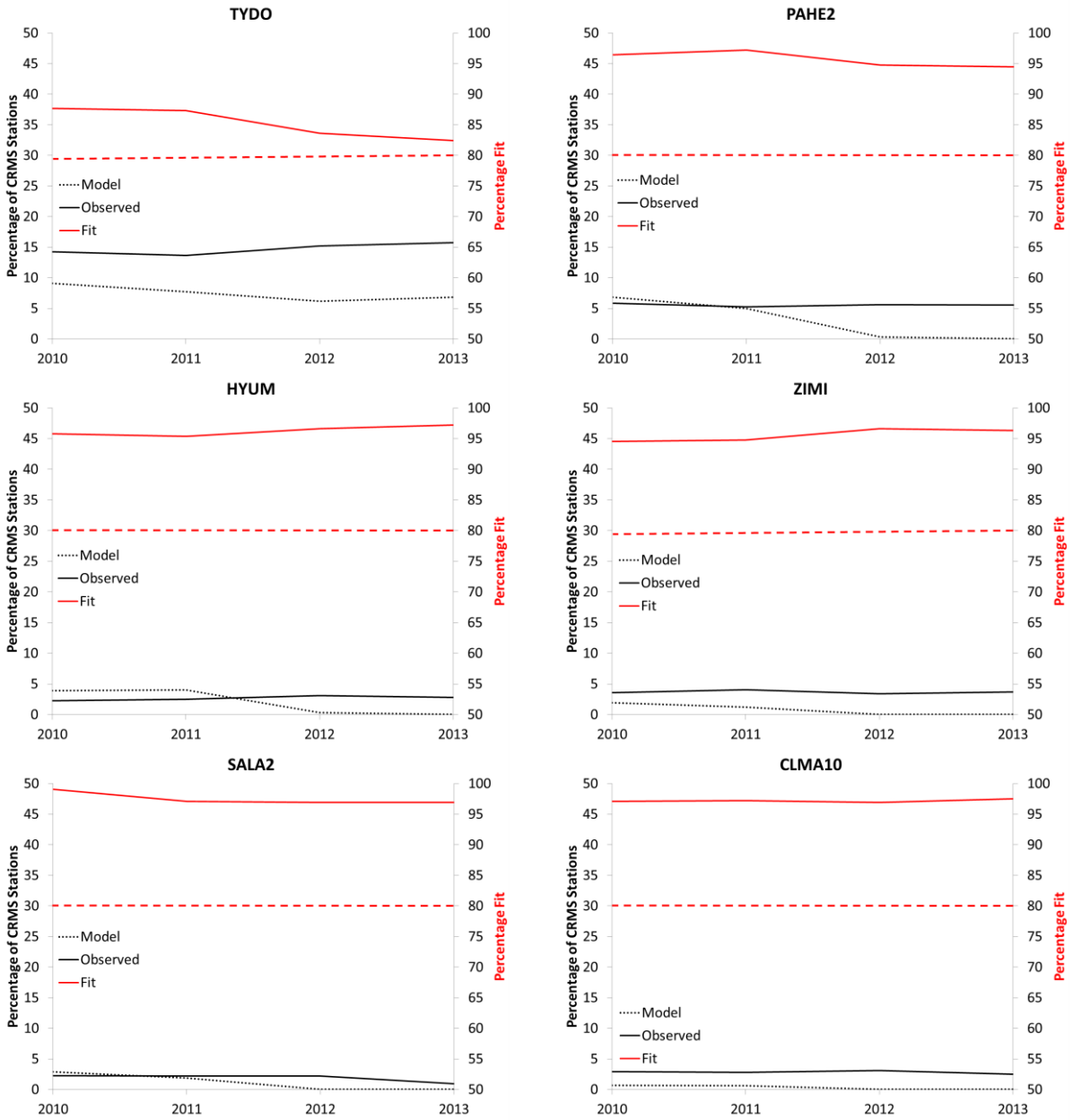

Figure 58: Calibration Results for the Fresh Marsh Species. The red dashed line represents the goal of at least 80% fit of LAVegMod 2.0. Model fit (solid red line) below this line indicate a failure to attain the ambitious goal.

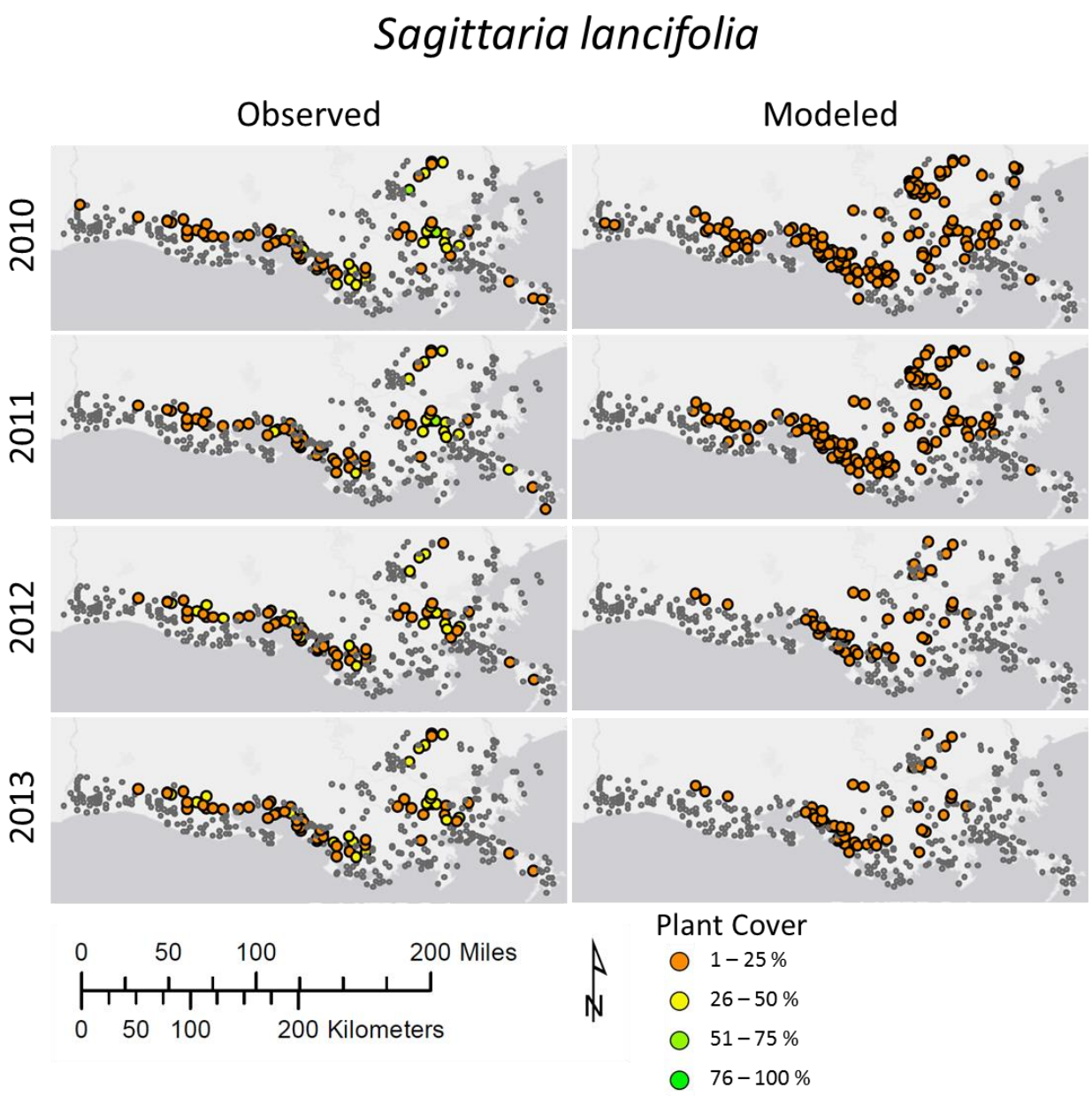

Figure 59: Spatial Distribution of Sagittaria lancifolia as Observed at CRMS Sites and as Predicted for Those Same Sites by the Calibrated LAVegMod 2.0.

5.4 Discussion

In general, LAVegMod 2.0 performed well against the observed distributions of most species. LAVegMod 2.0 used the 2010 initial condition map that was developed for LAVegMod 1.0, and therefore some species that were not present in the earlier version were completely or partially (brackish species were also mapped as individual species) estimated by equally distributing the class they were represented by in LAVegMod 1.0 (Table 12). Considering, some of the lowest levels of agreement are for those species in Table 12. The actual production runs will be performed using an initial condition map developed for LAVegMod 2.0, and model

performance is expected to greatly improve for these species. In general, LAVegMod 2.0 shows better performance for the rarer species. It is generally easier to predict the absence of a species correctly than it is to predict the presence of a species (van Horssen et al., 1999).

Table 12: Species Not Present in LAVegMod 1.0 and How They Were Apportioned to the Initial Condition Map Used for LAVegMod 2.0 Calibration.

LAVegMod 1.0 Class	LAVegMod 1.0 Abbreviation	LAVegMod 2.0 Species	LAVegMod 2.0 Abbreviation	Percentage of Area
Swamp forest	SWAMP	*Taxodium distichum*	TADI2	33%
		Nyssa aquatic	NYAQ2	33%
		Salix nigra	SANI	33%
Thin mat	THIN	*Eleocharis baldwinii*	ELBA2	50%
		Hydrocotyle umbellata	HYUM	50%
Brackish marsh	BRACK	*Spartina patens*	SPPA	33%
		Distichlis spicata	DISP	33%
		Spartina alterniflora	SPAL	33%

Very few vegetation models have attempted calibration, primarily because of lack of observed data. Poiani and Johnson (1993) calibrated a prairie wetlands model but provide no details only mentioning visual comparison of aerial photographs and model output. Benjankar et al. (2010) conducted an excellent review of comparing observed vegetation distribution in vegetation models and describe the evaluation of fit for their floodplain vegetation model. In this floodplain vegetation model, cells were only 10 x10 m and were allowed only one vegetation type per cell. Using this approach, overall accuracy was only 18%. Using information from surrounding cells and merging plant species into vegetation types in the model algorithm improved the prediction and raised it to 80%. LAVegMod 2.0 outperforms this significantly based on individual species. Since several other subroutines in the ICM (e.g., HSI and morphology) use vegetation types, it is assumed that the accuracy improves when species are aggregated into vegetation types.

6.0 Re-calibration of Salinity Parameters for Version 3

Upon completion of multi-decadal FWOA model runs, it was evident that, during later simulation years, the hydrology subroutine was simulating spikes in salinity in several hydrologic compartments. These salinity spikes began to occur after several decades of land loss and sea level rise when the hydraulic connectivity was substantially different than the conditions under which the ICM had been calibrated. These salinity spikes were also prone to occur only in compartments that had relatively small bodies of water (e.g., large land-to-water ratio within compartment) under initial conditions.

The underlying source for these salinity spikes was two-fold: first, an increase in hydraulic connectivity via the overland flow network was more active in later decades, which resulted in the activation of flow in links that did not receive much (or any) flow during the calibration period. The second reason for these spikes was a pre-existing assumption within the hydrology subroutine that the salinity in the marsh portion of a compartment was always equal to the salinity in the open water region of the same compartment. This assumption lead to an instability in calculations of salinity mass transfer when a large difference in marsh and open water salinity should have been maintained (e.g., large rainfall events on the marsh surface draining fresh water into a saline water body, or overland flow of saline water during a surge-like event to an open water body with relatively fresh water). During the original ICM calibration, the adjustment of the salinity diffusivity term in all hydraulic links corrected for these conditions. In later decades when the hydraulic connectivity was altered by higher sea level and land loss, links that originally had not been very active, received substantially higher amounts of flow, resulting in salinity spikes due to these instabilities introduced by this original assumption.

Prior to the start of alternative-level model runs, adjustments were made to the mass balance equations in the hydrology subroutine which improved the salinity transfer equations between the open water and marsh regions of compartments. This resulted in more stable calculations in later decades and resulted in more accurate conservation of salinity mass; however, the original calibration of the diffusivity term was no longer valid for hydraulic links in impacted regions of the model. Comparing salinity concentrations from the updated hydrology subroutine to the original calibration identified which regions of the model domain were adversely impacted by the new salinity calculation method. A brief calibration exercise was then repeated for these regions. The diffusivity term was adjusted (as described in Section 2.2.3) until the model was predicting salinity concentrations with the updated equations as accurately as it had been following the original calibration exercise. The updated and re-calibrated model was as accurate as the previous version, but was updated to better conserve salinity mass across the overland flow network in later years.

The updated salinity transfer equations, when applied to the hydraulic network utilizing diffusivity values from the original calibration, were considered Version 2 of the ICM. Once the diffusivity terms had been re-calibrated to account for the updated salinity transfer equations, it was referred to as Version 3. This version, Version 3 of the ICM, was utilized for all alternative-level and plan-level simulations. To accurately determine the impact of project implementation, the FWOA was re-run using Version 3.

As can be seen in Tables 13 and 14, the ICM performance for both the calibration and validation periods was essentially unchanged for Version 3 as compared to Version 1 (Tables 4 and 5 in Section 2.3). The model results for salinity tended to be lower in Version 3 as compared to Version 1; therefore, the model error was slightly smaller for the calibration period in regions where the mean observed salinity was greater than 1 ppt. The model error was slightly higher in the freshest regions of the model domain where the observed mean salinity was less than 1 ppt. These trends generally held across both the calibration and validation periods; however, the magnitude of the changes in error from Version 1 to Version 3 is insignificant.

Table 13: Updated Calibration Period (2010-2013) Mean Model Performance Statistics from Version 3 - Statistics are Aggregated Across All Model-Observed Pairs.

		No. Stns	Mean		Median		Standard Deviation		Root Mean Square Error			
Parameter	units		*Obs*	*Pred*	*Obs*	*Pred*	*Obs*	*Pred*	*Daily*	*2 week*	*Monthly*	*Annual*
Salinity (0-1 ppt)	ppt	*55*	0.4	0.6	0.2	0.4	0.4	0.5	0.6	0.6	0.5	0.4
Salinity (1-5 ppt)	ppt	*51*	2.8	3.0	2.2	2.3	2.1	2.2	2.3	2.1	1.9	1.2
Salinity (5-20 ppt)	ppt	*74*	11.6	11.0	11.2	10.7	5.0	4.4	4.2	3.7	3.4	1.9
Salinity (>20 ppt)	ppt	*4*	22.0	22.3	21.8	22.9	6.2	3.9	6.1	5.6	5.4	3.9

Table 14: Updated Validation Period (2006-2009) Mean Model Performance Statistics from Version 3 - Statistics are Aggregated Across All Model-Observed Pairs.

		No. Stns	Mean		Median		Standard Deviation		Root Mean Square Error			
Parameter	*units*		*Obs*	*Pred*	*Obs*	*Pred*	*Obs*	*Pred*	*Daily*	*2 week*	*Monthly*	*Annual*
Salinity (0-1 ppt)	*ppt*	*47*	0.4	0.6	0.2	0.4	0.4	0.5	0.7	0.6	0.4	0.4
Salinity (1-5 ppt)	*ppt*	*59*	3.3	3.1	2.7	2.7	2.2	1.9	3.0	2.9	2.1	1.8
Salinity (5-20 ppt)	*ppt*	*74*	11.3	10.8	10.9	10.8	4.4	3.3	4.6	4.4	3.4	2.6
Salinity (>20 ppt)	*ppt*	*4*	21.7	21.7	22.0	22.3	5.4	3.3	6.9	6.3	4.4	3.6

Figures 60 through 65 show the model and observed salinity concentrations at three example sites across the model domain for both the calibration and validation periods from Version 3. Compared to these same figures from Version 1 of the model, there is very little change, demonstrating the very slight differences between Version 1 and Version 3 of the salinity result.

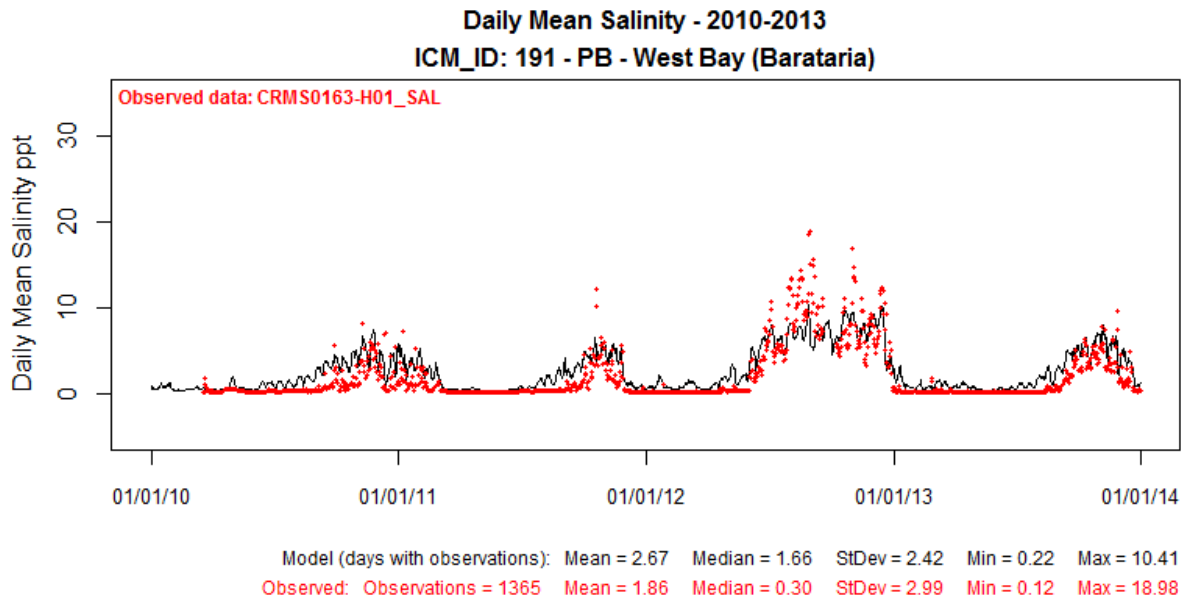

Figure 60: Modeled (black line) and Observed (red dot) Daily Mean Salinity for ICM Compartment 191 in the Pontchartrain/Barataria Region for Calibration Period (2010-2013). Results are from Version 3 of the Model.

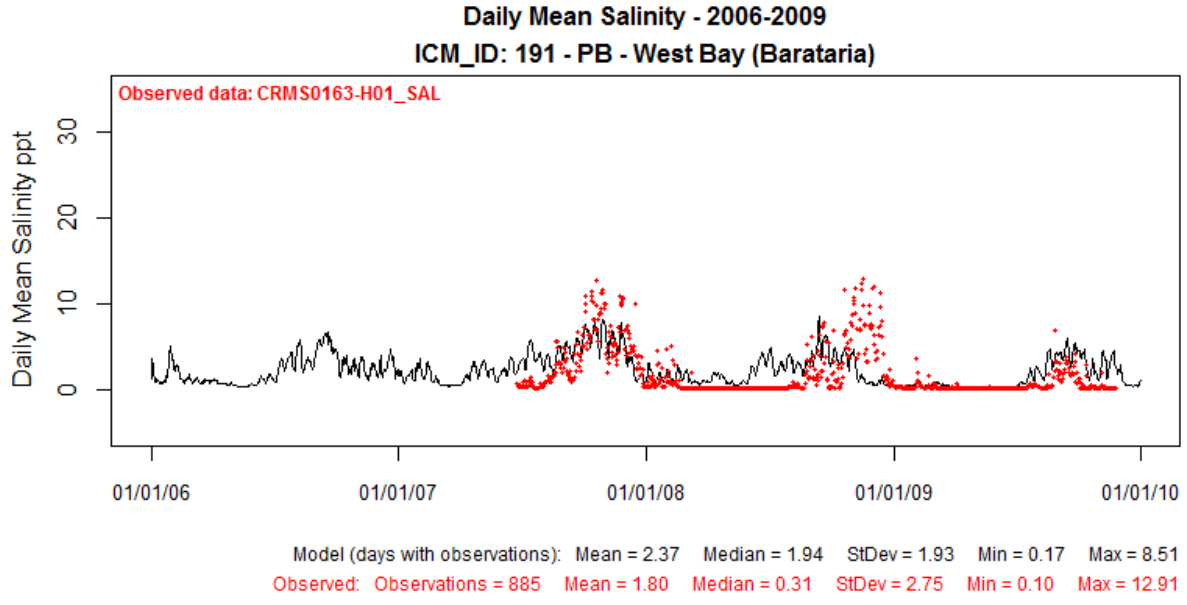

Figure 61: Modeled (black line) and Observed (red dot) Daily Mean Salinity for ICM Compartment 191 in the Pontchartrain/Barataria Region for Validation Period (2006-2009). Results are from Version 3 of the Model.

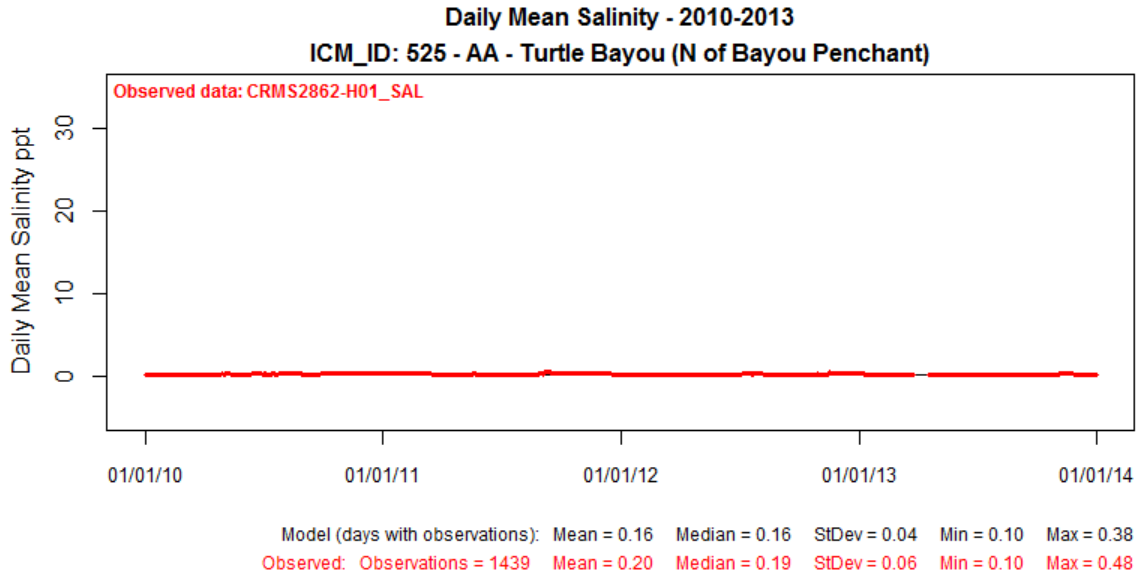

Figure 62: Modeled (black line) and Observed (red dot) Daily Mean Salinity for ICM Compartment 525 in the Atchafalaya Region for Calibration Period (2010-2013). Results are from Version 3 of the Model.

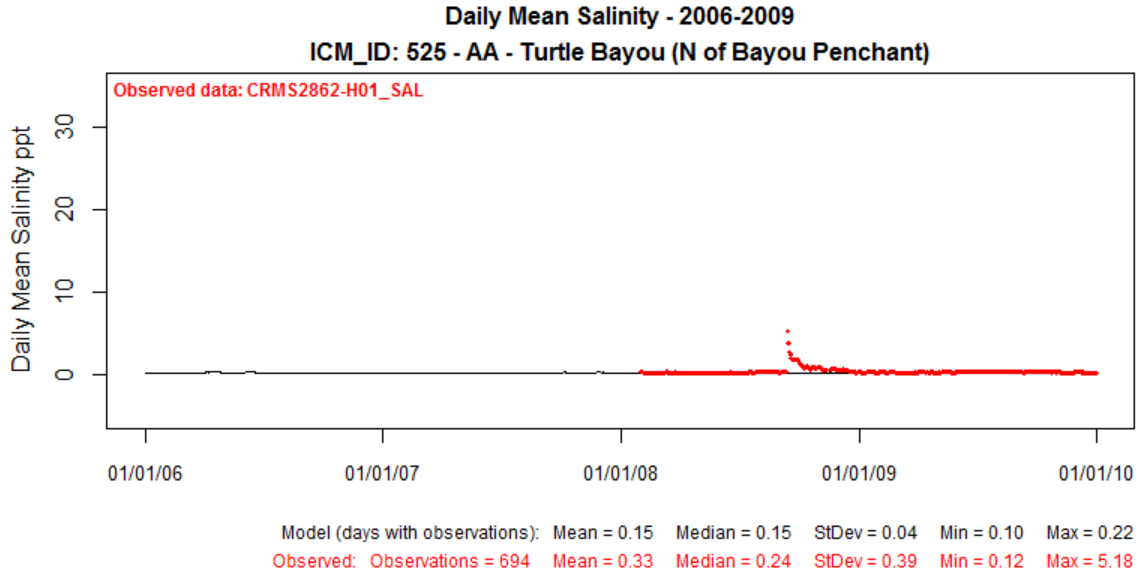

Figure 63: Modeled (black line) and Observed (red dot) Daily Mean Salinity for ICM Compartment 525 in the Atchafalaya Region for Validation Period (2006-2009). Results are from Version 3 of the Model.

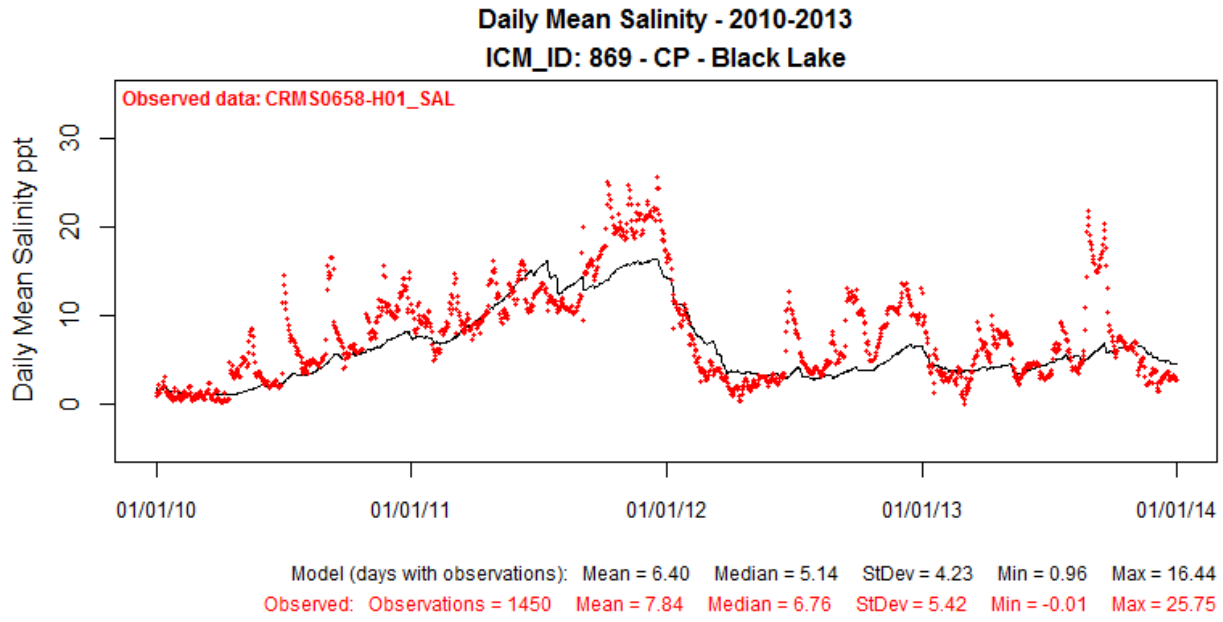

Figure 64: Modeled (black line) and Observed (red dot) Daily Mean Salinity for ICM Compartment 869 in the Chenier Plain Region for Calibration Period (2010-2013). Results are from Version 3 of the Model.

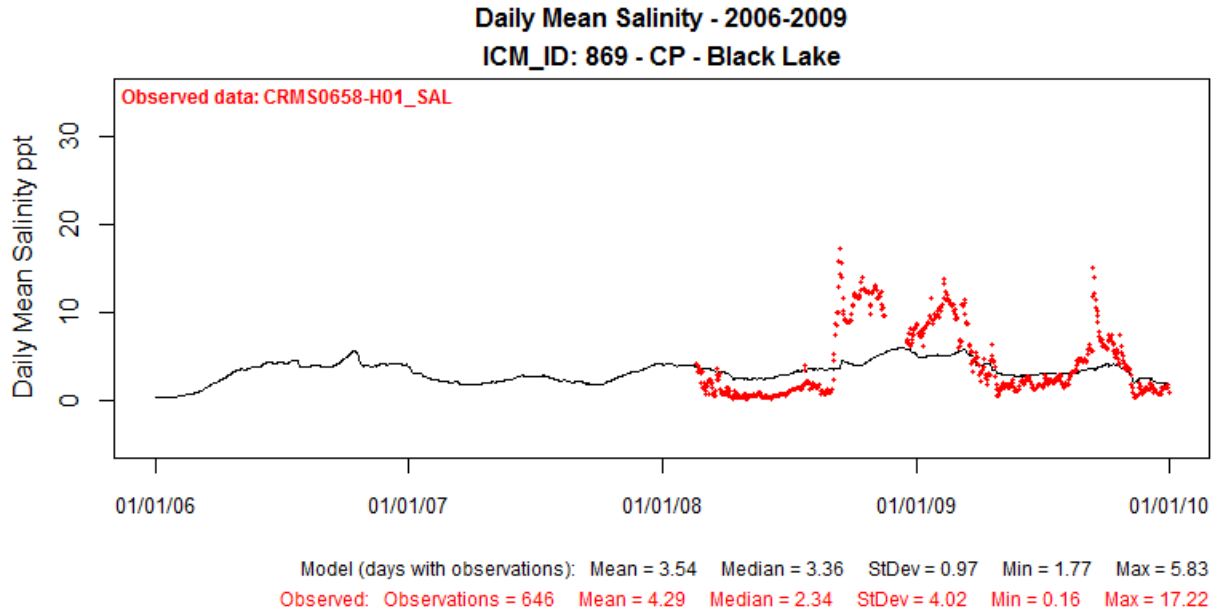

Figure 65: Modeled (black line) and Observed (red dot) Daily Mean Salinity for ICM Compartment 869 in the Chenier Plain Region for Validation Period (2006-2009). Results are from Version 3 of the Model.

7.0 Closing Remarks and Next Steps

Calibration and validation for the 2017 Coastal Master Plan ICM is documented in this report. Model subroutines including hydrology, morphology, barrier islands, and vegetation were fully calibrated against field measurements using both graphical and statistical metrics, and results show that the ICM is able to reproduce the observed hydro-morphological evolution at a satisfactory level. The calibrated model parameters are suitable for evaluating impacts from various projects or changes in operation conditions in the Louisiana coastal zone. Since the model was calibrated and validated based on certain hydrological conditions, exceeding the environmental conditions present during calibration and validation may result in reduced model accuracy and capability. The future environmental scenarios will, by necessity, be dissimilar to the calibration and validation periods, which may impose additional uncertainty to the model output.

This calibration and validation effort undertaken for the ICM provides a thorough understanding of model performance, sensitivities, and limitations. These strengths and limitations are further investigated in a systematic manner in Attachment C3-24: ICM Uncertainty Analysis.

The ICM is capable of simulating complex physical and ecological processes. While the wealth of data available for this effort is substantial, the data required for a fully robust model is nonetheless even more substantial. The spatial and temporal richness of the water level and salinity dataset further accentuates the data gaps with respect to other important parameters such as TSS and TKN. Improving input boundary condition datasets to better capture temporal fluctuations will greatly improve the model's ability to capture complex higher-order processes such as water quality and sediment dynamics.

Future model validation efforts for landscape-based subroutines (morphology, vegetation, and barrier islands) would be improved if the spatial resolution of the observed data better matched the resolution of model output. Full assessment of the model performance could not be achieved when data from individual soil cores are used to validate model output that is orders of magnitude coarser. Special effort on aggregate and spatial statistical methods would likely lead to better quantitative understanding of model strengths and weaknesses in prediction of vegetation cover, accretion, land change rates, and barrier island processes.

8.0 References

Benjankar, R., Glenn, N. F., Egger, G., Jorde, K., and Goodwin, P. (2010). Comparison of field-observed and simulated map output from a dynamic floodplain vegetation model using remote sensing and GIS techniques. *GIScience and Remote Sensing*, *47*(4), 480-497.

Couvillion, B.R. and Beck, H. (2013). Marsh collapse thresholds for coastal Louisiana estimated using elevation and vegetation index data. In: Brock, J.C.; Barras, J.A., and Williams, S.J. (eds.), Understanding and Predicting Change in the Coastal Ecosystems of the Northern Gulf of Mexico, *Journal of Coastal Research, Special Issue, 63*, 58–67.

Couvillion, B.R., Barras, J.A., Steyer, G.D., Sleavin, W., Fischer, M., Beck, H., Trahan, N., Griffin, B., and Heckman, D. (2011). Land area change in coastal Louisiana from 1932 to 2010. *U.S. Geological Survey Scientific Investigations Map 3164*, scale 1:265,000, 12 p. pamphlet.

De Mutsert, K., Lewis, K.A., Buszowski, J., Steenbeek, J., and Milroy, S. (2015). 2017 Coastal Master Plan Modeling: C3-20. Ecopath with Ecosim. Version I. (pp. 1-100). Baton Rouge, Louisiana: Coastal Protection and Restoration Authority. http://coastal.la.gov/a-common-vision/2017-master-plan-update/technical-analysis/modeling/

Folse, T.M., West, J.L., Hymel, M.K., Troutman, J.P., Sharp, L.A., Weifenbach, D.K., McGinnis, T.E., Rodrigue, L.B., Boshart, W.M., Richardi, D.C., Miller, C.M., and Wood, W.B. (2008), revised 2012. A Standard Operating Procedures Manual for the Coastwide Reference Monitoring System-Wetlands: Methods for Site Establishment, Data Collection, and Quality Assurance/Quality Control. Louisiana Coastal Protection and Restoration Authority. Baton Rouge, LA. 207 pp.

Kent, M. and Coker, P. (1995) Vegetation Description and Analysis: A practical approach. John Wiley and Sons.

Meselhe, E., McCorquodale, J.A., Shelden, J., Dortch, M., Brown, T.S., Elkan, P., Rodrigue, M.D., Schindler, J.K., and Wang, Z. (2013). Eco-hydrology component of Louisiana's 2012 Coastal Master Plan: Mass-Balance Compartment Model. In: Peyronnin, N.S. and Reed D.J. (eds.), Louisiana's 2012 Coastal Master Plan Technical Analysis. *Journal of Coastal Research, 67,pp.* 16-28.

Meselhe, E.A. and Rodrigue, M.D. (2013). Models Performance Assessment Metrics and Uncertainty Analysis. Report, Louisiana Coastal Area Program Mississippi River Hydrodynamics and Delta Management Study. https://www.lca.gov/Library/ProductList.aspx?ProdType=22andfolder=0.

Patankar, S. (1980). Numerical Heat Transfer and Fluid Flow. CRC Press. pp. 214.

Piazza, S.C., Steyer, G.D., Cretini, K.F., Sasser, C.E., Visser, J.M., Holm, Jr., G.O., Sharp, L.A., Evers, D.E., and Meriwether, J.R. (2011). Geomorphic and ecological effects of hurricane Katrina and Rita on coastal Louisiana Marsh communities. *U.S. Geological Survey, Open File Report, 2011-1094*, 126p.

Poiani, K.A. and Johnson, W.C. (1993). A spatial simulation model of hydrology and vegetation dynamics in semi-permanent prairie wetlands. *Ecological Applications,* 279-293.

Thomson, G., Thompson, W., Wycklendt, A., Swigler, D., and Gielow, R. (2011). Chenier Ronquille Barrier Island Restoration Project (BA-76) – 30% Design Report. Boca Raton, Florida: Coastal Planning and Engineering, Inc. 140p. (Report prepared for the Louisiana Office of Coastal Protection and Restoration).

Van Horssen, P.W., Schot, P.P., and Barendregt, A. (1999). A GIS-based plant prediction model for wetland ecosystems. Landscape Ecology, 14(3), 253-265.

Additional Information

Attachment C3-23.1: Hydrology Station Locations
Attachment C3-23.2: Model Performance - Stage
Attachment C3-23.3: Model Performance - Flow
Attachment C3-23.4: Model Performance - Salinity
Attachment C3-23.5: Model Performance - Total Suspended Solids
Attachment C3-23.6: Model Performance - Temperature
Attachment C3-23.7: Model Performance Total Kjeldahl Nitrogen
Attachment C3-23.8: Model Performance - Total Phosphorus